



Vaal University of Technology
Your world to a better future

**SYNTHESIS, CHARACTERIZATION AND ANTIMICROBIAL ACTIVITY OF
COBALT AND COBALT SULPHIDE NANOPARTICLES AGAINST SELECTED
MICROBES THAT ARE FOUND IN WASTEWATER**

Research proposal submitted for the degree Magister Technologiae

In the Faculty of Applied and Computer Sciences

Department of Biotechnology

Name of Student: Moukangoe Getrude Phuti

Student number: 209117559

Supervisor: Dr M. Klink

**Co-supervisors: Mr N. Laloo
: Dr V. Pakade**

DEDICATION

This dissertation is dedicated to my late father Lucas Tumishi Rammutla and my late sister Junior Chuene Rammutla, and to my husband and children for believing in me they are my pillar of strength.

PRESENTATIONS

- i. **G.P. Moukangoe**, E. Morifi, K. Kotlhao, M. Moloto, V. Pakade, J. Modise, N. Laloo, M.J. Klink, (2016). The Preparation and Characterisation of Doped Cobalt Nanoparticles and their Antimicrobial Activity against selected Waterborne Pathogens, CREW: International Conference on Environment, Materials and Green Technology, 24 – 25 November 2016, VUT Southern Gauteng Science and Technology Park, Sebokeng, South Africa. [Poster Presentation]
- ii. K. Kotlhao, N.E. Volofu, G.P. Moukangoe, V. Pakade, F. Mtunzi, M.J. Klink, (2018). The synthesis and Characterization Cobalt Oxide Nanoparticles and their Anti-Microbial Activity against selected Waterborne Pathogens, International Conference of pure and Applied Chemistry (ICPAC-2018), 2 -6 July 2018, Mauritius [Poster Presentation]

DECLARATION

I, Moukangoe Getrude Phuti, declare that this dissertation is my own work. It is being submitted in fulfilment of the degree, Magisters Technologiae in Biotechnology, at Vaal University of Technology. All the sources that I have used or quoted have been indicated and acknowledged by means of complete references and this work has not been submitted before for any other degree.

.....

Moukangoe Getrude Phuti

.....

Date

ACKNOWLEDGEMENTS

I would like to thank all the people who contributed one way or the other towards my study:

Firstly, I would like to thank almighty God, who gave me strength to finish my study. His mercy, love and protection have taken me so far. Through Him all things are possible.

I would like to thank my supervisor, Dr Michael Klink, for his advice and mentorship. He has assisted and helped me to execute this project timeously. He encouraged and supported me not to give up.

I would also like to express my gratitude to the department of Biotechnology at Vaal University of Technology (VUT), for allowing me to study in their institution and use their resources.

Very special thanks to Hersol Manufacturing Laboratories (LTD) for buying me the reagents and allowing me to do the synthesis and characterisation at their company, and to all the laboratory analysts who contributed towards my studies and helped me to understand chemistry at Hersol.

I would like to show gratitude to all my friends who kept me rational throughout this journey. At times it got stressful and I truly appreciated having them around. They were my stress relievers.

In addition, I would like to acknowledge National Research Foundation (NRF) and VUT for their financial support throughout the study. I would have not made it without them.

With special thanks to my mother Josephine Rammutla who kept on motivating and advised me to hold hard and become the woman I am today, and my sisters Emmah, Lindy and my only brother Wilford for their love and support.

To all my children (Hlakudi, Tumishi, Mathlaku and Phuti) for filling my life with joy and love and for giving me hope of life and so much to pray about.

Lastly, I would also like to express my sincere gratitude and thanks to my wonderful loving, caring and supporting husband Phasoane Isaac Moukangoe who supported and encouraged me through this journey.

ABSTRACT

Water shortages, water pollution and climate changes are highly interrelated global issues. These have raised immense concerns about serious adverse effects on the quality, treatment and re-use of wastewater. A major role of water is for vitality of life on earth. Water is recognized as source of evolution from origin to degree of civilization, since it is an essential resource its treatment becomes a necessity for day to day for life.

Nanoparticles and their application in treatment of wastewater is becoming a major area of research. It is mainly applicable to the removal of major contaminants like microorganisms. This study was carried out with an objective to investigate the antibacterial and antifungal potentials of nanoparticles. Cobalt and cobalt complexes of urea and thiourea were synthesized and characterized using UV-Vs, PL, FTIR, TEM, SEM, XRD and TGA techniques. The Co particles are in a mixture of rod, agglomerates with irregular shape around 50 – 100 nm in diameter. The Co/Thiourea particles appear to be around 10 – 30nm in size. The Co complexed with urea images showed spherical to hexagonal shape with 50 nm size in diameter.

The antimicrobial activity was determined using Minimum Inhibitory and bactericidal concentration and the well diffusion method. The antibacterial and antifungal activities of ratios (1:1, 1:2, 1:3, 2:1 µg/mL) of doped cobalt nanoparticles were tested against a panel of five Gram-negative bacteria - (*Escherichia coli*, *Pseudomonas aeruginosa*, *Shigella enterica*, *Salmonella typhi* and *Salmonella sonnei*) human pathogenic bacteria; and two fungal strains - *Aspergillus niger* and *Candida albicans*. Zones of inhibition as a consequence of nanoparticles were compared with that of different standards like Neomycin for antibacterial activity and Amphotericin B for antifungal activity. The results showed a remarkable inhibition of the bacterial growth against the tested organisms. The most striking feature of this study is that Cobalt, Urea and Thiourea nanoparticles have antifungal activity comparable or more effective (as in case of Thiourea on *A. niger*) than Amphotericin B and nearly promising antibacterial activity although not comparable to Neomycin.

Keywords: Nanoparticles, Co, Co/Tu, Co/U, MIC, *Pseudomonas aeruginosa*, *Shigella enterica*, *Escherichia coli*, *Salmonella sonnei*, *Salmonella typhi*, *Candida albicans* and *Aspergillus niger*.

TABLE OF CONTENTS

Dedication	i
Presentations	ii
Declaration	iii
Acknowledgements	iv
Abstract	v
CHAPTER ONE	1
INTRODUCTION	1
1. Background	1
2. Rationale and motivation	4
3. Problem statement	4
4. Research aim	5
5. Research objectives	6
6. Significance of the study	6
7. Structure of the dissertation	7
8. Conclusions	7
CHAPTER TWO	8
LITERATURE REVIEW	8
2.1. Introduction	8
2.2. Water shortage	8
2.3. Water pollution and challenges	9
2.4. Wastewater and challenges	10

2.5. Nanoparticles	11
2.5.1. Properties of nanoparticles	12
2.5.2. Structural properties	12
2.6. Application of nanoparticles in wastewater	12
2.8. Cobalt nanoparticles	15
2.9. Cobalt/urea nanoparticles	16
2.10. Cobalt/thiourea nanoparticles	17
2.11. Characterization techniques	18
2.11.1. Introduction	18
2.11.2. UV-Vis spectroscopy (UV-Vis)	18
2.11.3. Photoluminescence Spectroscopy (PL)	19
2.11.4. Fourier-transform Infrared spectroscopy (FT-IR)	19
2.11.5. X-ray diffraction (XRD)	20
2.11.6. Transmission Electron Microscopy (TEM)	20
2.11.7. Scanning Electron Microscopy (SEM)	21
2.11.8. Thermogravimetric analysis (TGA)	21
2.12. Antibacterial activity	21
2.13. Microbial routes for nanoparticles synthesis	22
2.14.1. Bacteria	22
2.14.1.1. <i>Escherichia coli</i>	23

2.14.1.2. <i>Pseudomonas aeruginosa</i>	23
2.14.1.3. <i>Salmonella typhi</i>	24
2.14.1.4. <i>Salmonella enterica</i>	25
2.14.1.5. <i>Shigella sonnei</i>	26
2.14.2. Mould	26
2.14.3. Yeast	27
CHAPTER THREE	29
RESEARCH DESIGN AND METHODOLOGY	29
3.1. Materials and methods	29
3.2. Experimental procedure	30
3.2.2 Synthesis of cobalt nanoparticles using Co-precipitation method	30
3.3. Synthesis of cobalt with urea and thiourea complexes	30
3.3.1. Complexes of thiourea with cobalt	31
3.3.2. Complexes of urea with cobalt	31
3.4. Characterization techniques	31
3.4.1. Introduction	31
3.4.2. UV-Visible spectroscopy (UV-Vis)	31
3.4.3. Photoluminescence spectroscopy (PL)	32
3.4.4. Transmission Electron Microscopy (TEM)	32
3.4.5. Fourier Transform Infrared Spectroscopy (FT-IR)	32

3.4.6. X-ray diffraction (XRD)	32
3.4.7. Scanning Electron Microscope (SEM)	33
3.4.8. Thermogravimetric analysis (TGA)	33
3.5. Heavy metals	33
3.6. Antibacterial activity	33
3.6.1. Introduction	33
3.6.2. Bacterial culture preparation	34
3.6.2.1. Preparation of the nanoparticles	34
3.6.2.2. Preparation of Mueller Hinton Broth (MHB)	34
3.6.2.3. Preparation of Mueller Hinton Agar (MHA)	34
3.6.2.4. Preparation of bacteria cultures	35
3.6.2.5. Preparation of resazurin dye	35
3.6.2.6. Preparation of neomycin	35
3.6.2.7. Serial dilution preparation and MIC determination	35
3.6.2.8. Well agar diffusion procedure	36
CHAPTER FOUR	37
SYNTHESIS AND CHARACTERIZATION RESULTS	37
4.1. Introduction	37
4.2. UV-Visible spectroscopy (UV-Vis)	37
4.3. Photoluminescence spectroscopy (PL)	40

4.4. FT-IR Spectral analysis (FT-IR)	43
4.5. Transmission Electron Microscopy (TEM)	44
4.6. Scanning Electron Microscopy (SEM)	48
4.7. X – ray diffraction spectral analysis (XRD)	51
4.8. Thermogravimetric analysis (TGA)	52
4.9. Heavy metals	55
CHAPTER FIVE	59
ANTIMICROBIAL RESULTS	59
5.1. Introduction	59
5.2. Minimum Inhibitory concentration	59
5.3. Well agar diffusion method	65
5.4. Antibacterial activities of nanoparticles	66
5.4.1. Cobalt on <i>E.coli</i>	67
5.4.2. Cobalt on <i>S.typhi</i>	67
5.4.3. Cobalt on <i>S.sonnei</i>	68
5.4.4. Cobalt on <i>P.aeruginosa</i>	69
5.4.5. Cobalt on <i>S.enterica</i>	70
5.4.6. Cobalt/Urea on <i>E.coli</i>	71
5.4.7. Cobalt/Urea on <i>S.typhi</i>	72
5.4.8. Cobalt/Urea on <i>S.sonnei</i>	73

5.4.9. Cobalt/Urea on <i>P.aeruginosa</i>	74
5.4.10. Cobalt/Urea on <i>S.enterica</i>	75
5.4.11. Cobalt/Thiourea on <i>E.coli</i>	77
5.4.12. Cobalt/Thiourea on <i>S.typhi</i>	78
5.4.13. Cobalt/Thiourea on <i>S.sonnei</i>	79
5.4.14. Cobalt/Thiourea on <i>P.aeruginosa</i>	80
5.5. Antifungal activities of nanoparticles	82
5.5.1. Cobalt on <i>A.niger</i>	82
5.5.2. Cobalt/Urea on <i>A.niger</i>	84
5.5.3. Cobalt/Thiourea on <i>A.niger</i>	85
5.5.4. Cobalt on <i>C.albicans</i>	86
5.5.5. Cobalt/Urea on <i>C.albicans</i>	87
5.5.6. Cobalt/Thiourea on <i>C.albicans</i>	88
CHAPTER SIX	90
CONCLUSION AND RECOMMENDATIONS	90
6.1. Introduction	90
6.2. Summary and interpretation of research findings	90
6.2.1. Characterization of Cobalt, Cobalt/Urea and Cobalt/Thiourea	90
6.2.2. Antibacterial properties of Cobalt, Cobalt/Urea and Cobalt/Thiourea	91
6.2.3. Antifungal properties of cobalt, cobalt/urea and cobalt/thiourea	91

6.3. Recommendations	92
6.3.1. Recommendation regarding antibacterial properties	92
6.3.2. Recommendation regarding the antifungal	92
6.3.3. Recommendation on study design	92
6.4. Contributions of the study	92
6.5. Limitations of the study	93
6.6. Concluding remarks	93
REFERENCES	94

LIST OF FIGURES

Figure 2.1: Pictures of water scarcity	09
Figure 2.2: A size comparison of nanoparticles	13
Figure 2.3: Structure of urea	17
Figure 2.4: Structure of thiourea	17
Figure 3.1: Research design	29
Figure 3.2: Schematic representation for the synthesis of cobalt doped nanoparticles	30
Figure 4.1: UV – Vis absorption spectrum of Thiourea	37
Figure 4.2: UV-Vis spectrum of Cobalt/Thiourea	38
Figure 4.3: UV – Vis absorption spectrum of Cobalt/Urea	39
Figure 4.4: PL spectrum of Cobalt	40
Figure 4.5: PL spectrum of Cobalt/Thiourea	41
Figure 4.6: PL spectrum of Cobalt/Urea	42
Figure 4.7: FTIR spectra of Cobalt/Thiourea	43
Figure 4.8: FTIR spectra of Cobalt/Urea	44
Figure 4.9: TEM image of Cobalt	45
Figure 4.10: TEM image of Cobalt/Thiourea	46
Figure 4.11: TEM image of Cobalt/Urea	47
Figure 4.12: SEM image of Cobalt	48
Figure 4.13: SEM image of Cobalt/Urea	49
Figure 4.14: SEM image of Cobalt/Urea	50
Figure 4.15 XRD pattern of Cobalt/Thiourea	51

Figure 4.16: XRD pattern of Cobalt/Urea	52
Figure 4.17: TGA curves of Cobalt	53
Figure 4.18: TGA curves of Cobalt/Thiourea	54
Figure 4.19: TGA curves for Cobalt/Urea complexes	55
Figure 4.20: Cobalt heavy metal	56
Figure 4.21: Co/Urea heavy metal	57
Figure 4.22: Co/Thiourea heavy metal	58
Figure 5.1: MIC results of <i>S.typhi</i>	60
Figure 5.2: MIC results for <i>S.enterica</i>	61
Figure 5.3: MIC results for <i>S.sonnei</i>	62
Figure 5.4: MIC for <i>E. coli</i>	63
Figure 5.5: MIC results for <i>P.aeruginosa</i>	64
Figure 5.6: Well diffusion picture of the yeast,mould and bacteria	65
Figure 5.7: The mean inhibition diameter of Cobalt nanoparticles and Neomycin on <i>E.coli</i>	66
Figure 5.8: The mean inhibition diameter of Cobalt nanoparticles and Neomycin on <i>S.typh</i>	67
Figure 5.9: The mean inhibition diameter of cobalt nanoparticles and neomycin on <i>S.sonnei</i>	68
Figure 5.10: The mean inhibition diameter of Cobalt nanoparticles and Neomycin on <i>P.aeruginosa</i>	69
Figure 5.11: The mean inhibition diameter of cobalt nanoparticles and neomycin on <i>S.enterica</i>	70
Figure 5.12: The mean inhibition diameter of Urea nanoparticles and neomycin on <i>E.coli</i>	71
Figure 5.13: The mean inhibition diameter of urea nanoparticles and neomycin on <i>S.typhi</i>	72

Figure 5.14: The mean inhibition diameter of urea nanoparticles and neomycin on <i>S.sonnei</i>	73
Figure 5.15: The mean inhibition diameter of urea nanoparticles and neomycin on <i>P.aeruginosa</i>	75
Figure 5.16: The mean inhibition diameter of urea nanoparticles and neomycin on <i>S.enterica</i>	76
Figure 5.17: The mean inhibition diameter of thiourea nanoparticles and neomycin on <i>E.coli</i>	77
Figure 5.18: The mean inhibition diameter of cobalt nanoparticles and neomycin on <i>S.typhi</i>	78
Figure 5.19: The mean inhibition diameter of thiourea nanoparticles and neomycin on <i>S.sonnei</i>	79
Figure 5.20: The mean inhibition diameter of thiourea nanoparticles and neomycin on <i>P.aeruginosa</i>	80
Figure 5.21: The mean inhibition diameter of thiourea nanoparticles and neomycin on <i>S.enterica</i>	81
Figure 5.22: The mean inhibition diameter of cobalt nanoparticles and amphotericin B on <i>A.niger</i>	83
Figure 5.23: The mean inhibition diameter of urea nanoparticles and neomycin on <i>A.niger</i>	84
Figure 5.24: The mean inhibition diameter of thiourea nanoparticles and amphotericin B on <i>A.niger</i>	85
Figure 5.25: The mean inhibition diameter of cobalt nanoparticles and amphotericin on <i>C.albicans</i>	86
Figure 5.26: The mean inhibition diameter of urea nanoparticles and amphotericin B <i>C.albicans</i>	87
Figure 5.27: The mean inhibition diameter of Thiourea and Amphotericin B on <i>C.albicans</i>	89

LIST OF TABLES

Table 2.1: Applications of nanoparticles	14
Table 3.1: Organisms that used for the antibacterial	34
Table 5.1: The difference in median values of <i>E.coli</i> treated with Cobalt and Neomycin	67
Table 5.2: The difference in median values of <i>S.typhi</i> treated with Cobalt and Neomycin	68
Table 5.3: The difference in median values of <i>S.sonnei</i> treated with Cobalt and Neomycin	69
Table 5.4: The difference in median values of <i>P.aeruginosa</i> treated with Cobalt and Neomycin	70
Table 5.5: The difference in median values of <i>S.enterica</i> treated with Cobalt and Neomycin	71
Table 5.6: The difference in median values of <i>E.coli</i> treated with Urea and Neomycin	72
Table 5.7: The difference in median values of <i>S.typhi</i> treated with Urea and Neomycin	73
Table 5.8: The difference in median values of <i>S.sonnei</i> treated with Urea and Neomycin	74
Table 5.9: The difference in median values of <i>P.aeruginosa</i> treated with urea and Neomycin	75
Table 5.10: The difference in median values of <i>S.enterica</i> treated with urea and Neomycin	76
Table 5.11: The difference in median values of <i>E.coli</i> treated with thiourea and Neomycin	78
Table 5.12: The difference in median values of <i>S.typhi</i> treated with thiourea and Neomycin	79
Table 5.13: The difference in median values of <i>S.sonnei</i> treated with thiourea and Neomycin	80

Table 5.14: The difference in median values of <i>P.aeruginosa</i> treated with Cobalt and Neomycin	81
Table 5.15: The difference in median values of <i>S.enterica</i> treated with thiourea and Neomycin	82
Table 5.16: The difference in median values of <i>A.niger</i> treated with Cobalt and Amphotericin B	83
Table 5.17: The difference in median values of <i>A.niger</i> treated with Urea and Amphotericin B	85
Table 5.18: The difference in median values of <i>A.niger</i> treated with Thiourea and Amphotericin B	86
Table 5.19: The difference in median values of <i>C.albicans</i> treated with Cobalt and Amphotericin B	87
Table 5.20: The difference in median values of <i>C.albicans</i> treated with Urea and Amphotericin B	88
Table 5.21: The difference in median values of <i>C.albicans</i> treated with Thiourea and Amphotericin B	89

LIST OF ABBREVIATIONS

<i>A.niger</i>	<i>Aspergillus niger</i>
<i>C.albicans</i>	<i>Candida albicans</i>
Co	Cobalt
<i>E.coli</i>	<i>Escherichia coli</i>
FTIR	Fourier Transform Infrared Spectroscopy
MHA	Mueller Hinton Agar
MHB	Mueller Hinton Broth
MIC	Minimal Inhibitory Concentration
NP	Nanoparticles
<i>P.aeruginosa</i>	<i>Pseudomonas aeruginosa</i>
PL	Photoluminescence spectroscopy
<i>S.enterica</i>	<i>Salmonella enterica</i>
<i>S.sonnei</i>	<i>Shigella sonnei</i>
<i>S.typhi</i>	<i>Salmonella typhi</i>
SD	Standard deviation
SEM	Scanning electron microscopy
TEM	Transmission electron microscopy
TGA	Thermogravimetric analysis
UV-Vis	Ultraviolet-visible spectroscopy
VUT	Vaal University of Technology
WHO	World Health Organization

CHAPTER 1

INTRODUCTION

This chapter provides a general overview of the study. It commences with the background to the study, followed by the statement of the research problem, research aim, specific objectives and purpose and significance of the study.

1. BACKGROUND

Water is our number one resource and plays a vital role in all living objects (Crane & Scott 2012). Water has a positive impact on different aspects of human life including, but not limited to health, food, energy and economy (Amin *et al.*, 2014). The ever-increasing populations all over the world put a strain on the supply of fresh water. Therefore, reliable and sustainable access to clean, safe and affordable water is considered to be one of the most essential resource for human beings (Marcelles *et al.*, 2009).

According to Sharma & Sharma, (2013), in the next two decades the average supply of water per person will drop by one third, possibly condemning millions of people to severe dehydration and unavoidable premature death. Access to clean water is a big challenge both in developing and developed countries (Ayanda & Petrik 2014). Clean water shortage is further compounded by microbial, wastewater contaminations and severe weather changes leading to water-borne diseases (Sadiq & Rodriguez 2004).

According to Nassar (2013), the traditional and old water treatment processes are not able to address the removal of toxic chemicals, organic materials and microorganisms present in raw water. Treatment technologies like activated carbon, oxidation, reverse osmosis (RO) membranes and activated sludge are also not becoming increasingly efficient to care for complex and intricate polluted water consisting of pharmaceuticals, surfactants, various industrial additives, and abundant toxic chemicals (Nassar 2013).

Highly efficient wastewater treatments are essential for improving the water quality of rivers, lakes and oceans and increasing the extremely small proportion of usable water. Above all, energy-intensive, complex wastewater treatment calls for energy-efficient, environmentally friendly methods and systems. Currently, nanotechnology offers potential advantages like low

cost, reuse and highly efficient way of removing and recovering microbial and wastewater pollutants (Ayanda & Petrik 2014). The World Health Organization (2015) defines nanotechnology as the manipulation of matter with at-least one dimension sized from 1 to 100 nanometres. Research in nanotechnology promises breakthroughs and exciting applications in areas such as medicine, data storage, food industry, molecular biotechnology, computing, defence, robotics, textiles, environment, sanitation (Pankaj *et al.* 2012) and desalination of water (Diallo *et al.* 2005).

Nanotechnology is revolutionizing many fields of applications and has great potential to change the traditional water supply and wastewater treatment model (Qu *et al.* 2013). The multifunctional and highly efficient processes of nanotechnology are providing possible affordable solutions to wastewater treatments that do not require large infrastructures or centralized systems (Qu *et al.* 2013). Various nano materials like carbon nanotubes (CNTs), nanomembranes, zeolites and dendrimers are being studied and are useful in the advanced water systems care (Crane & Scott 2012). There are many aspects of nanotechnology that are yet to be studied and employed to address the multiple problems of water quality.

The unique properties of nanomaterials can enable novel technologies for contaminant removal, microbial control, sensing and monitoring and resources recovery (Qu *et al.* 2013). The super high surface area, high reactivity and catalytic properties of nanomaterials greatly enhance the kinetics and efficiency of various chemicals and physicochemical processes. These processes are essential in water and wastewater treatment and therefore reduce system size as well as chemical and energy consumption (Prachi *et al.* 2013). These unique features have the potential to enable the pattern shift towards distributed wastewater treatment and water supply, a much-needed change in large metropolitan areas facing challenges of rapid population growth and aging infrastructure (Pendergast & Hoek 2011).

According to Dhermendra *et al.* (2008), dendrimers, metal – containing nanoparticles, zeolites and carbonaceous nanomaterial are the main four classes of nanoscale materials that are being evaluated as functional materials for water purification. These classes have a broad range of physicochemical properties that make them particularly attractive as separation and reactive media for water purification.

Nanoparticles are expected to play a crucial role in water purification (Tchobanoglous *et al.* 2014). The possible application of nanotechnology for the removal of toxic pollutants such as the pharmaceutical and personal care products, polycyclic aromatic hydrocarbons, polychlorinated biphenyls, phthalates, furans and dioxins, agrochemicals and pesticides, volatile organic compounds, viruses and bacteria, dyes, inorganic pollutants have been widely reported by several investigators such as (Nassar 2013; Lens *et al.* 2013; Sharma & Sharma 2013; Olushola & Leslie 2014) in the field of nanotechnology. The principal way nanotechnologies might help in removing water problems is by solving the technical challenges associated with water contaminants including bacteria, viruses, toxic metals, pesticides and salts (Kanchi 2014). Dhermendra *et al.* (2008) reported that bacterial death is caused by considerable changes induced by the nanomaterial on the integrity of the cell membranes. Interestingly, results by other authors in the field have shown that environmental nanotechnology could be effectively utilized for the removal of organic and inorganic contaminants from sewage, municipal, industrial and process of wastewater for safer use (Lens *et al.* 2013).

The potential impact of nanomaterials on human health and the environment is unclear. The environmental fate and toxicity of a material are critical issues in materials selection and design for water purification. There is no doubt that nanotechnology is better than other techniques used in water treatment, but today the knowledge about the environmental fate, transport and toxicity of nanomaterial is still in its infancy (Lens *et al.*, 2013).

Several studies claim that nanotechnologies offer a more affordable, effective, efficient and durable way of water purification using less toxic methods (Obare & Meyer 2004, Pankaj *et al.* 2012, Diallo *et al.* 2005, Dhermendra *et al.* 2008). There are many aspects of nanotechnology to address the multiple problems of water quality in order to ensure the environmental stability. Further research is therefore required to intensively study the use of advanced nanotechnology in water purification for safe human consumption. The purpose of this study is to assess the antimicrobial activity of doped cobalt nanoparticles against selected microbes that are found in wastewater.

2. RATIONALE AND MOTIVATION

Water contains different contaminants at different locations. Nanotechnology may potentially provide a variety of options to “tailor-make” solutions to filter out contaminants such as heavy metals and biological toxins, including waterborne disease-causing pathogens, as well as organic and inorganic solutes (Amin *et al.* 2014). Nanotechnology provides a platform for offering affordable and safe drinking water by providing relatively inexpensive water purification systems and the rapid and low-cost detection of impurities (Salman *et al.* 2014). The unique characteristic; such as high surface area can be used efficiently for removing toxic metal ions, diseases causing microbes, organic and inorganic solutes from water (Prachi *et al.* 2013). Although nanoparticles are a relatively cheap and effective antibacterial agent in drinking water treatment, it is important to develop products that do not leach nanoparticles into the final purified product, since this poses additional public health concerns (Prachi *et al.* 2013). The antimicrobial activities of doped cobalt, Co/urea and Co/thiourea nanoparticles against microorganisms commonly found in wastewater needs investigated to find new ways to address the challenge of water contamination and wastewater treatment.

3. PROBLEM STATEMENT

Conventional wastewater treatment methods involve biosorption, and aerobic and anaerobic treatment methods which are probably of the most expensive approaches. Biological treatment systems such as activated sludge and biological trickling filters are unable to remove a wide range of emerging contaminants and most of these compounds remain soluble in the effluent (Funk *et al.* 2015). Chlorination, though providing residual protection against regrowth of bacteria and pathogens, results in undesirable tastes and odors in addition to the forming of different disinfection by products (DBPs) in potable drinking water (Saliby *et al.* 2013). Ozonation has been considered to be a less attractive alternative due to high costs and short lifetime (Funk *et al.* 2015). Both ultraviolet (UV) photolysis and ion exchange, though being advanced treatments, are not feasible alternatives for micro pollutants removal (Qu *et al.* 2013). Therefore, there is a need to develop a better water treatment technology to address these setbacks in water treatment (Saliby *et al.* 2013).

Membrane processes like microfiltration, ultrafiltration, nanofiltration, and reverse osmosis, which are pressure-driven filtration processes, are considered as some new highly effective processes (Walha *et al.* 2007). These are considered as alternative methods of removing huge

amounts of organic micro pollutants (Bodzek *et al.* 2004). Water or wastewater treatment by membrane techniques is cost-effective and technically feasible and can be better alternatives for the traditional treatment systems since their high efficiency in removal of pollutants meets the high environmental standards (Yoon *et al.* 2006). Nanofiltration and reverse osmosis have proved to be quite effective filtration technologies for removal of micro pollutants (Yoon *et al.*, 2006). Reverse osmosis is relatively more effective than nanofiltration but higher energy consumption in reverse osmosis makes it less attractive than nanofiltration where removal of pollutants is caused by different mechanisms including convection, diffusion (sieving), and charge effects (Braeken *et al.* 2006). Although nanofiltration based membrane processes are quite effective in removing huge loads of micro pollutants, advanced materials and treatment methods are required to treat newly emerging micro pollutants (Bolong *et al.* 2009).

Recent studies have shown that water purification processes that have functional properties such as high efficiency, low time and low cost are very important (Qu *et al.* 2013). The application of nanotechnology to the purification and treatment of wastewater pollutants is gaining popularity worldwide. Studies reveal the potential of resolving the current problems involving water quality and quantity by using nanotechnology (Obare & Meyer 2004, Bottero *et al.* 2006).

Since the water industry must meet the demands to produce drinking water of high quality, there is a clear need for the development of cost-effective and stable materials and methods to address the challenges of providing fresh water in adequate amounts. There is a need for inventions of new water treatment methods. However, they need to be stable, economical, and more effective as compared with the already existing techniques. To meet the aforementioned demands, traditional treatment technologies have to be updated, modified or replaced by efficient, cost-effective, and reliable methods. Thus, this study seeks to develop new methods of water treatment using an advanced nanotechnology.

4. RESEARCH AIM

The main goal of this study is to assess antimicrobial activity of doped cobalt, Co/urea and Co/thiourea nanoparticles against bacteria and fungi (yeast and mould) commonly found in wastewater.

5. RESEARCH OBJECTIVES

Despite advances in disinfection technology, outbreaks from waterborne infections are on the rise, thus requiring new innovations of preventing these outbreaks.

The objectives of this research are therefore to:

- 5.1 To synthesize cobalt nanoparticles using a chemical reduction method.
- 5.2 To synthesize complexes of cobalt with thiourea using a template method.
- 5.3 To synthesize complexes of cobalt with urea using a direct solid-state reaction method.
- 5.4 To characterize the nanoparticles using Transmission Electron Microscopy (TEM), Scanning Electron Microscopy (SEM), Fourier Transform Infrared (FT-IR) Spectroscopy, X-ray diffraction (XRD) and Thermogravimetric Analysis (TGA).
- 5.5 To detect heavy metals in the nanoparticles.
- 5.6 To test antimicrobial activity of nanoparticles against bacteria and fungi (yeast and mould) using well agar diffusion and minimum inhibitory concentration methods.

6. SIGNIFICANCE OF THE STUDY

Since water contamination is a public health concern, contaminants can be more effectively removed even at low concentrations. Contaminants that were previously impossible to remove could be easily removed.

Nanotechnology could radically reduce the number of steps, materials and energy needed to purify water. This will make water purification processes easier to implement in rural areas and associated communities.

7. STRUCTURE OF THE DISSERTATION

This study is divided into following five chapters:

Chapter 1: This chapter is based on the research proposal and explains what the study intended to achieve. It describes the following in detail: the background to the problem, the purpose of the study, as well as the objectives.

Chapter 2: This chapter reviews literature from different settings that is relevant to this study.

Chapter 3: This chapter provides the research design and methods, as well as the materials used, the analytical techniques and the instrumentation used.

Chapter 4 & 5: This chapter provides the results of the findings.

Chapter 6: This chapter provides the discussion of the findings.

Chapter 7: This chapter includes conclusion, recommendations and limitations of the study.

8. CONCLUSIONS

This chapter briefly discussed the study background to the problem, problem statement, purpose and significance of the study. It was important to note that the chapter provided a clear message of the intention of this study and contributed to the shortage and pollution of water. Such insight requires enhancement. The researchers believe that an extensive review of the literature is a good starting point for enhancing such an understanding. It was therefore imperative to conduct a literature review on this subject, nanotechnology for waste water treatment. The next chapter is a review of the literature on the synthesis, characterization and antimicrobial activity of doped cobalt nanoparticles against selected microbes that are found in wastewater.

CHAPTER 2

LITERATURE REVIEW

2.1 INTRODUCTION

Literature review refers to a systematic process whereby a search is performed to determine the existing body of knowledge relating to the proposed topic under study (Anita *et al.* 2004). The purpose of a literature review is “to determine the extent to which the topic under study is covered in the existing body of knowledge” (Babbie & Mouton 2002). The literature review presented in this chapter focuses on the water shortage, water pollution, characterisations of the nanoparticles, antimicrobial activity and nanotechnology form a major part of this review.

2.2 WATER SHORTAGE

Water is the most vital substance in our life (Mara 2003). Clean drinking water is important for overall health and plays a substantial role in infant and child health and survival (Anderson *et al.* 2002; Fewtrell *et al.* 2005; Ross *et al.* 1988; Vidyasagar 2007). Approximately one-sixth of the world’s population lacks access to clean drinking water (Vorosmarty *et al.* 2010). According to World Health Organisation (2010), over 2.6 billion people lack access to clean water. The world is facing formidable challenges in meeting rising demands of clean water as the available supplies of freshwater are depleting due to extended droughts, population growth, more stringent health-based regulations and competing demands from a variety of users (Vorosmarty *et al.* 2010).

There is a limited possibility of an increase in the supply of fresh water due to competing demand of increasing populations throughout the world (Privette & Smink 2017). Water-related problems are expected to increase further due to climate changes and due to population growth over the next two decades (Hangchan 2011). Shortage of fresh water supply is also a result of the exploitation of water resources for domestic, industry and irrigation purposes in many parts of the world (Anneberg 2010).



Figure 2.1: Pictures of water scarcity

2.3 WATER POLLUTION AND CHALLENGES

Water pollution is the addition of any material to water that alters its chemical, physical or microbial composition to such an extent that it causes harm to man and other organisms (Chen & Zhang 2013). Pollution of surface or ground water sources is another cause of reduced fresh water supplies (Gao *et al.* 2012). Pollution of natural water is a problem for half of the world's population (Chen & Zhang 2013). Each year, it is estimated that about 4 billion people worldwide are expected to have no access to clean and sanitised water supply and millions of people die of severe water related diseases (Gao *et al.* 2012). These statistical figures are expected to grow in the near future as there is an increase in contamination by discharge of micro pollutants and contaminants into the natural water cycles (Zhang *et al.* 2011). The problem with water is expected to worsen in the coming decades, with water scarcity occurring globally, even in regions currently considered 'water-rich' (Zhang *et al.* 2011).

Water pollutants include toxic organic and inorganic chemicals, suspended solids and harmful microorganisms (Russo *et al.* 2015). Aquifers around the world are depleting and being polluted due to multiple problems of saltwater intrusion, soil erosion, inadequate sanitation, and contamination of ground or surface waters by detergents, fertilizers, pesticides, chemicals and heavy metals (Funk *et al.* 2015). Water contamination has implication for human health which arises when contaminated water by chemicals and micro-organisms are consumed (Russo *et al.* 2015). Most of these contaminations end up in natural water as a result of industrial, agricultural and domestic activities (Plaza *et al.* 2013).

In general terms, the greatest microbial risks are associated with ingestion of water that is contaminated with human or animal faeces. Wastewater discharges in fresh waters and costal seawaters are the major source of faecal microorganisms, including pathogens (Szylak-

Szydlowski *et al.* 2016). Carte & Howsam 1997, Fewtrell *et al.*, 2005 suggested that poor health related to water is a result of unclean drinking water and of inadequate sanitation.

Water-borne diseases caused by various bacteria, viruses, and protozoa have been the causes of many outbreaks (Craun *et al.* 2006). In developing countries water-borne diseases infect millions (Fenwick 2006). World Health Organization (WHO 2014) reported that, each year 3.4 million people, mostly children (1.4 million), die from water-related diseases. According to United Nations Children's Fund (UNICEF) assessment, 4000 children die each day as a result of contaminated water (UNICEF 2014). World Health Organization (WHO 2010) reports that over 2.6 billion people lack access to clean water, which is responsible for about 2.2 million deaths annually, of which 1.4 million are in children. Improving water quality can reduce the global disease burden by approximately 4% (WHO 2010).

Clasen *et al.* 2007 and World Health Organization (WHO 2010) have reported a global concern with the effects of unclean drinking water because water-borne diseases are a major cause of morbidity and mortality. The World Health Organization (2005) estimated that worldwide about 1.8 million people die from diarrheal diseases annually. Persons with compromised immune systems, such as those with AIDS, are especially vulnerable to water-borne infections, even those which are not typically threatening to healthy individuals (Kgalushi & Laurent 2005).

2.4 WASTEWATER AND CHALLENGES

Wastewater is any water that has been affected by human use. It is therefore a combination of domestic, commercial, agricultural or industrial activities. Wastewater can contain any physical, chemical and biological pollutants which are often discharged to a receiving water body like a river, lake or ocean (Tilley *et al.* 2016).

If the wastewater contains human feces, as is the case for sewage, then it may also contain pathogens of one of the four types:

- Bacteria (for example *Salmonella*, *Shigella*, *Campylobacter*, *Vibrio cholerae*),
- Viruses (for example hepatitis A, rotavirus, enterovirus),
- Protozoa (*e.g.* *Entamoeba histolytica*, *Giardia lamblia*, *Cryptosporidium parvum*) and

- Parasites (*e.g.* *Ascaris* (roundworm), *Ancylostoma* (hookworm), *Trichus* (whipworm) (WHO 2006; Anderson *et al.* 2016).

At a global level, around 80% of wastewater produced is discharged into the environment untreated, causing widespread water pollution (World Water Assessment Programme 2017). This usually has serious impacts on the quality of an environment and on the health of people. The occurrence of new or emerging micro contaminants in polluted water or wastewater has rendered existing conventional water/wastewater treatment plants ineffective to meet the environmental standards (Crane & Scott 2012).

There are numerous processes that can be used to clean up wastewaters depending on the type and extent of contamination. A combination of these technologies can meet strict treatment standards and make sure that the processed water is hygienically safe, meaning free from bacteria and viruses (WHO 2006).

Wastewater can be treated in wastewater treatment plants which include physical, chemical and biological treatment processes. Treated wastewater can be reused in industry, in artificial recharge of aquifers, in agriculture and in the rehabilitation of natural ecosystems. In rarer cases it is also used to augment drinking water supplies. Nanotechnology is fast gaining popularity in the purification and treatment of wastewater pollutants (Obare & Meyer. 2004). Studies reveal the potential of resolving the current problems involving water quality and quantity by using nanotechnology (Bottero *et al.*, 2006).

2.5 NANOPARTICLES

Nanotechnology is being developed at several levels: materials, devices and systems (Salata 2004). Nanoparticles are less than a few 100 nm. This reduction in size brings about significant changes in their physical properties with respect to those observed in bulk materials. They can be metallic, mineral, polymer-based or a combination of materials (Rana & Kalaichelvan, 2013). Most of these changes are related to the appearance of quantum effects as the size decreases, and are the origin of phenomena such as the super Para magnetism, Coulomb blockade, surface plasmon resonance, *etc.* The increase in the surface area to volume ratio is also a consequence of the reduction in size. It leads to the appearance of surface effects related to the high number of surface atoms, as well as to a high specific area, which are important from a practical point of view (Salata 2004).

2.5.1 PROPERTIES OF NANOPARTICLES

Once the particle size is reduced below 100 nm, the solid particles begin to demonstrate unusual properties from the bulk material based on quantum mechanics (Bhusan 2007). The surface related properties and the quantum properties play a fundamental role in making the difference in the properties of the bulk material with that of the nanoparticles (Roduner 2006). They exhibit: size effects - Depending on the material used to produce nanoparticles, properties like solubility, transparency, color, absorption or emission wavelength, conductivity, melting point and catalytic behavior are changed only by varying the particle size. Properties like dispersibility, conductivity, catalytic behavior and optical properties alter with different surface properties of the particle. If the surface properties are not controlled, nanoparticles quickly turn into larger particles due to agglomeration. Most of the size dependent effects are then lost. For the application of nanoparticles, it is therefore crucial to control their agglomeration behavior (Born *et al.*, 2006).

2.5.2. Structural properties

The large specific surface area of the nanoparticles is an important property related to reactivity, solubility, sintering performance *etc.* and is also related with the mass and heat transfer between the particles and their surroundings. Furthermore, the crystal structure of the particles may change with the particle size in the nanosized range in many cases. This is attributed to the compressive force exerted on the particles as a result of the surface tension of the particle itself. The critical particle size of the crystal structure and the size effect differ with the materials (Grosset *et al.*, 2016).

2.6. APPLICATION OF NANOPARTICLES IN WASTEWATER

The application of nanotechnology to the purification and treatment of wastewater pollutants is gaining popularity worldwide. Researchers have shown that semiconductors and metallic nanoparticles can be used as photocatalysts for water treatment (Bora & Dutta 2014).

Nanotechnology is still in the discovery phase of new materials that are being synthesized for specific applications. Typically, during this phase of development, researchers focus mainly on identifying new properties and applications. As a result, the examination of any unintended properties of the material or concerns about the efficiencies of the material is often deferred. Most of the semiconductors and metallic nanoparticles used as photocatalysts in the water treatment are physiologically toxic and non-biodegradable. But to keep the pace with extremely

rapid growth in nanotechnology in the field of remediation of water pollutants, there is the need to develop very efficient but environmentally friendly nanomaterials such as bio composites for water treatment (Brar *et al.*, 2010).

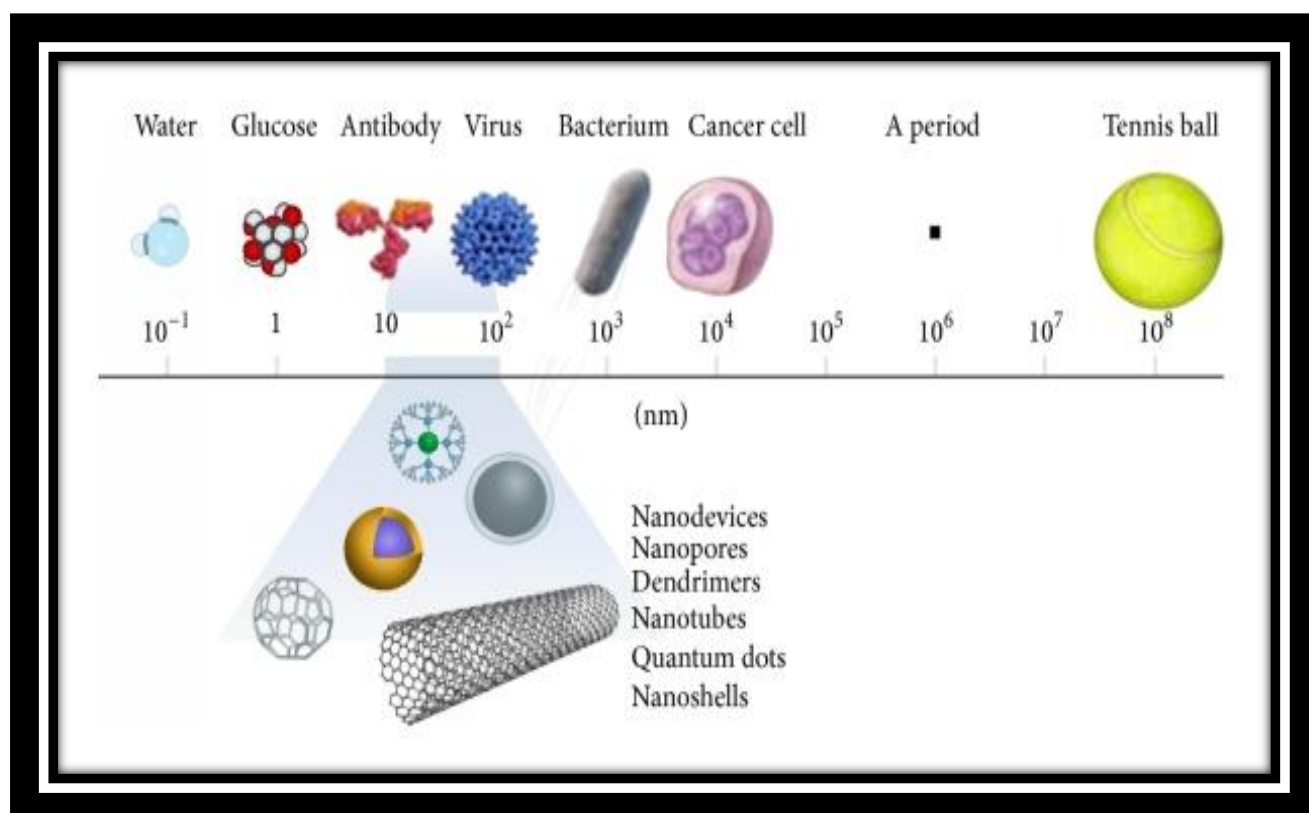


Figure 2.2: A size comparison of nanoparticles with other larger-sized materials (Amin *et al.* 2014)

At this scale, materials possess novel and significantly changed physical, chemical and biological properties mainly due to their structure, higher surface area to volume ratio offering treatment and remediation, sensing and detection and pollution prevention (Brar *et al.*, 2010). These unique properties of nanomaterials, for example high reactivity and strong adsorption are explored for application in water/waste treatment based on their functions in unit operations as highlighted in Table 2.1.

Table 2.1: Applications of nanoparticles in wastewater treatment (Amin *et al.* 2014)

Applications	Examples of nanomaterials	Novel properties
Adsorption	CNTs/ nanoscale metal oxide and nanofibers.	High specific surface area and assessable adsorption sites, selective and more adsorption sites, short intraparticle diffusion distance, tuneable surface chemistry, easy reuse, and so forth
Disinfection	Nano silver/titanium dioxide (Ag/TiO ₂) and CNTs.	Strong antimicrobial activity, low toxicity and cost, high chemical stability ease of use.
Photocatalysis	Nano-TiO ₂ and Fullerene derivatives.	Photocatalytic activity in solar spectrum, low human toxicity, high stability and selectivity and low cost.
Membranes	Nano-Ag/TiO ₂ /Zeolites/Magnetite and CNTs.	Strong antimicrobial activity, hydrophilicity low toxicity to humans, high mechanical and chemical stability, high permeability and selectivity, photocatalytic activity.

Nanoparticles can penetrate deeper and thus can treat wastewater which is generally not possible by conventional technologies. The higher surface area-to-volume ratio of nanomaterials enhances the reactivity with environmental contaminants (Theron *et al.* 2010).

In the context of treatment and remediation, nanotechnology has potential to provide both water quality and quantity in the long run through the use of, for example, membranes enabling water

reuse and desalination (Theron *et al.* 2010). In addition, it yields low-cost and real-time measurements through the development of continuous monitoring devices (Bora & Dutta 2014).

Nanoparticles, having high absorption, interaction and reaction capabilities can behave as colloid by mixing with aqueous suspensions and they can also display quantum size effects. Energy conversation leading to cost savings is possible due to their small sizes. However, overall usage cost of the technology should be compared with other techniques in the market (Khan *et al.* 2016).

Nanomaterials have effectively contributed to the development of more efficient and cost-effective water filtration processes since membrane technology is considered as one of the advanced wastewater treatment processes (Li *et al.*, 2011). Nanomaterials have been frequently used in the manufacturing of membranes, allowing permeability control and fouling-resistance in various structures and relevant functionalities. Both polymeric and inorganic membranes are manufactured by either assembling nanoparticles into porous membranes or blending processes. The example of nanomaterials used in this formation include, for example metal oxide nanoparticles like TiO₂. Carbon nanotubes have resulted in desired outputs of improved permeability, inactivation of bacteria (Das *et al.* 2012).

Finally, nano fibrous media have also been used to improve the filtration systems due to their high permeability and small pore size properties. They are synthesized by a new and efficient fabrication process, namely electrospinning and may exhibit different properties depending on the selected polymers. In short, the development of different nanomaterials like nano sorbents, nano catalysts, zeolites, dendrimers, and nanostructured catalytic membranes has made it possible to disinfect-disease causing microbes, removing toxic metals and organic and inorganic solutes from waste water (Elmi *et al.* 2014).

2.8 COBALT NANOPARTICLES

Cobalt is considered to be the first catalyst made from nonprecious metal with properties closely matching those of platinum. Cobalt also serves as a model system for the macroscopic magnetic response, because the low to moderate crystal anisotropy allows the effects of size, shape, internal crystal structure and surface anisotropy to be observed in a single system. The low crystal anisotropy of cobalt also promotes its study as a model system for the effects of size, shape, crystal structure and surface anisotropy on their macroscopic magnetic response (Sun & Murray, 1999).

A variety of methods for the preparation of magnetic colloid dispersions have been reported. Cobalt is one of the most important ferromagnetic metals due to its three metastable phases with different crystallographic structures, namely the hexagonal closed packed (hcp) phase, the face centred cubic (fcc) phase and the epsilon phase (Gabriella *et al.*, 2015).

Because of the difference in crystal structure, variations in physical and magnetic properties between the two polymorphs arise. HCP-Co is slightly denser than FCC-Co, even though both phases are close-packed structures. HCP-Co is also magnetically harder than the FCC phase due to its magnetic anisotropy and high coercivity as compared to the symmetrical and low coercivity FCC phase. Thus, the highly anisotropic HCP-Co is more desirable for magnetic recording and other permanent magnet applications (Gabriella *et al.*, 2015).

2.9 Cobalt/Urea nanoparticles

The rich coordination chemistry of transition metals has led to the design and development of novel ligands with unique structures and functional characteristics. Currently, significant efforts are being directed towards the design of specific ligand architecture in synthetic and applied chemistry (Zhang *et al.* 2013). One such area is the study of the coordination chemistry of the transition metals, such as zinc, cadmium, mercury, cobalt and lead in attempt to design specific ligands that can selectively bind these metals. Recently, the coordination chemistry of cobalt and cadmium (II) has received increased attention mainly due to their significance and impact on the environment and human body. In fact, the toxic effect of cadmium (II) is associated with its competition with cobalt for a variety of important binding sites in cells such as gene regulation (Hu *et al.* 2016).

Urea may be prepared in the laboratory by the interaction of ammonia with carbonyl chloride, alkyl carbonates, chloroformates or urethans. Industrially, urea is prepared by allowing liquid carbon dioxide and liquid ammonia to interact and heating the formed ammonium carbamate at 130-150°C under about 35 atmospheric pressure. The carbamate is decomposed to form urea and water according to the following reaction;



Urea is also extensively used in the paper industry to soften cellulose and has been used to promote healing in infected wounds and many other applications in the field of medicine (Karak & Bhattacharyya 2011)

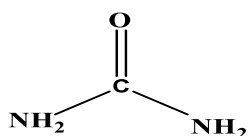


Figure 2.3: Structure of urea.

Crystal structure studies have shown that in solid urea, both nitrogen atoms are identical. Bond length measurements in urea give the C-N distance as 1.37 Å, while, in aliphatic amines the C-N bond length is 1.47 Å. This indicates that the C-N bond in urea has some double bond character (about 28%) (Hu *et al.* 2016).

Complexes of urea with some metal ions are used as fertilizers. Complexes of urea with zinc sulphate and nitrate, $(\text{Zn}(\text{CON}_2\text{H}_4)_6)\text{SO}_4 \cdot \text{H}_2\text{O}$ and $(\text{Zn}(\text{CON}_2\text{H}_4)_4)(\text{NO}_3)_2 \cdot 2\text{H}_2\text{O}$ have very important application in this field. These complexes were found to increase the yield of rice more than a dry mixture of urea zinc salt does. Calcium nitrate-urea complex, $(\text{Ca}(\text{urea})_4)(\text{NO}_3)_2$, was used also as an adduct fertilizer. For example, metal-urea complexes have a pharmaceutical application that the platinum-urea complex was recorded a significant effect as an antitumor agent (Zhang *et al.* 2013).

Urea plays a big role in the dried particles by preventing the interconnection between precipitated particles. With further heating by flame, urea decomposed and primary particles disintegrated producing nanoparticles (Terashi *et al.*, 2008).

In the study of Flame-assisted spray pyrolysis (FASP), Urea was used to produce BaTiO₃ nanoparticles with relatively high tetragonality and controlled sizes from 23 to 33 nm in one-step process. The addition of urea into the precursor was the key factor for the formation of tetragonal BaTiO₃ nanoparticles; the lack of urea addition led to the formation of submicrometric BaTiO₃ (Terashi *et al.*, 2008).

2.10 Cobalt/Thiourea nanoparticles

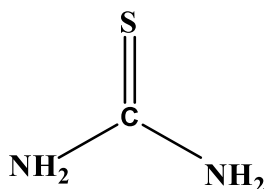


Figure 2.4: Structure of thiourea

Thiourea is a white crystalline solid. It is soluble in water, soluble in polar protic and aprotic organic solvents and insoluble in non-polar solvents. It is analysed mainly by high performance liquid chromatography (HPLC) with subsequent ultraviolet (UV) detection. Based on thiourea use pattern, the hydrosphere is expected to be its main environmental target compartment. Measured concentrations of the chemical in surface waters are not available (Binzet *et al.* 2013).

Thiourea will be biodegraded by an adapted microflora only after extended acclimation periods. Thus, under conditions not favouring biotic or abiotic removal, thiourea may be present in surface waters and sediment particles, however, is not to be expected as indicated by soil to groundwater seems possible, particularly under conditions unfavourable for biotic degradation (Karak & Bhattacharyya 2011).

Thiourea is an antioxidant. After oral administration to humans and animals, it is almost completely absorbed and is excreted largely unchanged via kidneys (Binzet *et al.* 2013). Thiourea in the synthesis of nanoparticles it is used as a precursors and stabilizing agents (Jianxi *et al.* 2003).

2.11 CHARACTERIZATION TECHNIQUES

2.11.1 INTRODUCTION

It is very important to understand the properties and applications of the characterization of materials. The technical application of nanoparticles mainly depends on their surface. It is therefore crucial to the chemist to control the surface and thus the properties of single particles. However, the qualitative and quantitative analysis of the surface of a single nanoparticle ensemble is challenging (Born *et al.* 2006). The techniques that are adopted to characterize the nanoparticles are: UV-Visible Spectroscopy (UV), Photoluminescence spectroscopy (PL), Fourier-transform infrared spectroscopy (FT-IR), Scanning electron microscopy (SEM), Transmission electron microscopy (TEM), Nuclear magnetic resonance (NMR) and Thermogravimetric analysis (TGA).

2.11.2. UV-Vis Spectroscopy

UV-Vis spectroscopy is determined through exciting electrons from the ground to excited states (absorption) and relaxing from the excited to ground states (emission). It deals with the study of electronic transitions between orbitals or bands of atoms, ions or molecules in gaseous,

liquid and solid state (Lili & Youshi, 2007). Small metallic nanoparticles are proven to have the property for absorption and scattering electromagnetic radiation. The absorption of electromagnetic radiation by metallic nanoparticles originates from the coherent oscillation of the valence band electrons induced by an interaction with the electromagnetic field (Guo *et al.*, 2004). These resonances are known as surface plasmons, which occur only in the case of nanoparticles and not in the case of bulk metallic particles (Lili & Youshi, 2007). Hence, UV-Vis spectroscopy can be utilized to study the unique optical properties of nanoparticles (Niara *et al.*, 2015).

2.11.3 Photoluminescence Spectroscopy

It is a contactless, non-destructive method to probe the electronic structure of materials. The intensity and spectral content of the emitted photoluminescence is a direct measure of various important material properties, including band gap determination, impurity levels and defect detection and recombination mechanisms (Lili & Youshi, 2007). Light is directed onto a sample, where it is absorbed and imparts excess energy into the material in a process called photo-excitation. Photo-excitation causes electrons within a material to move into permissible excited states. These electrons return to their equilibrium states, by a radiative process or by a non-radiative process. The quantity of the emitted light is related to the relative contribution of the radiative process (Niara *et al.*, 2015).

2.11.4 Fourier-transform Infrared spectroscopy (FT-IR)

The vibrational technique involved is the interactions of photons with species in a sample that results in energy transfer to or from the sample via vibrational excitation or de-excitation. These vibrational frequencies provide information about chemical bonds in the detecting samples. It deals with the vibration of chemical bonds in a molecule at various frequencies depending on the elements and types of bonds. After absorbing electromagnetic radiation, the frequency of vibration of a bond increases leading to transition between ground state and several excited states. These absorption frequencies represent excitations of vibrations of the chemical bonds and thus are specific to the type of bond and the group of atoms involved in the vibration. The energy corresponding to these frequencies correspond to the infrared region of the electromagnetic spectrum (Hari *et al.* 2005).

2.11.5 X-ray diffraction

X-ray diffraction has been used to determine the crystal structure of solids, including lattice constants and geometry, identification of unknown materials, orientation of single crystals, defects (Wang, 2000). The X-ray diffraction patterns are obtained by measurement of the angles at which an X-ray beam is diffracted by the crystalline phases in the specimen. Bragg's equation relates the distance between two hkl planes (d) and the angle of diffraction (2θ) as: $n\lambda = 2d\sin\theta$, where, λ = wavelength of X-rays, n = an integer known as the order of reflection (h , k and l represent Miller indices of the respective planes) (Bragg and Bragg, 1949). From the diffraction patterns, the uniqueness of nanocrystal structure, phase purity, degree of crystallinity and unit cell parameters of the nanocrystalline materials can be determined. X-ray diffraction technique is non-destructive and does not require elaborate sample preparation, which partly explains the wide use of XRD methods in material characterization. X-ray diffraction broadening analysis has been widely used to determine the crystal size of nanoscale materials. The average size of the nanoparticles can be estimated using the Debye-Scherrer equation: $D = k\lambda / \beta\cos\theta$ where D = thickness of the nanocrystal, k is a constant, λ = wavelength of X-rays, β = width at half maxima of (111) reflection at Bragg's angle 2θ (Saini *et al.* 2013).

2.11.6 Transmission electron microscopy (TEM)

Electron microscopes are scientific instruments that use a beam of energetic electrons to examine objects on a very fine scale. The transmission electron microscope (TEM) was the first type of electron microscope to be developed and is patterned exactly on the light transmission microscope except that a focused beam of electrons is used instead of light to "see through" sample. It was developed by Max Knoll and Ernst Ruska in Germany in 1931. Transmission electron microscopy is typically used for high resolution imaging of thin films of a solid sample for nano structural and compositional analysis. The topographic information obtained by TEM in the vicinity of atomic resolution can be utilized for structural characterization and identification of various phases of nanomaterial (Wang *et al.* 2013). The technique involves: (i) irradiation of a very thin sample by a high-energy electron beam, which is diffracted by the lattices of a crystalline or semi-crystalline material and propagated along different directions, (ii) imaging and angular distribution analysis of the forward-scattered electrons (unlike SEM where backscattered electrons are detected), and (iii) energy analysis of the emitted X-rays (Li *et al.* 2014).

2.11.7 Scanning Electron Microscope (SEM)

It is a very useful imaging technique that utilised a beam of electrons to acquire high magnification images of samples. The SEM maps reflect electrons and allows imaging of thick (~ mm) samples. SEM images are formed by scanning a beam across the sample and forming the image point-by-point. The SEM is an instrument that produces a largely magnified image by using electrons instead of light to form an image. A beam of electrons is produced at the top of the microscope by an electron gun. The electron beam follows a vertical path through the microscope, which is held within a vacuum. The beam travels through electromagnetic fields and lenses, which focus the beam down toward the sample. Once the beam hits the sample, electrons and X-rays ejected from the sample. Detectors collect these X-rays, backscattered electrons and secondary electrons and convert them into a signal that is sent to a screen similar to a television screen (Michler & Balta-Calleja 2012). This produces the final image.

2.11.8 Thermogravimetric analysis

Thermogravimetric analysis (TGA) is conducted on an instrument referred to as a thermogravimetric analyzer. A thermogravimetric analyzer continuously measures mass while the temperature of a sample is changed over time. Mass, temperature, and time in thermogravimetric analysis are considered base measurements while many additional measures may be derived from these three base measurements (Janet & Szafert 2017).

Thermal analysis is an appropriate methodology to assess a wide range of properties of substances. Many of them associated with a particular technique. Whereby, the identification is made the physical and chemical stability is checked, changes of phase are detected and fundamental kinetic studies are performed (Bruce *et al.* 2008).

2.12 Antibacterial activity

Determining the effectiveness of a nanoparticle as an antibacterial agent requires experimental techniques that measure bacteria viability after exposure. While numerous techniques have been developed to determine the antibacterial activity of nanoparticles, many of them are flawed in their own way. As a result, multiple techniques are often used in a single study to compare and confirm antibacterial results. Furthermore, Gram-positive and Gram-negative bacteria may respond to antibacterial nanoparticles differently and also assay differently. Therefore, studies often include both Gram-positive and Gram-negative species in a variety of assays to determine antibiotic efficacy. Due to the importance of developing novel antibacterial

treatments, bacteria plating is a technique that can be used to evaluate bacterial susceptibility to nanoparticles (Ricco & Assadian 2011).

2.13 Microbial routes for nanoparticles synthesis

Many studies show that microorganisms, both unicellular and multicellular have the ability to synthesize inorganic materials. The biological synthesis can be considered a bottom-up approach where nanoparticle formation occurs due to the reduction/ oxidation of metallic ions via biomolecules such as enzymes, sugars, and proteins secreted by the microorganism (Prabhu & Poullose 2012). However, a complete understanding of nanoparticle synthesis mechanism occurring in microorganisms is yet to be developed. This is because each type of microorganism tends to behave and interact differently with particular metallic ions. The interaction and biochemical processing activities of a specific microorganism and the influence of environmental factors such as pH and temperature ultimately determine the formation of nanoparticles with a particular size and morphology (Makarov *et al.*, 2014). Nanoparticle formation can be either extracellular or intracellular depending on the microorganism (Wang *et al.*, 2012).

2.14 Bacteria

Bacteria are the most common of the microbial pathogens found in wastewater. There are a wide range of bacterial pathogens and opportunistic pathogens which can be detected in wastewaters. Many of the bacterial pathogens are enteric, however, bacterial pathogens which cause non-enteric illnesses such as *Legionella* spp, *Mycobacterium* spp., and *Leptospira* have also been detected in wastewaters (Dhillon *et al.*, 2012).

Gastrointestinal infections are among the most common diseases caused by bacterial pathogens in wastewater. Acute microbial diarrheal diseases are a major public health problem in developing countries. People affected by diarrheal diseases are those with the lowest financial resources and poorest hygienic facilities. Children under five, primarily in Asian and African countries, are the most affected by microbial diseases transmitted through water (Muirhead & Monaghan 2012).

Water-borne bacterial infections *Vibrio cholerae* causing cholera and salmonellosis caused by a number of *Salmonella* species, and dysentery, caused by various *Shigella* species as well as some *Salmonella* species. Dysentery – like infections have also recently been found to be

caused by a disease caused by *Salmonella* spp, has been traced food stuffs irrigated with wastewater (Kumar *et al.* 2013).

The contamination of food by water containing known toxin producing organisms such as *Shigella sonnei*, *Salmonella* spp, *E. coli* or *Clostridium perfringens* can cause outbreaks of food poisoning (Muirhead & Monaghan 2012).

As well as the established pathogens, a number of opportunistic pathogens can be found in untreated and treated wastewaters. These opportunistic pathogens include *Pseudomonas*, *Streptococcus* and *Aeromonas* species (Oikonomou *et al.* 2012). These opportunistic pathogens can be commonly isolated from a wide range of environmental water samples including wastewaters. They are often members of natural microbial populations and, at times, can be major members of these populations (Seil & Webster, 2012). Many opportunistic pathogens, being members of the natural microbial population, have the ability to rapidly increase in number when given sufficient nutrients. As wastewaters often have high nutrient loads, high numbers of these opportunistic pathogens can be present, increasing the risk of infections occurring from them (Oikonomou *et al.* 2012).

2.14.1 *Escherichia coli*

Escherichia coli (*E. coli*) is a Gram negative, rod shaped bacteria that lives in the lower guts of warm blooded ruminant animals and humans. The normal strains of *E.coli* that inhabit the guts of these animals are beneficial. But some strains of *E. coli* such as the infamous O157:H7 strain are very dangerous. If water or food containing this strain of *E. coli* is ingested, serious illness and death can occur (Gaffield *et al.* 2003).

E. coli is unique in that it can survive outside the body of its host for an extended period, making it an excellent choice as an indicator organism for the presence of animal waste in the environment. A water source becomes contaminated with *E. coli* when animal waste makes its way into the water.

2.14.2 *Pseudomonas aeruginosa*

Pseudomonas aeruginosa is a common Gram-negative, rod-shaped bacterium that can cause disease in humans. It is a multidrug resistant associated with serious illnesses such as pneumonia and sepsis (Poole 2004). It is an opportunistic pathogen affecting the immune-compromised but can also infect the immune-competent as in hot tub folliculitis (Balcht & Smith 1994).

Pseudomonads are a large group of free-living bacteria that live primarily in soil, seawater, and fresh water. Pseudomonads are highly versatile and can adapt to a wide range of habitats and can even grow in distilled water. This adaptability accounts for their constant presence in the environment (Poole 2004). They are responsible for food spoilage and degradation of petroleum products and materials. In normal healthy humans, they are responsible for eye and skin diseases (Botzenhart and Doring 1993). They also cause serious life-threatening illnesses in burn and surgical patients and in immune-compromised individuals (Bodey et al. 1983).

P. aeruginosa is also known for contaminations recreational waters and tap water associated with outbreaks; however, the relative role water plays in the transmission of this bacterium to humans is still unclear (Hollyoak *et al*, 1995).

According to Hardalo and Edberg (1997), the range of infections caused by *P. aeruginosa* is narrow and related to specific changes in the defense and immune status of the host. They claim (multiple times) that the bacterium does not attack normal tissue. In many cases, this is true. However, *P. aeruginosa* is a well-established cause of ear and/or skin infections in healthy non-compromised hosts. It may be argued that extended water-to-skin contact damages tissue by removing fatty acids, oils, and keratin layers. This type of damage is unavoidable, as are minor tiny scratches caused by the wearing of contact lenses which can predispose a person to infection. The type of infections caused by *P. aeruginosa* is actually quite large, and this bacterium is a leading cause of illness in compromised hosts

2.14.3 *Salmonella typhi*

Salmonella typhi is a Gram-negative bacterium also known as *Salmonella enterica* serotype, growing in the intestine and blood (CDC 2013). Typhoid is spread by eating or drinking food or water contaminated with the faeces of an infected person (WHO 2008). Humans are the only known carriers of the bacteria. An asymptomatic human carrier is an individual who is still excreting *S. typhi* in their stool a year after the acute stage of the infection. Human carriers are responsible for the transmission of the bacteria in endemic regions of the world (Eng *et al*; 2015).

Multiple drug resistant (MDR) *Salmonella* strains, represent an increased hazard for human health and that may contribute to the dissemination of drug resistances are also detected in surface water in developed countries. Surface runoff was shown to play a main role as driver of *Salmonella* load in surface waters (Crump *et al*. 2016). Accordingly, analysis of serovars

indicated a mixed human and animal origin of *Salmonella* contribution to surface waters, emphasizing the role of wild animals in water contamination. Data relating to *Salmonella* prevalence in surface and drinking water in developing countries are quite rare. Nevertheless, data on water-borne outbreaks as well as case control studies investigating the risk factors for endemic typhoid fever confirmed the relevance of water as source for the transmission of this disease. In addition, epidemiological studies and *Salmonella* surveys, consistently provided an undeniable evidence of the relevance of MDR *Salmonella typhi* strains in water-borne typhoid fever in developing countries (Levantesi *et al.* 2012).

2.14.4 *Salmonella enterica*

Salmonella is one of the leading causes of intestinal illness all over the world as well as the etiological agent of more severe systemic diseases such as typhoid and paratyphoid fevers. While water is known to be a common vehicle for the transmission of typhoidal *Salmonella* serovars, non-typhoidal salmonellae are mainly known as foodborne pathogens (Levantis *et al.* 2012).

Salmonella enterica is a genus of rod-shaped (bacillus) Gram-negative bacteria of the family Enterobacteriaceae. The two species of *Salmonella* are *Salmonella enterica* and *Salmonella bongori*. *S. enterica* is the type species and is further divided into six subspecies that include over 2,600 serotypes (Gal-Mor *et al.* 2014).

Salmonella enterica is a non-spore-forming, predominantly motile enterobacteria with cell diameters between about 0.7 and 1.5 µm, lengths from 2 to 5 µm, and peritrichous flagella (Fàbrega & Vila 2013). It is also a facultative aerobe, capable of generating ATP with oxygen ("aerobically") when it is available, or when oxygen is not available, using other electron acceptors or fermentation ("anaerobically"). *Salmonella enterica* subspecies are found worldwide in all warm-blooded animals and in the environment.

Salmonella species are intracellular pathogens (Jantsch *et al.* 2011); certain serotypes can cause food-borne infection and illness. *S. enterica* serotypes can be transferred from animal-to-human and from human-to-human. They usually invade only the gastrointestinal tract and cause salmonellosis (Ryan & Ray 2004).

2.14.5 *Shigella sonnei*

Shigella sonnei (S. sonnei) is a species of shigella. Together with *Shigella flexneri*, it is responsible for 90% of Shigellosis cases (Jain *et al.* 2005). Shigellosis is one of the most contagious types of diarrhea caused by bacteria *Shigella sonnei*. It is a Gram-negative, rod-shaped, nonmotile, nonspore-forming bacterium (Holt *et al.* 2012).

Shigellae are transmitted by the direct faecal-oral route. As a consequence, food has the potential to be contaminated through the soiled fingers of patients or carriers. The transfer of shigellae by flies breeding on faeces has been established as a very important transmission route during some outbreaks. *Shigella sonnei* can be found in surface waters and also within contaminated drinking water (Steven *et al.* 2014).

2.15 Mould

Biosynthesis of nanoparticles utilizing fungi is widespread among many research groups globally and the synthesis occurs at both extracellular and intracellular locations. For example, fungi such as *Aspergillus niger*, has been frequently reported for their biosynthetic ability to create both Ag and Au nanoparticles (Gade *et al.* 2008). Moreover, studies have shown that fungi are capable of producing mono dispersed nanoparticles and particle sizes over a wide range of different chemical compositions. Fungi possess some additional attributes when compared to their bacterial counterparts for the synthesis of metallic nanoparticles. For instance, fungi secrete large amounts of proteins and enzymes per unit of biomass, which results in larger amounts of nanoparticles being, manufactured (Narayan & Sakthivel 2010). Studies have shown that some fungi possess high intracellular metal uptake volume and the synthesized particles tend to be small in size (Mukherjee *et al.* 2002). However, the culture conditions can have a significant influence during the biosynthesis of metallic nanoparticles. For example, the biological reduction of Au ions was carried out using *Trichothecium* spp. Biomass under stationary conditions synthesized extracellular nanoparticles. In contrast, agitation of the biomass tended to produce intracellular nanoparticles (Wang *et al.* 2012). Fluorescence spectra have shown that extracellular synthesis of nanoparticles by the fungi results from the action of bioactive reducing agents secreted from the cell wall and it produces protein-stabilized nanoparticles. The study was able to show that the same proteins released by the fungal biomass were present in the solution and also bound to the surfaces of nanoparticles (Hulkoti & Taranath 2014). Both extracellular and intracellular synthesis of nanoparticles using fungi has been investigated. In the case of intracellular synthesis, extraction procedures

in downstream processing suffer from the drawback of low yields. In contrast, extracellular synthesis produces nanoparticles at the cell surface or at the periphery of the cell, which means they can be readily recovered in downstream processing (Dhillon *et al.* 2012 & Kathiresan *et al.* 2009). A very notable feature of some fungi is their ability to synthesize nanoparticles of different chemical compositions.

2.16 Yeasts

Yeasts, like many other microorganisms, have the ability to absorb and accumulate significant amounts of toxic metals from their surrounding environment (Mandal *et al.* 2006). *Candida albicans* is the common pathogenic species because it expresses higher levels of putative virulence factors compared to other *Candida* species. It is known to cause superficial infections such as oral candidiasis as well as severe systematic infections. Antifungal drugs are available that can successfully treat candidiasis. However, it has been discovered that *C.albicans* is developing resistance to the drugs used currently; they have side effects and are costly. Therefore, there is compelling need for the development of a new antifungal drugs that can successfully treat many fungal infections including oral candidiasis with minimal effect on the host and available at a cheaper cost. (Sudha *et al.* 2013)

The genus *Candida* comprises about 200 yeast species, with *C.albicans* accounting for most of candidal infections. However, in recent times, the prevalence of other candidal species in the mouth such as *C. glabrata*, *C. tropicalis*, *C. krusei*, *C. dubliniensis* and *C. parapsilosis* appear to have been on the increase as pathogens. It has been reported that candidal species occur as commensals on the normal oral and oro-pharyngeal epithelium of up to 60% of immunocompetent, non-hospitalized subjects who are free of clinically detectable oral candidosis (Farah *et al.*, 2010). *C.albicans* exists in the mouth in three different morphological forms: the yeast cell, also termed blastopore or blastoconidium, the septate filamentous form termed the pseudohypha, and the non-septate filamentous form, the hypha. The yeast cell is commensal, avirulent, does not invade the oral epithelium, and in a healthy host, induces regulatory immune responses mediated by keratinocytes and epithelial immunocytes releasing into the local microenvironment a number of biological agents which induce protective immune responses, preventing the development of clinical infection (Feller *et al.* 2014).

The transition from the commensal yeast form to the potentially pathogenic filamentous forms occurs in response to local micro-environmental stress signals on a background of systemic and local predisposing factors This transition is associated with the production of virulence

factors that promote the adhesion of the fungus to the epithelium, colonization, proliferation, and then invasion of the oral epithelium with evasion of protective immune responses by the fungus (Prabhu & Poullose 2012).

The transition of *Candida* from a commensal to a pathogenic form causing clinical infection is associated to a great extent with any reduction in the inherent fitness of the immune system. To a lesser extent the transition is influenced by changes in the microenvironment in response to antibiotic treatment, xerostomia, malignancy, systemic chemotherapy, pregnancy, or diabetes with possible secondary reduction in the fitness of the immune system (Zhang *et al.* 2015).

To add to the complexity of the pathogenesis of oral candidosis, it is now evident that in the mouth, *Candida* usually resides in mixed fungal-bacterial biofilms encapsulated in, and protected by, a matrix of glycoproteins and polysaccharides. Within this biofilm, the bacterial-fungal interactions influence the morphogenetic status, virulence, proliferation and survival of *Candida*. Nutrient availability, saliva composition and flow dynamics, and the level of oral cleanliness are some of the local factors that determine the density, thickness and the biological properties of the mixed biofilm (Chauhan *et al.* 2013).

CHAPTER 3

RESEARCH DESIGN AND METHODOLOGY

This chapter outlines the research methodology, experimental techniques and instrumentation used by which the aim of this study was achieved. It also provides detailed information on the research materials and research procedure.

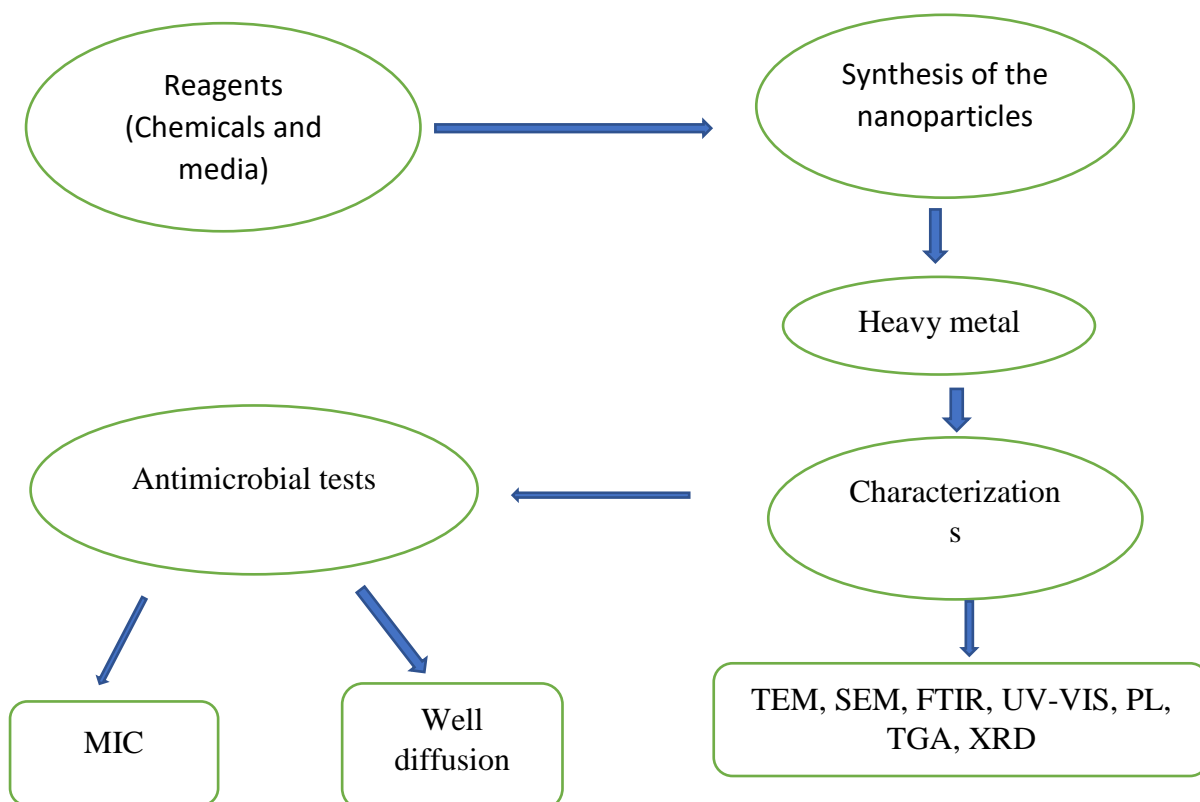


Figure 3.1: Research design

3.1 MATERIALS AND METHODS

Cobalt (II) chloride hexahydrate, cobalt (II) nitrate hexahydrate, benzil diethylenetriamine, Hydrazine monohydrate, Sodium citrate dehydrate, NaOH, H₂SO₄, Dimethylformamide, Urea, Thiourea and Sodium hydroxide were obtained from Sigma Aldrich and were used as purchased. Ether, acetone, methanol, ethanol and n-butanol (analytical grade) obtained from Sigma Aldrich were used without further purification and distilled water was also used as a solvent.

3.2 EXPERIMENTAL PROCEDURE

3.2.2 Synthesis of cobalt nanoparticles using Co-precipitation method.

The cobalt nanoparticles were synthesized without any capping agents by co-precipitation method. In this procedure 1:1, 1:2; 1:3 and 2:1 M ratio of $\text{Co}(\text{NO}_3)_2 \cdot 6\text{H}_2\text{O}$, and NaOH were dissolved in 20 ml distilled water under constant magnetic stirring. About 1.6 g NaOH solution was dropped in 148.48 g $\text{Co}(\text{NO}_3)_2 \cdot 6\text{H}_2\text{O}$ solution under constant stirring for 2 hours at room temperature. Then it was allowed to hold on overnight at room temperature. The cobalt hydroxide settles down and the excess solution found on top was discarded very carefully. The stock solution of precipitates was separated using a centrifuge and heated at 80°C for 5 hours. Finally, the black colour was obtained (Wadekar *et al.* 2017).

3.3 SYNTHESIS OF COBALT WITH UREA AND THIOUREA COMPLEXES

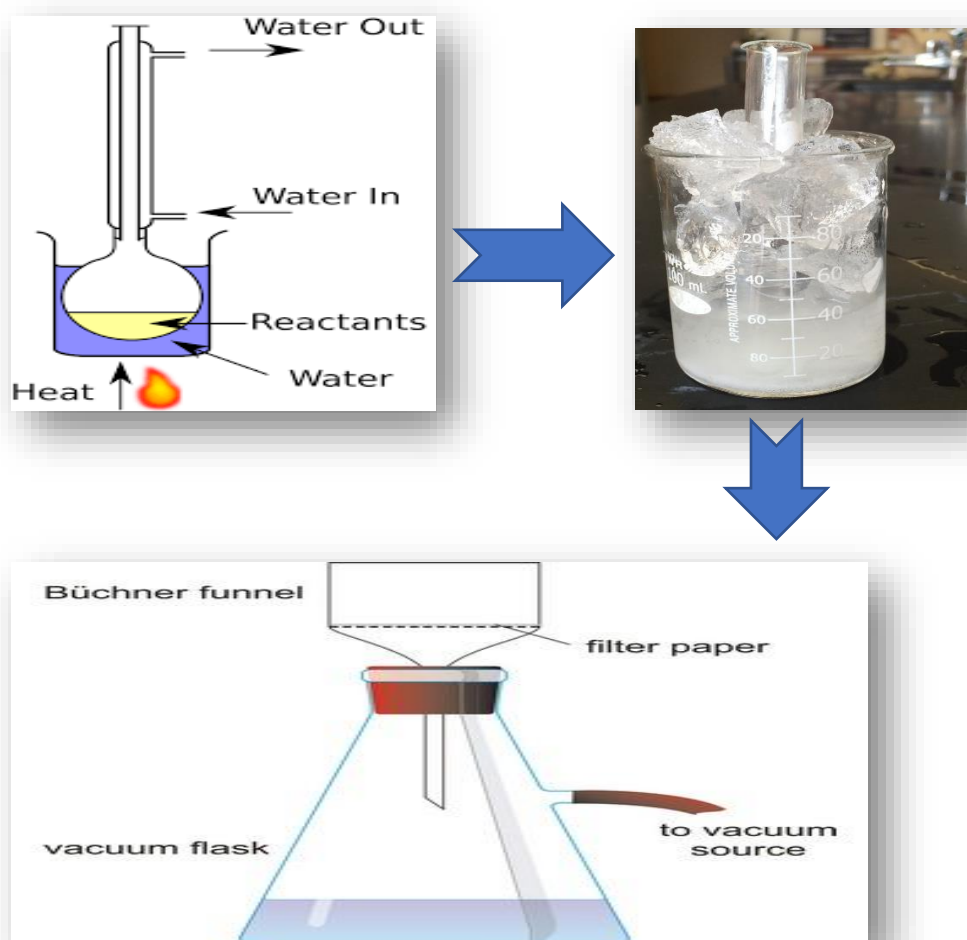


Figure 3.2: Schematic representation for the synthesis of cobalt doped nanoparticles

3.3.1 Complexes of thiourea with cobalt

$\text{CoCl}_2 \cdot 6\text{H}_2\text{O}$ (4.76 g) was dissolved in 30 mL n-butanol and 6.08 g of thiourea was added. The mixture was heated and refluxed for three hours on heating until complete dissolution of the entire solid was attained. The solution was cooled to room temperature and benzene was added until a slight permanent turbidity was produced. It was cooled in an ice chest and resulted in a blue solid precipitate. The precipitate was filtered and washed twice with ethanol and acetone under vacuum (Amutha *et al.* 2011).

3.3.2 Complexes of urea with Cobalt

The complexes of urea were prepared by mixing equal methanolic solutions of 4.76 g of $\text{Co}(\text{NO}_3)_2 \cdot 6\text{H}_2\text{O}$ in 25 mL of methanol with a 50 mL volume of 6.08 g of urea solution in methanol solvent. The mixture was stirred for about 12 hours under refluxed system at room temperature. The amount of the formed precipitate was increased during standing. The precipitate complex was filtered off and dried under vacuum (Omar, 2012).

3.4 CHARACTERIZATION TECHNIQUES

3.4.1 INTRODUCTION

The characterization of materials is important for understanding their properties and applications. This part describes experimental set ups utilized for various measurements towards the characterization of the synthesized nanoparticles. The techniques adopted to characterize the nanoparticles are: UV-Visible Spectroscopy, photoluminescence spectroscopy, Fourier transform infrared spectroscopy, Raman spectroscopy, scanning electron microscopy, transmission electron microscopy, nuclear magnetic resonance and X-ray diffraction.

3.4.2 UV-VISIBLE spectroscopy (UV-Vis)

The sample was prepared by dissolving the nanoparticles with distilled water to make a dilute sample solution and sonicated for 60 minutes. The UV-Vis was turned on to allow the lamps to warm up. A cuvette was filled with the distilled water and placed inside the spectrophotometer to read the blank results for the absorbance spectrum. This serves as blank control and helps account for light losses due to scattering or absorption by the solvent. The cuvette was rinsed twice with the diluted nanoparticles. The cuvette was filled quarter full (the cuvette should be clean of any fingerprints) and placed in the spectrophotometer in the correct direction and covered to prevent any ambient light. Absorbance spectrum was collected by

allowing the instrument to scan through different wavelengths to collect the absorbance (Nemade & Waghuley 2013).

3.4.3 Photoluminescence spectroscopy (PL)

The sample was prepared by dissolving the nanoparticles with distilled water to make a dilute sample solution and sonicated for 60 minutes. The UV-Vis was turned on to allow the lamps to warm up. A cuvette was filled with the distilled water and placed inside the spectrophotometer to read the blank results for the absorbance spectrum. This serves as blank control and helps account for light losses due to scattering or absorption by the solvent. The cuvette was rinsed twice with the diluted nanoparticles. The cuvette was filled quarter full (the cuvette should be clean of any fingerprints) and placed in the spectrophotometer in the correct direction and covered to prevent any ambient light. Absorbance spectrum was collected by allowing the instrument to scan through different wavelengths to collect the absorbance (Nemade & Waghuley 2013).

3.4.4 Transmission electron microscopy (TEM)

TEM images were recorded by JEOL JEM 1010 transmission electron microscope equipped with an AMT XR40 digital imaging camera at a magnification of 1000 x and a maximum accelerating voltage of 10 kV. Samples were dispersed in ethanol and it was ultrasonicated for 20 minutes. A drop of nanoparticles suspension was coated onto the copper grid, followed by negative staining with an aqueous solution of uranyl acetate at 1% (w/v). Particles diameter of approximately 300 randomly selected nanoparticles from different TEM micrographs was determined using the morphometry software image JV, 1.44 (Sun *et al.*, 2013).

3.4.5 Fourier transform infrared spectroscopy (FT-IR)

FT-IR absorption spectrum of nanoparticles was obtained from 16 scans at a resolution of 4 cm^{-1} in the region of 400-4000 cm^{-1} using a Bomem MB- 120 FT-IR spectrometer that is equipped with a potassium bromide beam splitter and a deuterated triglycine sulphate (DTGS) detector. To prepare the samples, a small quantity of freeze-dried nanoparticles was deposited on potassium bromide tablet surface prior to FT-IR analysis (Zhang *et al.*, 2015).

3.4.6 X-ray diffraction (XRD)

X-ray diffraction (XRD) patterns on powdered samples were carried out in the 2θ on a D8 diffractometer. Samples were placed in silicon zero background sample holder.

Measurements were taken using a glancing angle of incidence detector at an angle of 2° , for 2θ values over $20^\circ - 60^\circ$ in steps of 0.05° with a scan speed of $0.01^\circ 2\theta.s^{-1}$.

3.4.7 Scanning Electron Microscope (SEM)

The samples were prepared by placing a drop of diluted solution of sample in toluene onto a copper grid (Bao *et al.*, 2005). The samples were allowed to dry completely at room temperature. The HRTEM Joel JEM-2100 microscope was used to study the surface morphology of the sample operating at 200 kV (Plaza *et al.* 2013).

3.4.8 Thermogravimetric analysis (TGA)

The sample preparation for thermogravimetric analysis was done by weighing 10 mg of the complexes. These complexes were decomposed at temperature range of 50 to 930 °C. This analysis was performed on a Perkin Elmer Pyris 6 TGA under an inert atmosphere of dry nitrogen, and heating rate of 10 °C.Min-1.

3.5 HEAVY METALS

1.568 g of $\text{Pb}(\text{NO}_3)_2$ was dissolved into 100 ml of distilled water and diluted into 1 L of (1000 ml) of distilled water to make stock solution. A stock solution containing Pb^{2+} was prepared by dissolving a known quantity of lead nitrate ($\text{Pb}(\text{NO}_3)_2$) in deionized water. To 200ml of stock solution 0.15ml of 0.1M Nitric acid was added and heated in a glass evaporating dish on a water-bath until the volume is reduced to 20 ml. 2 ml of the concentrated solution complies with limit test A. The reference solution was prepared by using 10 ml of lead standard solution (1 ppm Pb) R and adding 0.075 ml of 0.1 M Nitric Acid. Blank solution was prepared by adding 0.0075 ml of 0.1 M Nitric acid.

To each solution, 2 ml of buffer solution pH 3.5 R. mix and added to 1.2 ml of thioacetamide reagent R. the solution was mixed immediately. The solution was examined after two minutes.

3.6 ANTIBACTERIAL ACTIVITY

3.6.1 Introduction

In this study the prepared nanoparticles were investigated against microorganisms which were purchased from Inqaba laboratory and preserved in the laboratory and used as references strains.

All the organisms that were used are tabled in Table 1.

Table 3.1: Organisms that were used for the antimicrobial studies

Bacteria	Mould	Yeasts
<i>Shigella sonnei</i>	<i>Aspergillus niger</i>	<i>Candida albicans</i>
<i>Salmonella typhi</i>		
<i>Salmonella enterica</i>		
<i>Escherichia coli</i>		
<i>Pseudomonas aeruginosa</i>		

3.6.2 Bacterial culture preparation

3.6.2.1 Preparation of the nanoparticles

About 0.2 g of each nanoparticles were weighed into a test tube (Urea, Thiourea & Cobalt) and diluted into 1 ml of distilled water to prepare 200 ppm of solution. The nanoparticles solution was sonicated for 45 minutes to disperse the particles. The test tubes were closed with the lid and wrapped with parafilm to avoid contamination and placed in the fridge (Okafor *et al.*, 2013)

3.6.2.2 Preparation of Mueller Hinton Broth (MHB)

MHB was used in serial dilutions of prepared nanoparticles. It was prepared by dissolving 21.0 g of MHB powder in 1 liter of distilled water, followed by heating it on a Bunsen burner. Sterilization of MHB at 121°C at 15 minutes was performed using an autoclave and it was then cooled in water bath for 45 minutes and stored at 4°C (Balouiri *et al.* 2015)

3.6.2.3 Mueller Hinton Agar (MHA)

About 38 g of MHA was dissolved in 1 liter of distilled water, mixed thoroughly and heated on a Bunsen burner and boiled for 1 minute to completely dissolve components. The MHA was autoclaved at 121°C for 15 minutes. The media was cooled at 45°C and poured into sterile petri dishes on a level, horizontal surface to give uniform depth. The agar was solidified at room temperature and stored at 4°C (Balouiri *et al.* 2015).

3.6.2.4 Preparation of bacteria cultures

A small amount of the bacterial strains from the culture was grown into the test tubes containing 9 ml of MHB. The test tube was covered with the lid and incubated overnight in an orbital shaker (150 rpm) at 37°C (Balouiri *et al.* 2015).

3.6.2.5 Preparation of resazurin dye

Resazurin dye was prepared at 0.015% by dissolving 0.015 g vortexed and filter sterilized and stored at 4°C for a maximum of two weeks after preparation (Mohammed *et al.* 2016).

3.6.2.6 Preparation of neomycin

About 0.10 g of neomycin was weighed and dissolved in 10ml of distilled water, dissolved completely and filter-sterilized. Stored kept at -20°C for a year after preparation (U.S. Pharmacopeia 35).

3.6.2.7 Serial dilution preparation and MIC determination

Minimum inhibitory concentration of the nanoparticles was determined using serial two-fold dilutions. The availability of bacterial cells was exposed to varying concentrations of the nanoparticles were analyzed in a 96 well microtiter plate using resazurin dye. Overnight cultures of the bacteria were diluted to approximately 10^6 CFU/ml. The nanoparticles were sonicated for forty minutes. About 100 µl of MH broth were dispensed in all the wells, followed by transferring 100 µl of the nanoparticles into wells 1 to 8, 100 µl of antibiotic (neomycin) was added to wells 9 and 10 as positive control. All the wells from 1 to 10 were diluted from one well to another (A to H) and with discarding the last amount, which gave us a serial dilution ranging from 2500 µl/ml to 1.22 µl/ml. After serial dilutions of the above-mentioned materials in each well, 100 µl of the bacterial strain was added to each well without exception according to McFarland theory to have a final concentration of about 1.0×10^6 bacteria /ml in each well. NP-free broth was used as negative control. After serial dilution of the above-mentioned materials in each well, 30 µl of resazurin dye was added to all the wells. The plates were then incubated aerobically at 37°C for the bacteria and at 42°C for yeast. After incubation, the plates were inspected for colour change. Resazurin dye indicates cell viability by changing from a blue/ non-fluorescent state to a pink/ highly fluorescent state upon chemical reduction resulting from aerobic respiration due to cell growth. The lowest concentration of nanoparticle suspension that inhibited cell growth (dye did not convert to red) was defined as the minimum inhibitory concentration. Each microorganism was tested in a different plate with duplicates of

each concentration of the nanoparticles. Two controls without nanoparticles were also included in each plate (Okafor *et al.*, 2013).

3.6.2.8 Well agar diffusion procedure

The MHA plate surface was inoculated by spreading a volume of the microbial inoculum over the entire agar surface. Then, a hole with a diameter of 6-8 mm was punched aseptically with a sterile tip and a volume (20 µl) of the antimicrobial agent and the nanoparticles with different concentrations were introduced into the well. The plates were then incubated at 37°C for 24 hours. The antibacterial activity was assayed by measuring the diameter of the inhibition zone formed around the wells. Amphotericin B was used as positive control and Mueller Hinton broth as negative control (Konate *et al.* 2012).

4.1 INTRODUCTION

In this chapter, all the characterization of the materials with the different techniques (UV-Vis, PL, FTIR, TEM, XRD, TGA and some metal analyses) were discussed.

4.2 UV-Visible spectroscopy

When a beam of light propagates through a sample which has the ability to interact with the electromagnetic radiation, part of the radiation is absorbed by the sample and the rest is transmitted through the sample. In UV-Visible spectroscopy, light is used to populate the unoccupied electronic states of the sample and transitions between the valence and conduction bands. The spectra were recorded in absorption mode and all samples were prepared by dissolving the nanoparticles in distilled water (Chandra & Kumar, 2012).

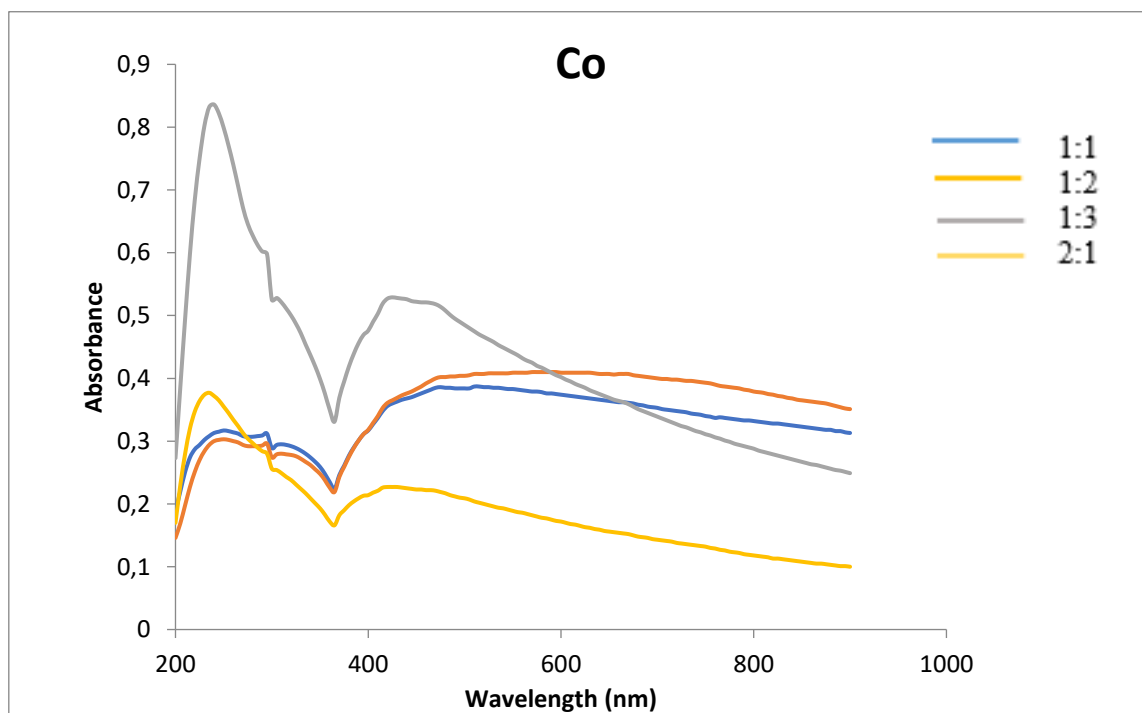


Figure 4.1: UV-Vis absorption spectrum of Co

Optical properties of cobalt in Figure 4.1 were recorded using UV- Vis spectroscopy observing a broad excitonic absorbance peak at 249 nm and 495 nm with a tail extending towards the longer wavelength as a results of quantum size effect. The broadening of excitonic absorption

band is because of the particle size. The particles 1:1, 1:2 and 2:1 showed the same peaks except 1:3 with excitonic peak. The absorption band gaps are blue shifted to a high energy compare with bulk cobalt. The blue shift phenomenon of the absorption edge has been described to a decrease in particle size. It is well known in case of semiconductors that the band gap between the valence and conduction band increases as the size of the particles decreases in the nano-scale range. The magnitude of the shift depends on the size of the semiconductors material (Bao *et al.*, 2005).

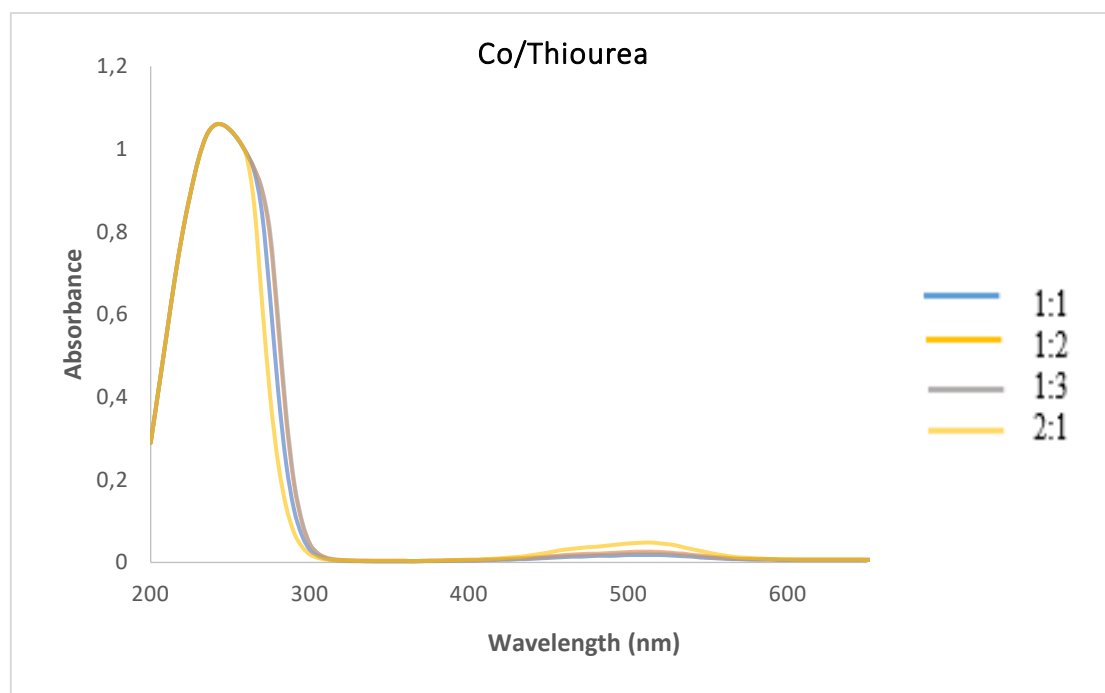


Figure 4.2: UV – Vis absorption spectrum of Cobalt/Thiourea

UV - Vis spectra of Cobalt thiourea complex Figure 4.2 depicts the UV spectra of ratio 1:1, 1:2, 1:3 and 2:1. It gave excitonic absorbance bands at 290 nm and 590 nm with a tail extending towards the longer wavelengths as a result of quantum size effects.

The absorption band gaps are blue shifted to a high energy compare to bulk cobalt with respect to reduced particle size of the material. The blue – shift in band-edge was further explained using the work reported by Jianxi and co-workers (2003). Jianxi *et al.*, (2003) discovered that not only the size of the nanoparticles has an influence on the band-gap but shape also plays an important role. Therefore, the blue-shifts in band-edge can be explained by the notion that the morphology (length and width of rods) of the particles has a great influence on the optical properties of the nanoparticles. With spherical particles, the diameter of the particle can be related to the optical properties of the particles, whereas with rod or wire-like particles, the

diameter does not account for the properties of the particles. Other reason accounting for the blue shift can be associated with the agglomeration of the particles due to ageing and external factors such as oxygen to penetrate into the pores of the particles (Wang *et al.*, 1991).

Transition state in CoS exists in several numbers. Gupta and co-workers proposed that the two maxima in absorbance are because of bulk state transition and surface transitions. The surface states include the localized states because of defect in bulk in addition to the surface states. The optical transition to and from the surface states will produce maxima at higher wavelengths (Gupta *et al.*, 2011).

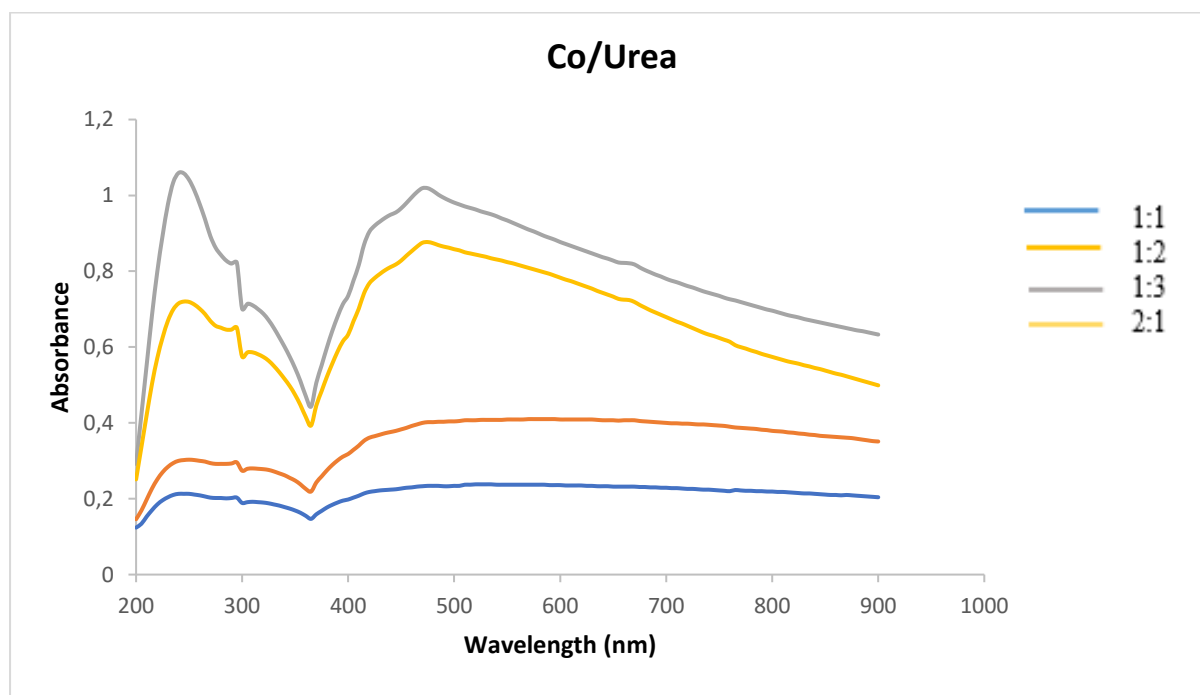


Figure 4.3: UV-Vis absorption spectrum of Co/Urea

UV-Vis spectrum of urea complex (Figure 4.3) showed absorption band edges at 290 nm and 495 nm respectively for ratio 1:1, 1:2, 1:3 and 2:1 ratios. Observation of absorption bands due to the electronic transition indicates that particles have a narrow size distribution as results of early stage formation of nanoparticles and indication of irregular shapes from lower concentration and more uniform shapes at a higher concentration (Jianxi *et al.*, 2003).

The phenomena can also be explained by means of absorption band in which at a low concentration is less visible and as the concentration is increased becomes more profound. The band edges are red-shifted from a low to high concentration due to increase in particles size. They are two types of emission usually gives sharp peaks near their band edges whereas trapped emission is always characterized by broad peaks with large Stokes shift (Gupta *et al.*, 2011).

4.3 Photoluminescence spectroscopy

Photoluminescence spectroscopy is a spontaneous emission of light from a material under optical excitation. The excitation energy and intensity are chosen to probe different regions and excitation concentrations in the sample.

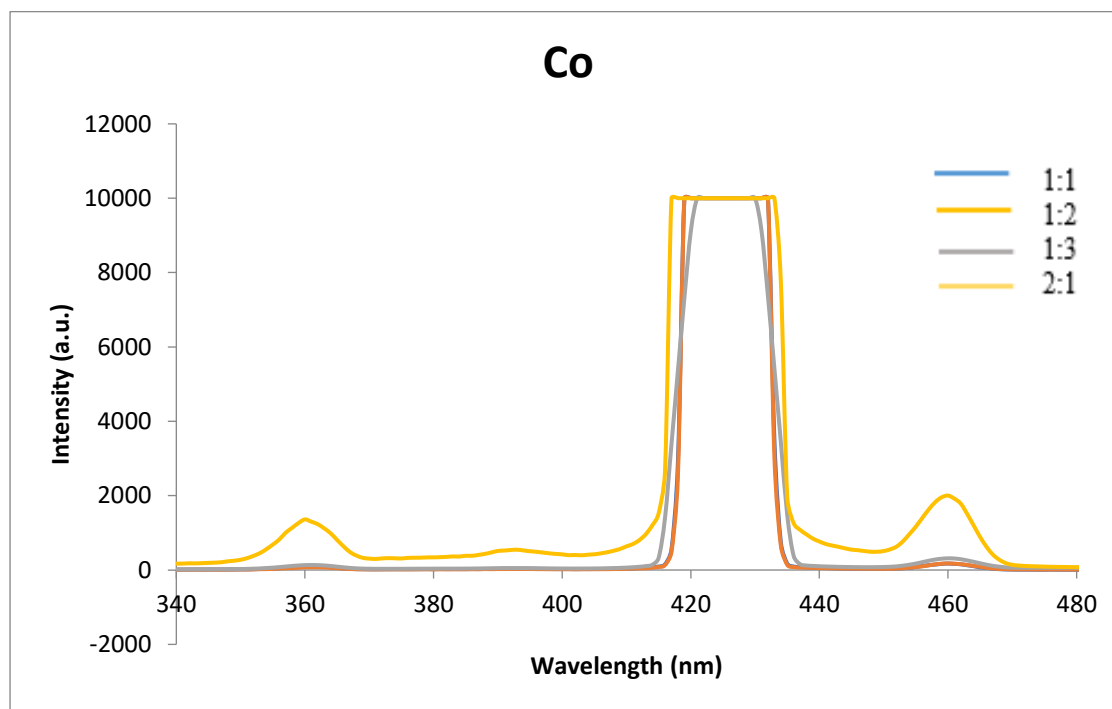


Figure 4.4: PL Cobalt graph

Figure 4.4; Red shift in emission maxima of cobalt to its absorption band edge as expected. The figure shows that emission spectra consist of broad band in range 415 – 435 nm, with two sharp peaks at 350 – 370 nm and 455 – 465 nm respectively, and a small peak at about 390 nm.

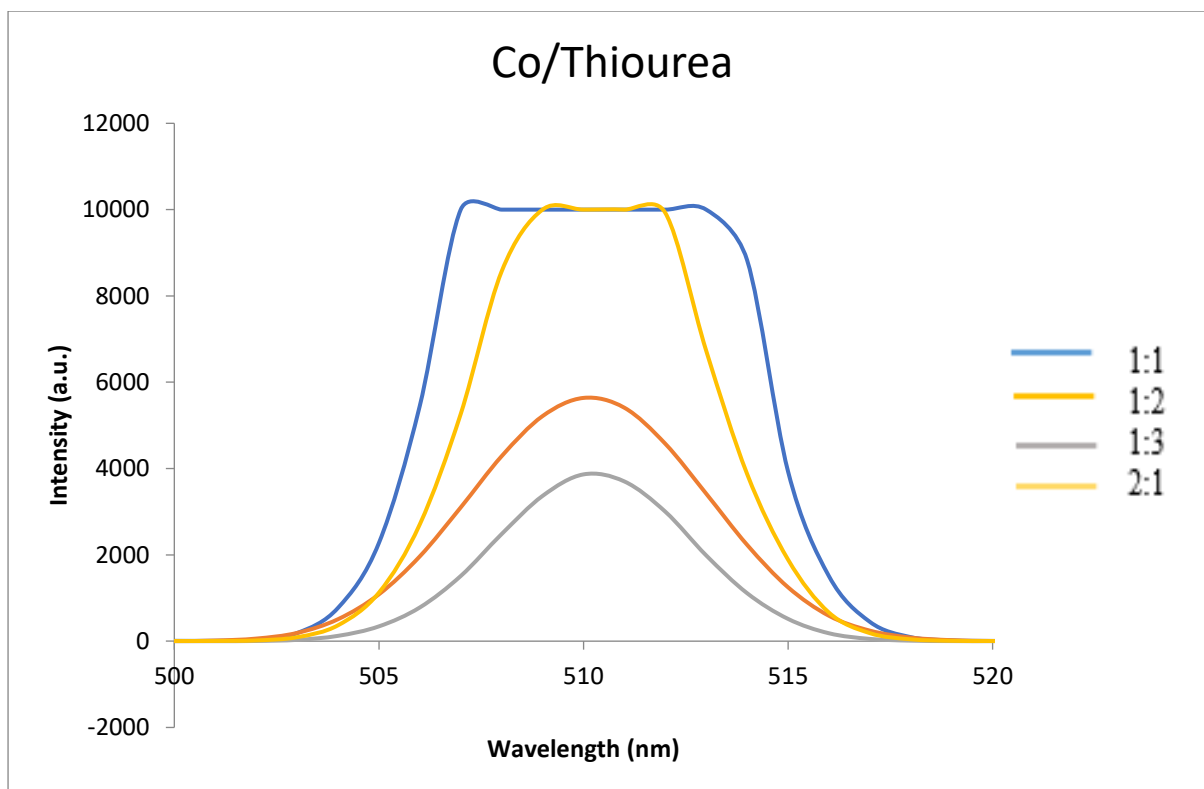


Figure 4.5: PL graph of Co/thiourea complex

Figure 4.5 Red shift from the respective band edges of the absorption spectra. The excitonic emission usually gives sharp peaks near their band edges. The narrowing of the peaks is observed as the monomer concentration is increased due to excitonic type of emission. Emission peak has a narrow shape, around 510 nm, which indicates the mono-dispersity and good passivation of the particles. Photoluminescence emission maxima of the samples were observed and are red shifted from their respective band edges of the absorption spectra (Wang *et al.*, 1991).

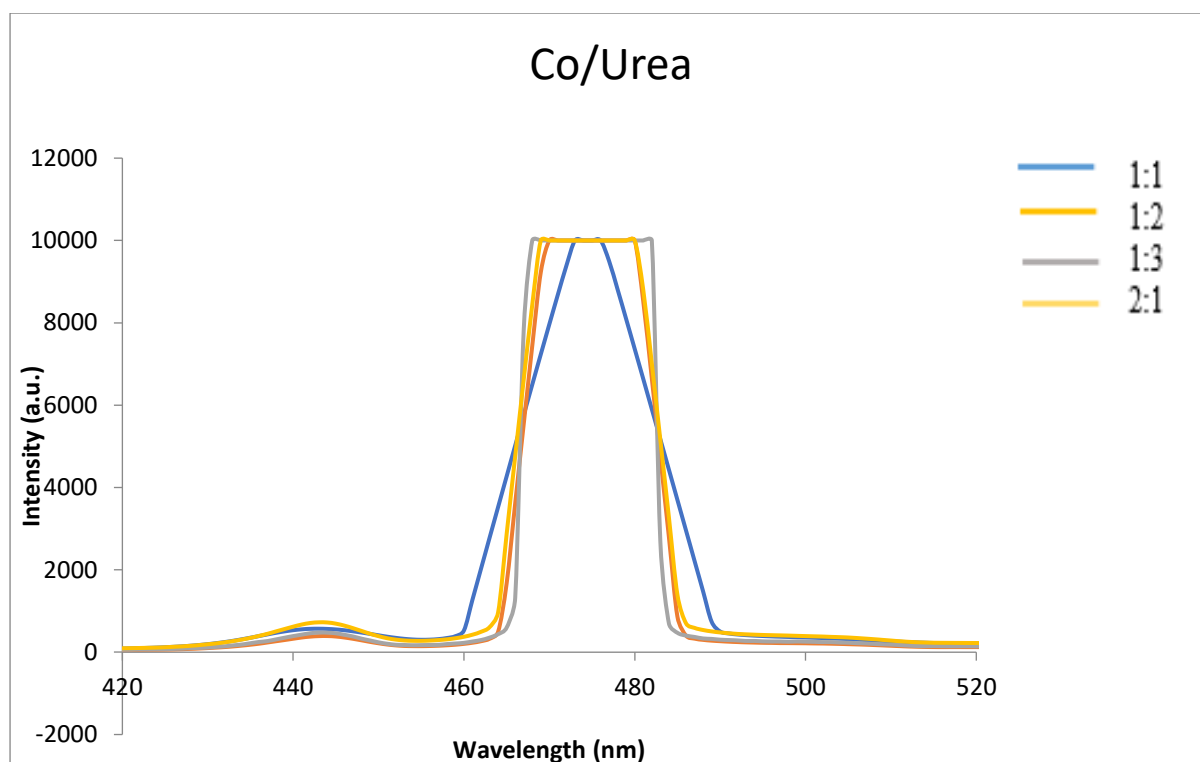


Figure 4.6: PL absorption spectrum of Co/urea

The PL spectrum of Co/urea complex, Figure 4.6, showed absorption band edges at 430 nm and 479 nm respectively for ratios 1:1, 1:2, 1:3 and 2:1. Observation of absorption band due electronic transition indicates that particles have narrow size distribution as results of early stage formation of nanoparticles and indication of irregular shapes from lower concentration and more uniform shapes at a higher concentration.

The narrowing of the peaks is observed as the monomer concentration is increased due to excitonic type of emission. These were caused by a faster growth as a result of increased concentration. The emission peaks for the sample prepared at low concentration have a broad shape which indicates the mono-dispersity and good passivation of the particles. However, for the nanoparticles prepared at high concentration, the emission is very narrow which indicate that the particles are poly-dispersed (Jianxi *et al.*, 2003).

4.4 FTIR SPECTRAL ANALYSIS

Thiourea, $(\text{CS}(\text{NH}_2)_2)_2$, has a large dipole moment and an ability to form extensive network of hydrogen bonds. A thermochemistry study with an emphasis on the fundamental measure of the total coordinate bond strength conducted by Moloto *et al.*, (2013) showed that thiourea has a low basicity and, in aqueous solution, forms complexes with metal ions which are of similar stability to that of the protonated ligand itself. The S-C-N bending modes for the Co complexes in all ratios observed at 1432 to 1453 cm^{-1} from the FTIR spectrum in Figure 4.7

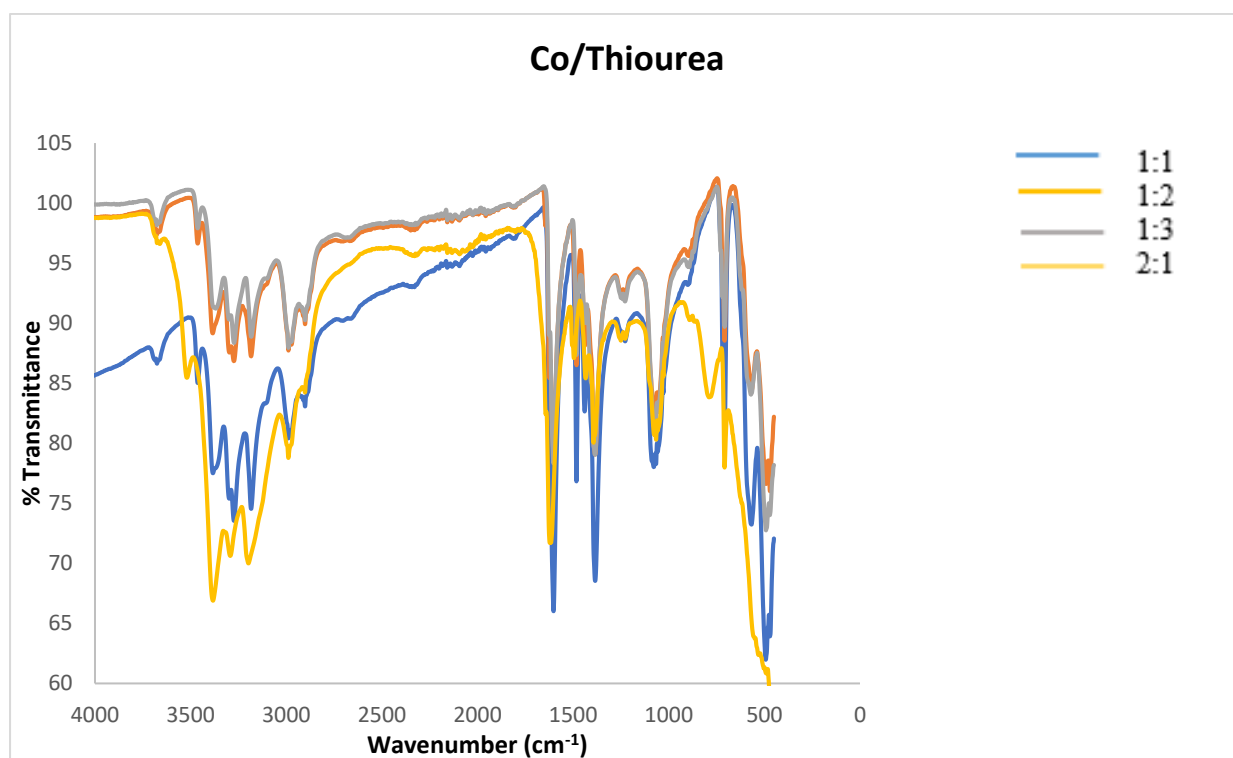


Figure 4.7: FTIR spectra Cobalt complexes with Thiourea

The spectrum showed a decrease in the frequency shifts to 1484 and 1487 cm^{-1} , respectively on coordination of the sulphur atom to the Co-metal. The N-H absorption bands are not shifted to the lower frequency which indicates that the nitrogen expected to bond Co is not present and the bonding must be between the sulphur and the Co-metal. These absorption bands includes: N-H stretching symmetric at 3189 cm^{-1} ; N-H stretching asymmetric at 3390 cm^{-1} ; and N-H rocking at 1099 cm^{-1} . Similarly from the N-C-N stretching mode at 1472 cm^{-1} there are no observable features of the Co-N bond but much enhanced sensitivity to coordination through sulphur. The free ligand show a band observed at 732 cm^{-1} , which is due to contribution of C-S stretching and has shifted to a lower frequency 721 cm^{-1} Co-thiourea. This signify a decrease

in the double bond character of the C=S which confirms the sulphur bonding of thiourea to cobalt (Moloto *et al.*, 2013).

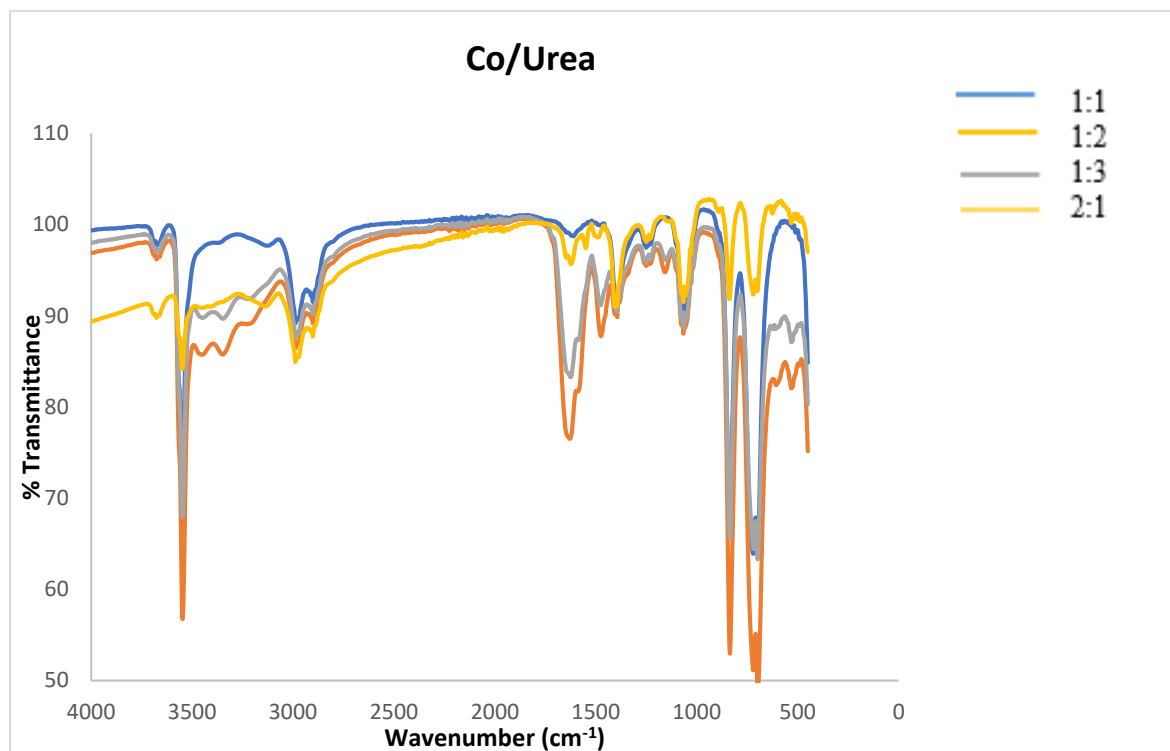


Figure 4.8: FTIR spectra of cobalt complexes with urea

The FTIR bands at 1632 cm^{-1} in the urea, $(\text{CO}(\text{NH}_2)_2)_2$, complex with Co with different ratios are assigned to C=O stretching vibration (Figure 4.8). All in plane vibration of NH_2 groups show small frequency shifts: N-H stretching asymmetric at 3493 cm^{-1} ; N-H bend symmetric 3190 cm^{-1} and N-H rocking at 1113 cm^{-1} . These may be due to the change in environment or consequence of the breaking of the coupling between NH_2 bending and OCN skeleton vibration. The C-N stretching band is seen at 1475 cm^{-1} (Chandra & Kumar, 2012).

4.5 Transmission Electron Microscopy

TEM is a very useful technique in characterizing the size and shape of the nanoparticles. Cobalt has been prepared at varied concentrations. The manner in which the reagents attaches itself to the Co metal could have influence on the other surrounding particles, thus affecting the mode of arrangement of the particles. The Co particles are in a mixture of rod and spherical and some percentages of bipodal, tripodal and tetrapodal morphologies as seen in Figure 4.9.

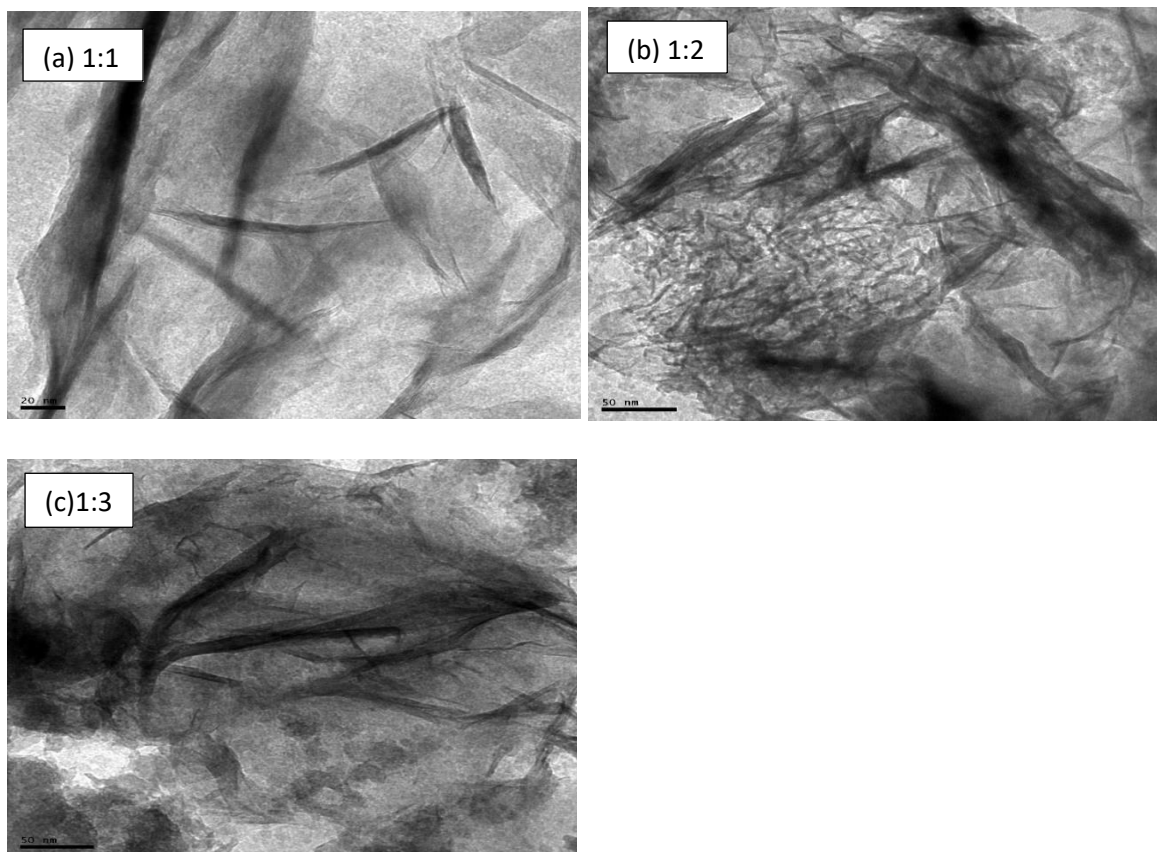


Figure 4.9: TEM image for Cobalt nanoparticles

The images showed particles from ratio 1:1, 1:2 and 1:3 to be agglomerated and it was difficult to measure the size of the particles.

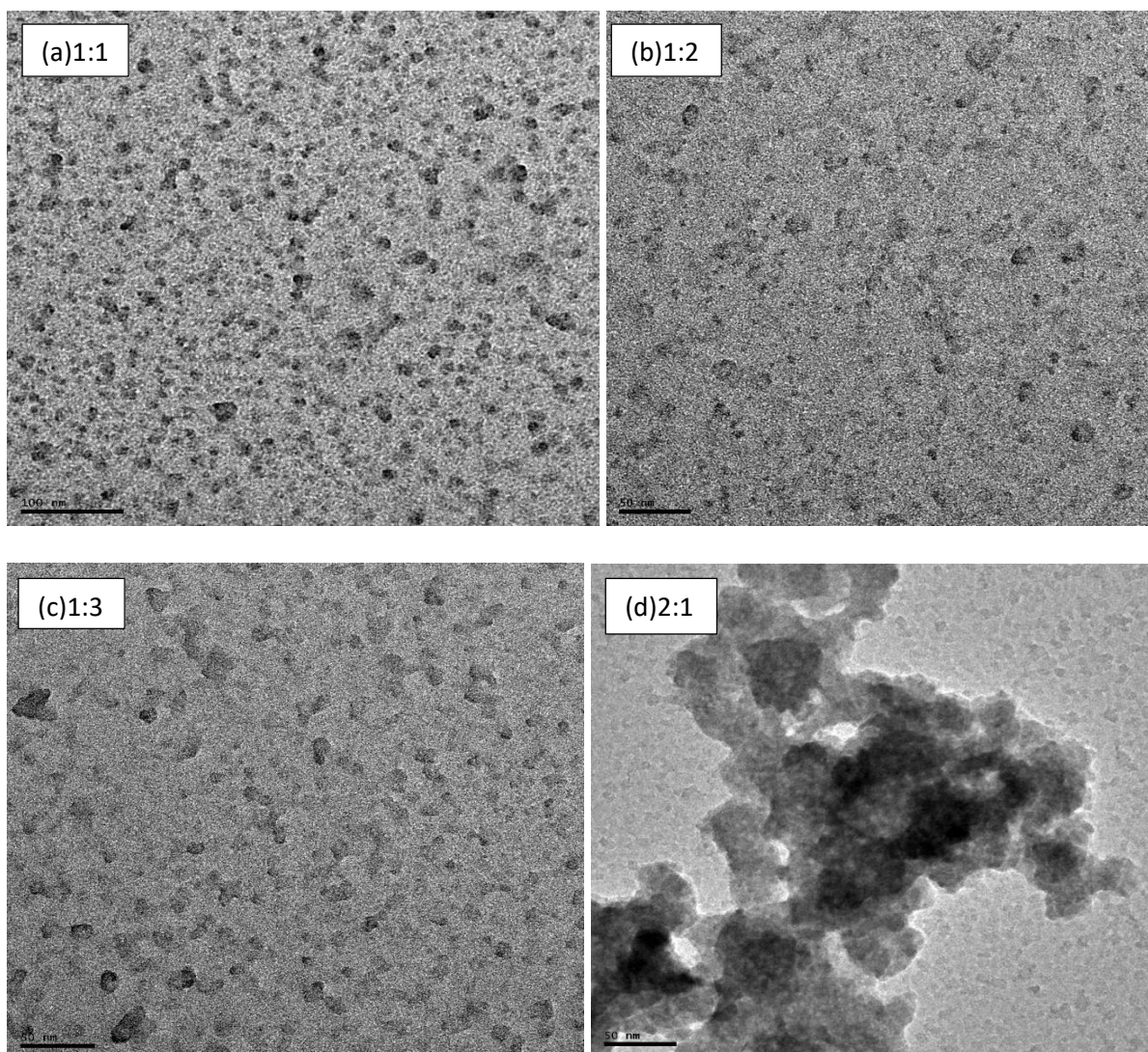


Figure 4.10: TEM image for Co/Thiourea nanoparticles

The TEM micrographs, Figure 4.10, showed that the particles from ratio 1:1, 1:2 and 1:3 appear to be well dispersed due to their small size and high surface energy. The particles appear to be around 10 – 30 nanometers in size. At ratio 2:1 particles are agglomerates with irregular shapes of about 50 nm.

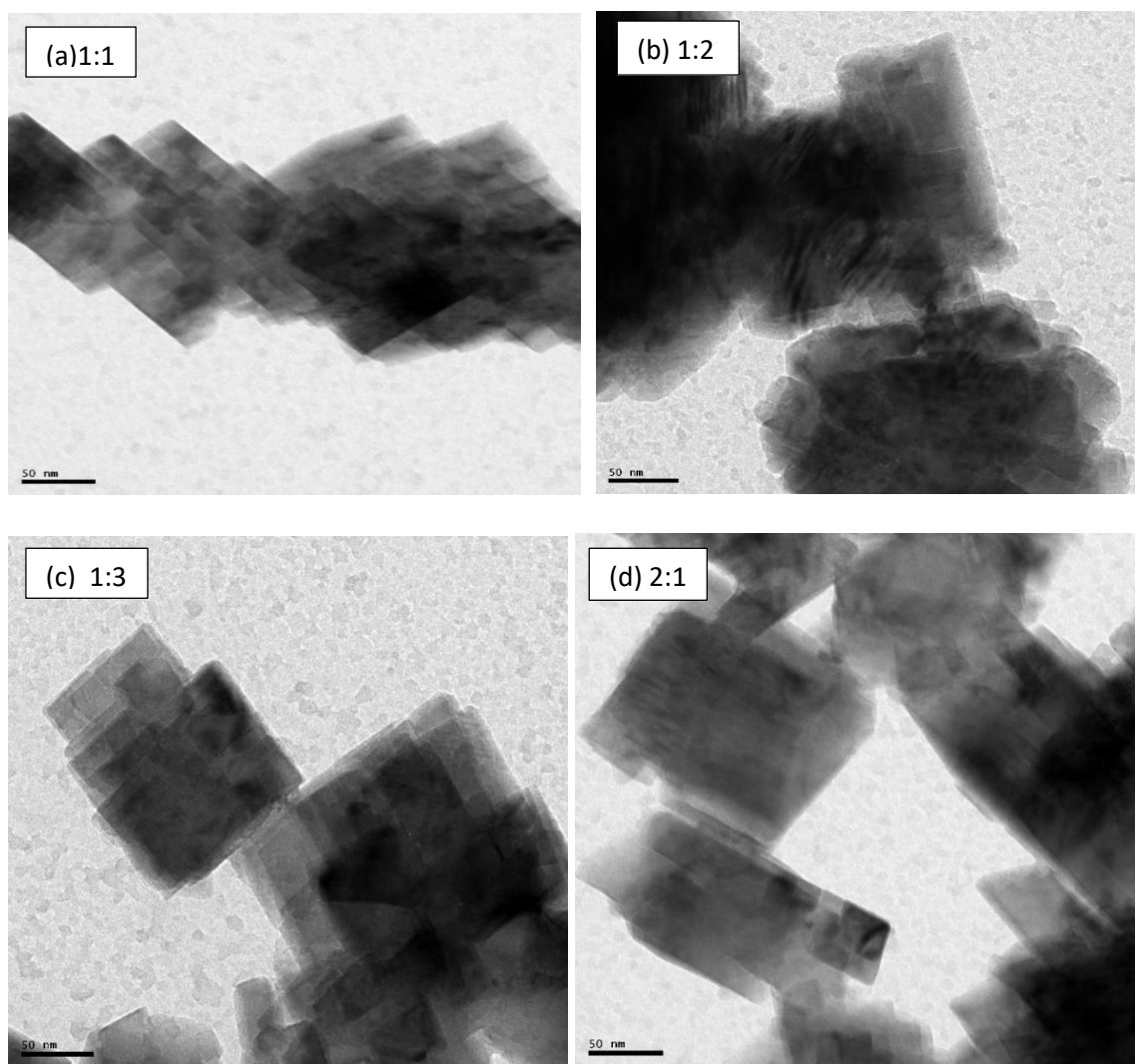


Figure 4.11: TEM image for Co/Urea

The Co complexed with Urea images showed particles from ratio 1:1, 1:2, 1:3 and 2:1 that appear spherical to hexagonal shape with 50 nm size in diameter (Figure 4.11). Similar particles were observed for Chandra & Kumar, 2012.

4.6. Scanning electron microscopy

SEM is a very useful technique in characterizing the morphology of the nanoparticles. It was observed that particles synthesized in ratio 1:1, 1:2 and 1:3 were more or less spherical in shape (Figure 4.12). Also, the particles were well dispersed and clusters for ratio 2:1, suggesting aggregation of nanoparticles.

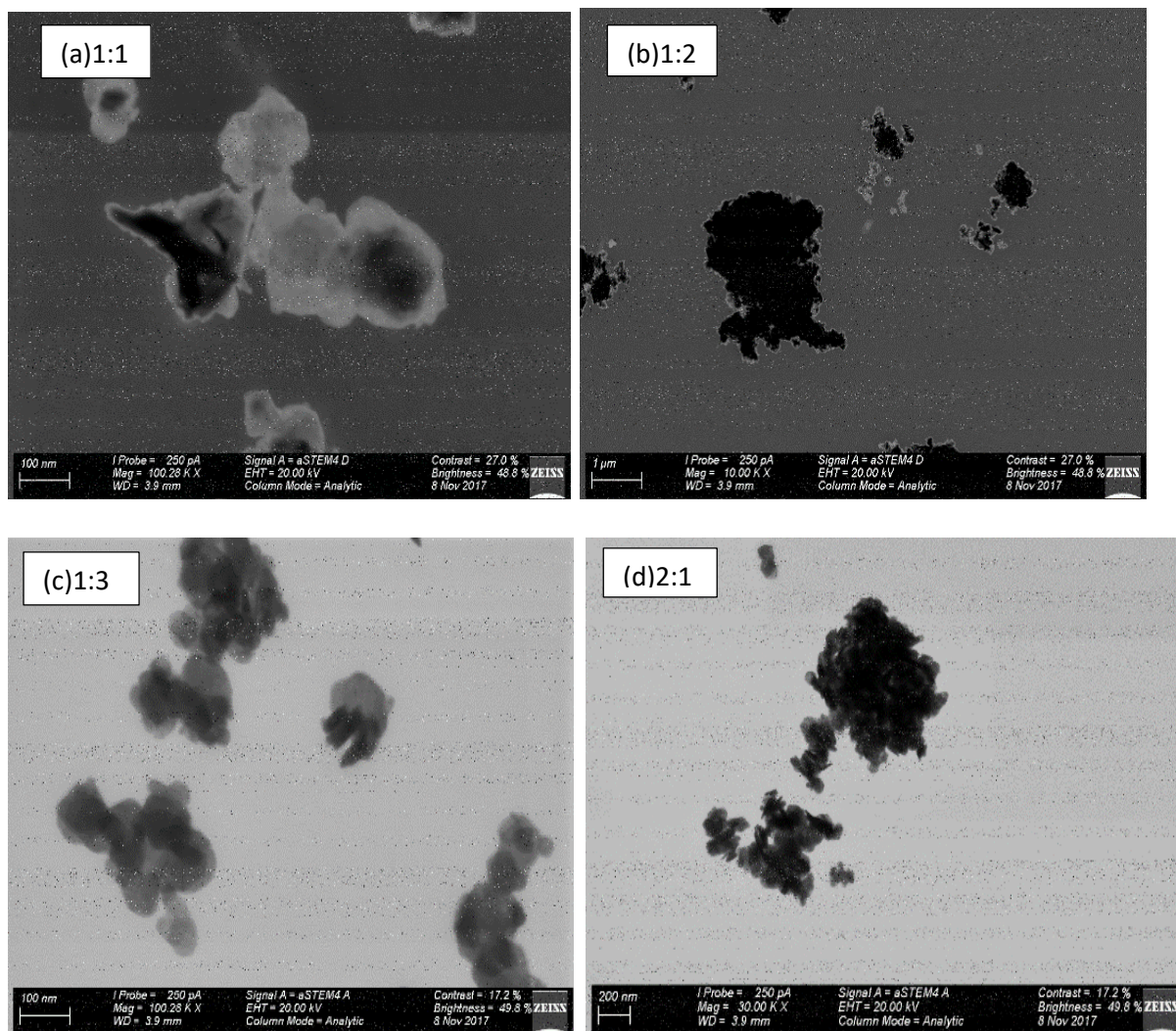


Figure 4.12: SEM image for Cobalt

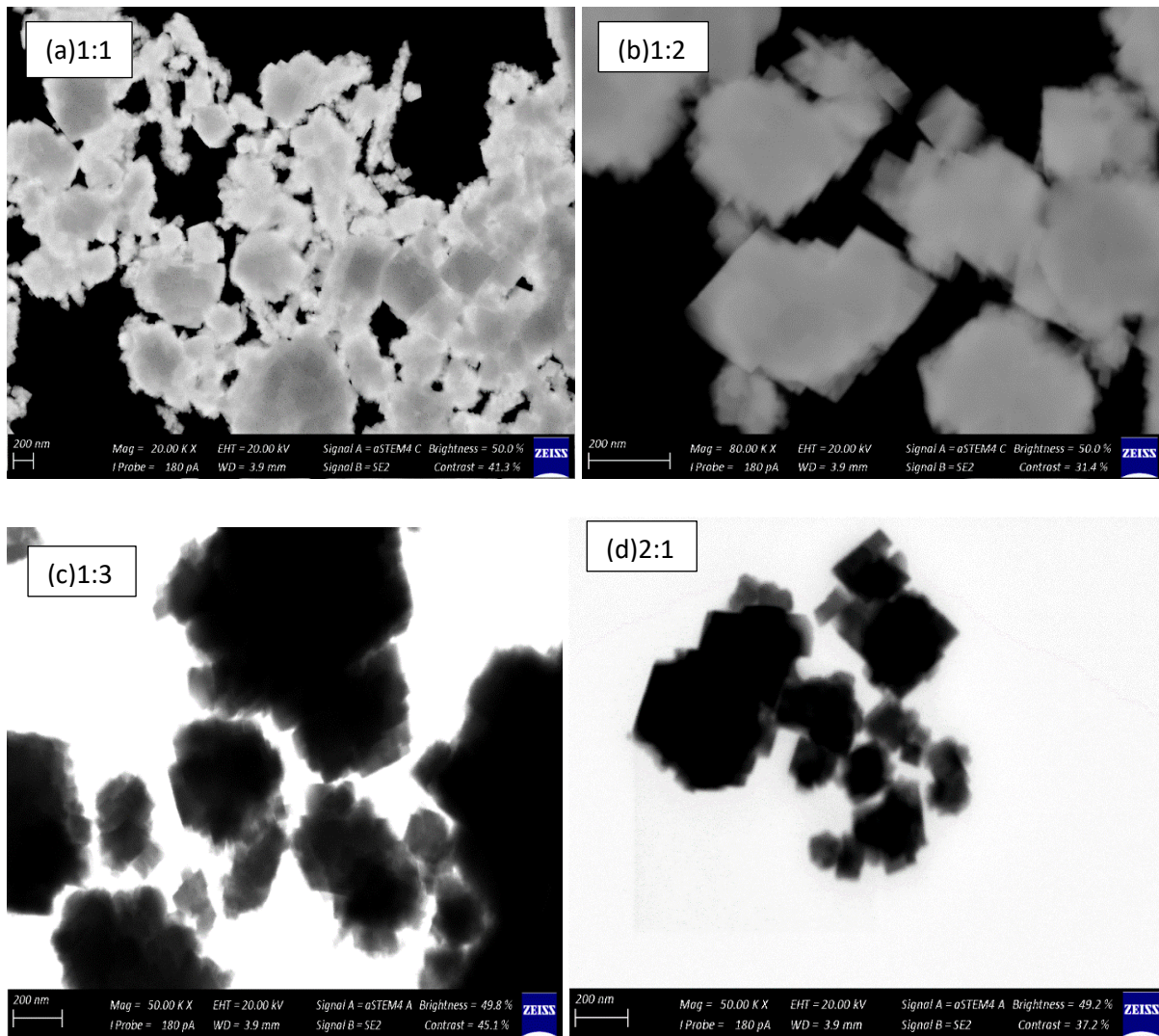


Figure 4.13: SEM image for Co/Urea

The SEM images are inconsistent with the absorption spectra in which particles increase when the concentration of the precursors was increased and the emission peaks are further evidence that broad peaks favouring large particles (Gupta *et al.*, 2011). Ratio 1:1 is agglomerated but from ratio 1:2 to 2:1 showed well dispersed nanoparticles (Figure 4.13).

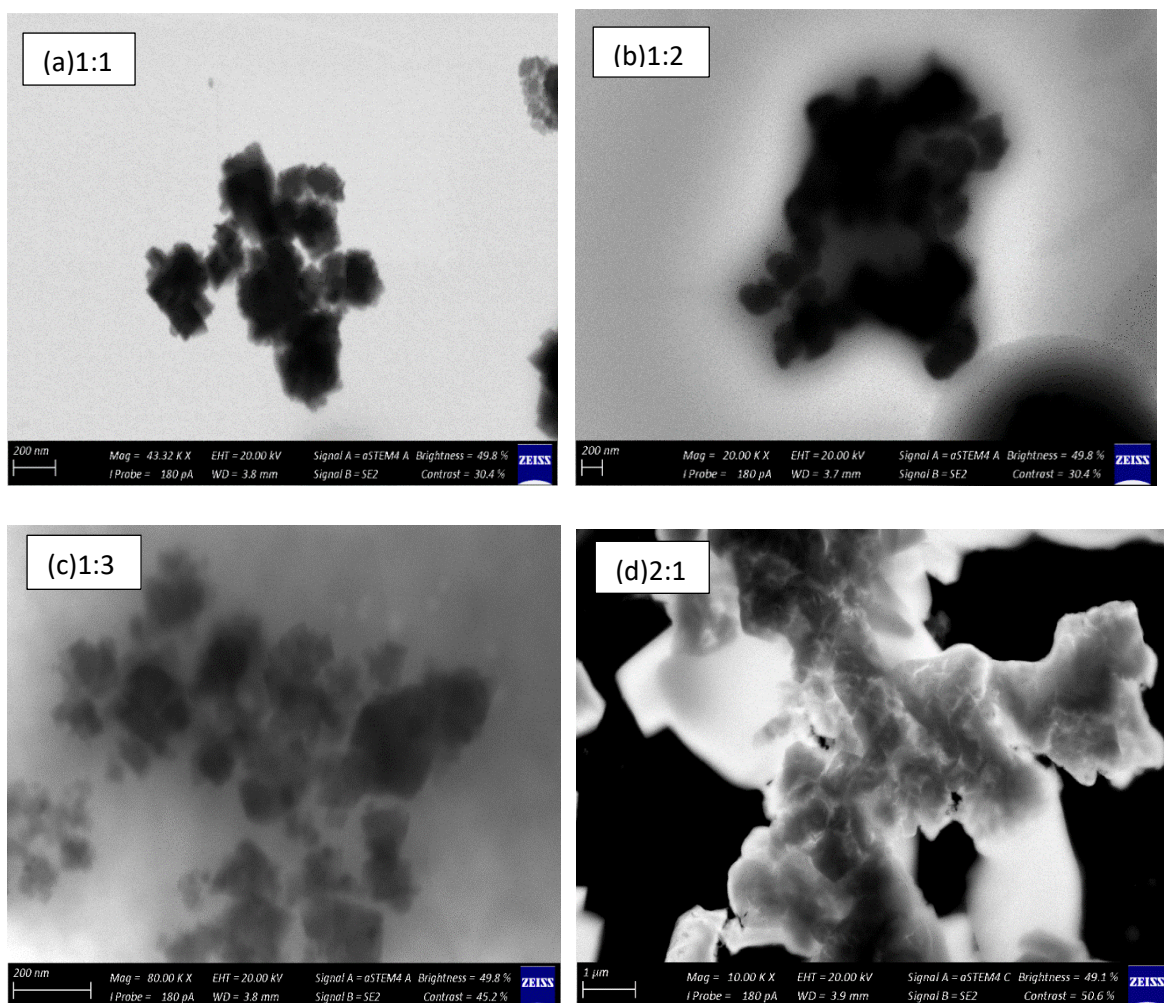


Figure 4.14: SEM image for Co/Thiourea 1:2

The SEM micrographs in Figure 4.14 showed that particles are irregular from low concentration to high concentration. The particles are irregular and agglomerated for 1:1 to 1:3 which makes difficult to determine the particle size. At ratio 2:1 particles are well dispersed and are irregular shapes ranging from 1 μ m.

4.7 XRD spectral analyses

XRD studies were performed to report on the crystallinity of the samples. Figure 4.15 shows diffraction peaks of Co/Thiourea which can be indexed to a face centered-cubic of cobalt hexahydrate.

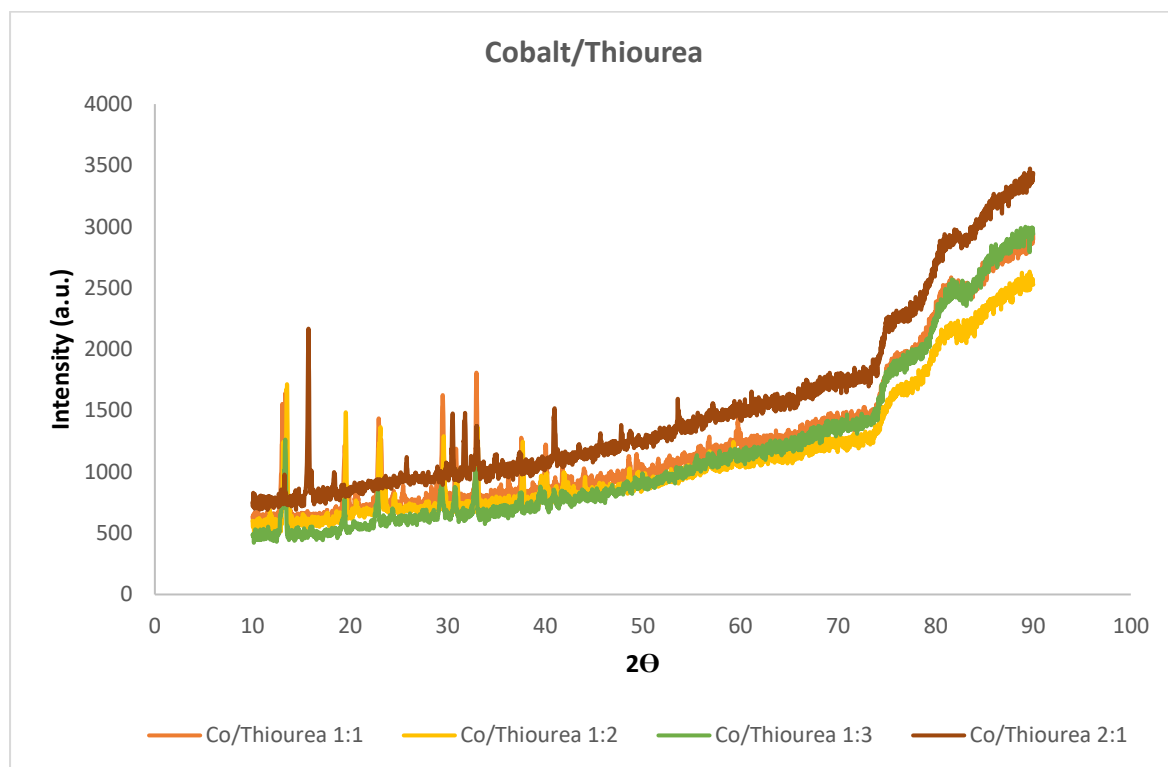


Figure 4.15: XRD patterns of Co/thiourea complexes

The diffraction peaks show a lot of impurities which might be as a result of insufficient washing of nanoparticles or recurring of impurities from the complex. The Bragg peaks are not well defined, which means the material is amorphous (Bragg & Bragg, 1949).

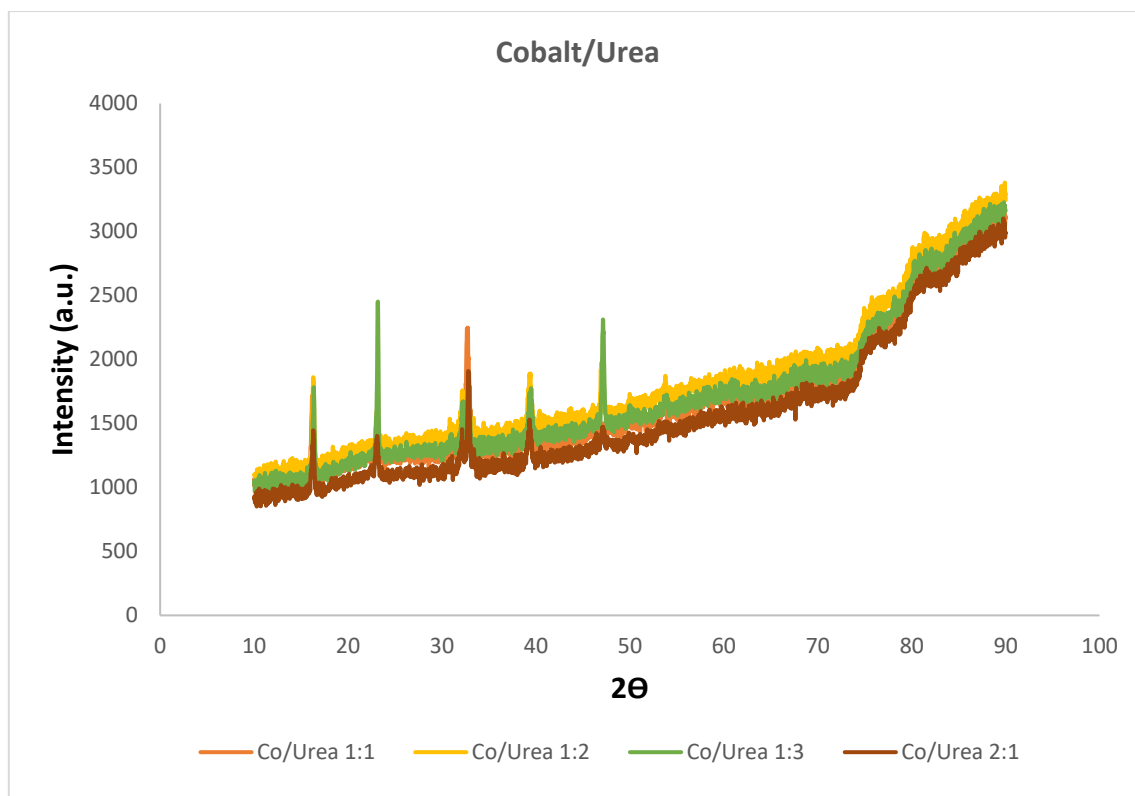


Figure 4.16: XRD patterns of Co/urea complexes

The XRD peaks for Co/urea (Figure 4.16) were not well defined, which means the material is amorphous. The hexagonal phase can be attributed to cobalt nanoparticles which exist either as cubic, orthorhombic or hexagonal phases. The existence of mixture of cubic and hexagonal phase with predominance of one over the other was reported by Bao *et al.*, (2005). The spectra show reasonable broadened peaks, with the higher concentration samples having slightly sharper peaks than the lower concentration samples.

4.8 Thermogravimetric analyses

Thermal decomposition studies on metal complexes have brought information on the mechanism and steps of decomposition by heating and therefore permit determination of kinetic parameters of the reaction. Thermal decomposition has been done due to interest in the isolation and identification of the solid decomposition products of complexes, interesting decomposition intermediate has been produced. Metal compound of thiourea and urea represent an extensive series of sulphur and oxygen bonded complexes with well-established structures (Bruce *et al.*, 2008).

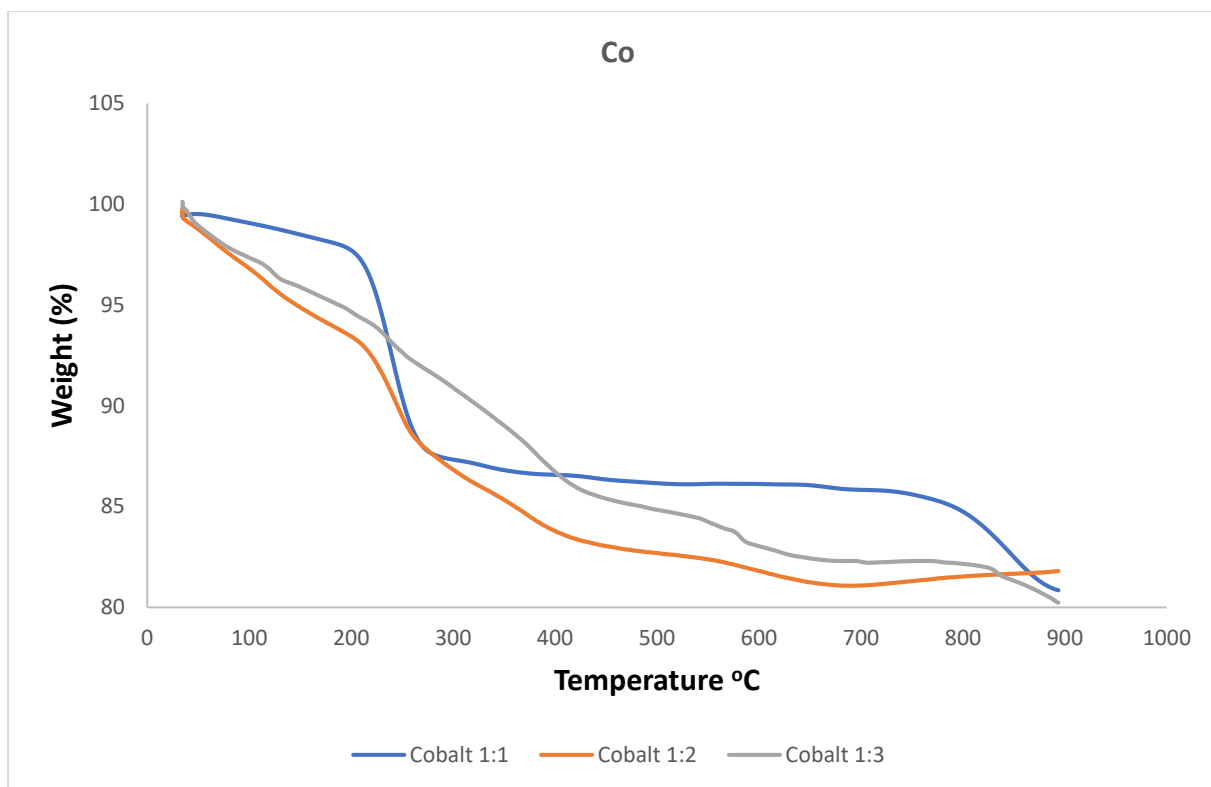


Figure 4.17: TGA curves for Cobalt

The TGA curves in Figure 4.17 indicate the three-steps decomposition ratio 1:1, 1:2 & 1:3 for cobalt. All the ratios for cobalt display first decomposition at 210°C to 240°C. There is a slow weight loss of the ratios which led to the formation carbon at a final temperature of 800°C. The periods of weight loss can be associated with the water, impurities and some reagents not reacted (Chandra & Kumar, 2012).

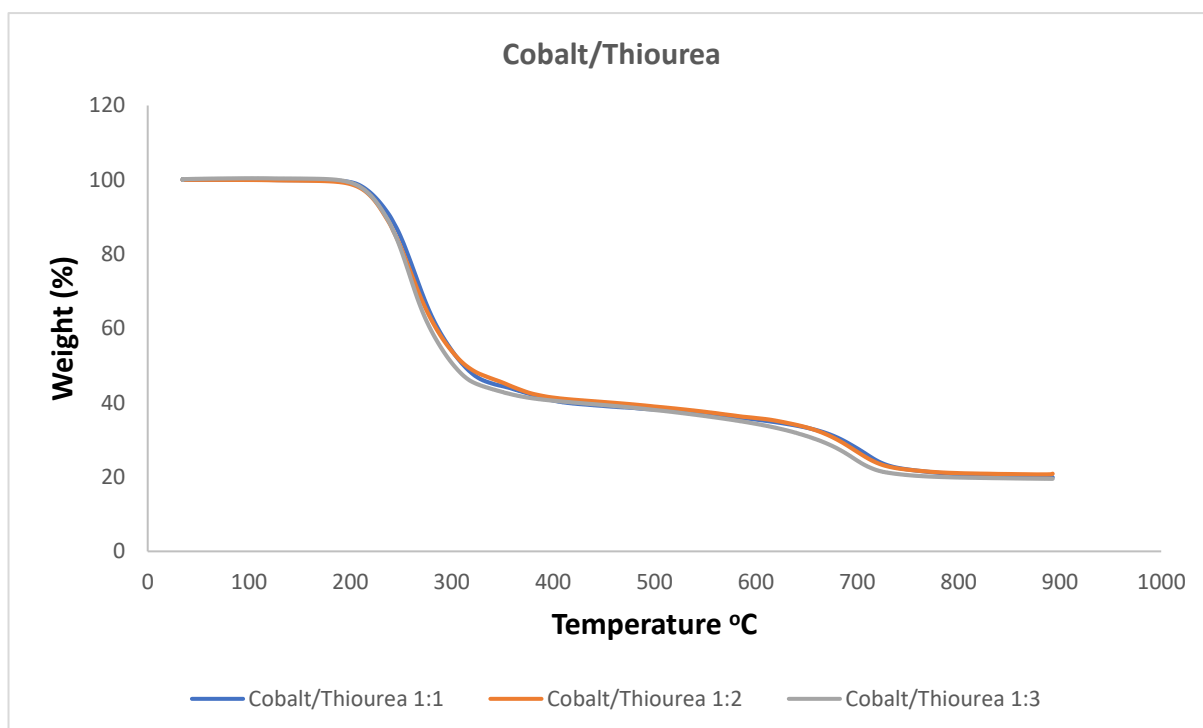


Figure 4.18: TGA curves for Co/thiourea complexes

The TGA curves in Figure 4.18, indicate the four-step decomposition ratio 1:1, 1:2, 1:3 & 2:1 of Co/thiourea complexes. All the ratios on Co/thiourea complexes display first decomposition at 200°C to 300°C. There is a slow weight loss of the ratios complexes which led to the formation of metal sulphide and oxide at a final temperature of 800°C (Jianxi *et al.*, 2003).

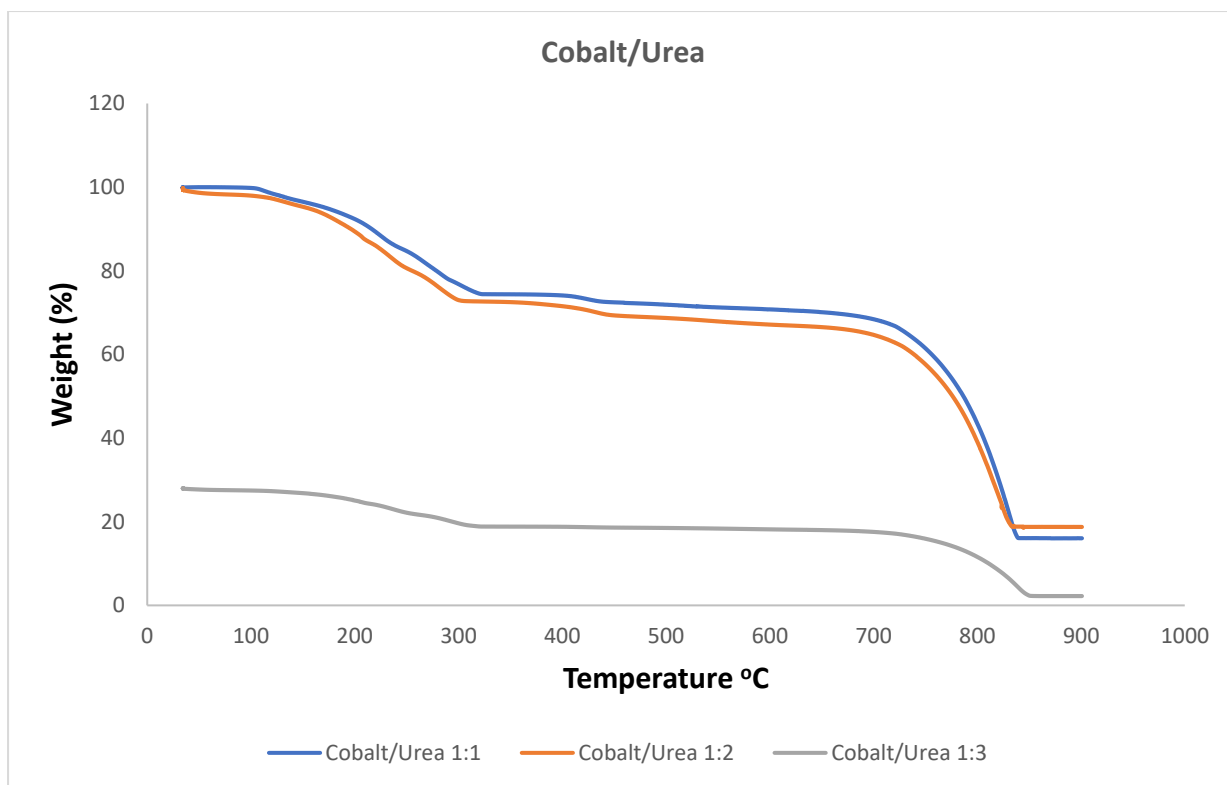


Figure 4.19: TGA curves for Co/Urea complexes

Figure 4.19 depicts the TGA curves for Urea Cobalt complexes with different ratios. Ratio 1:1, 1:2 show two steps decomposition with a sudden loss of weight on heating until 100°C which can be associated with loss of water and some volatile impurities remained during purification. The second decomposition started at 300°C, a period slow loss of weight led to the formation of metal oxide, which was completed at about 700°C. There is a slow weight loss of the ratios complexes which led to the formation of metal sulphide and oxide at a final temperature of 830°C. The TGA curve of ratio 1:3 started displaying at 180°C to 300°C, most organic molecules from the ligand are lost and followed by the slow period of weight loss from 800°C to 850°C (Bruce *et al.*, 2008).

4.9 Heavy metals

A heavy metal test was also conducted to measure the levels of potentially harmful metals in the nanoparticles. Removals of heavy metals in wastewater involves the use of biological techniques for the elimination of pollutants from wastewater. In this study the metals were tested against lead.

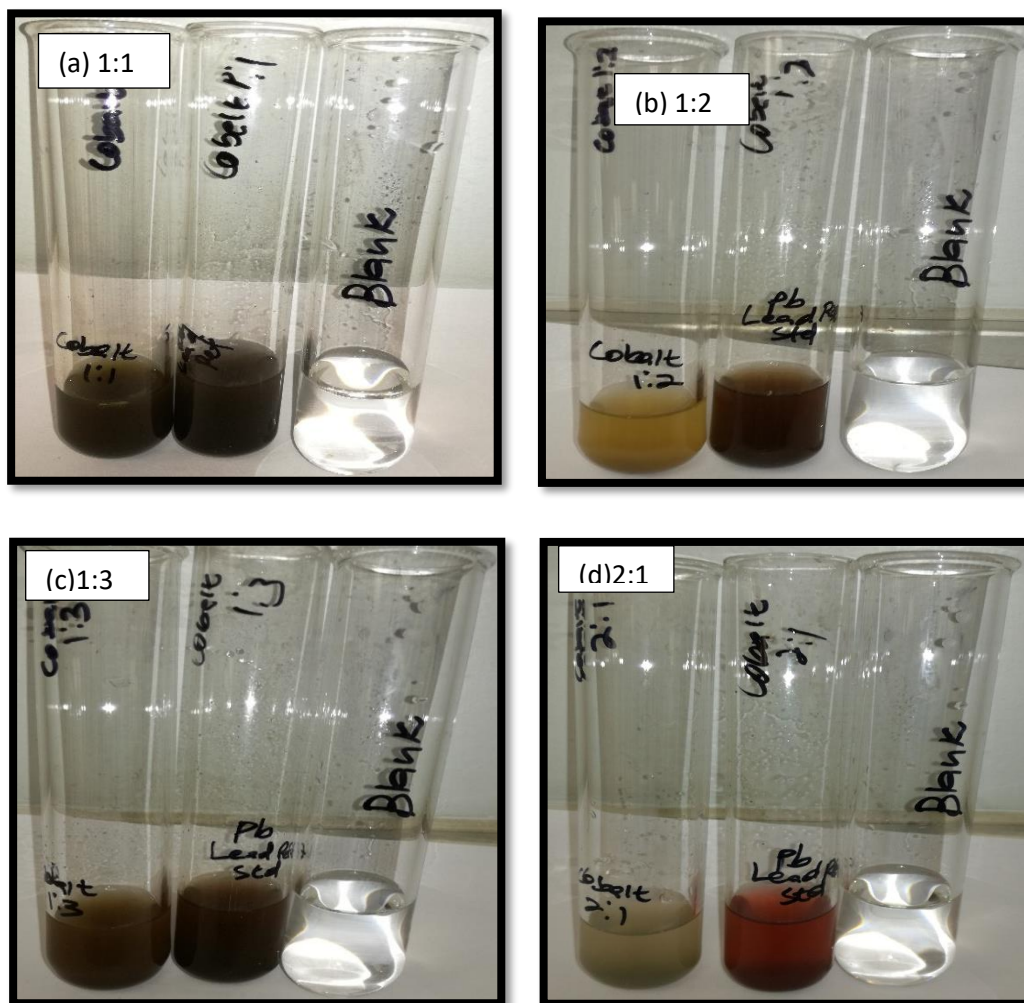


Figure 4.20: Cobalt heavy metal results

The nanoparticles were tested against 10 ppm of lead which showed to have less metals when compared to lead (Figure 4.20). Ratio 1:1 and 1:3 showed same colour light darker than the lead but ratio 1:2 and 2:1 they showed different colour from the lead. It shows that the cobalt nanoparticles have less metals.

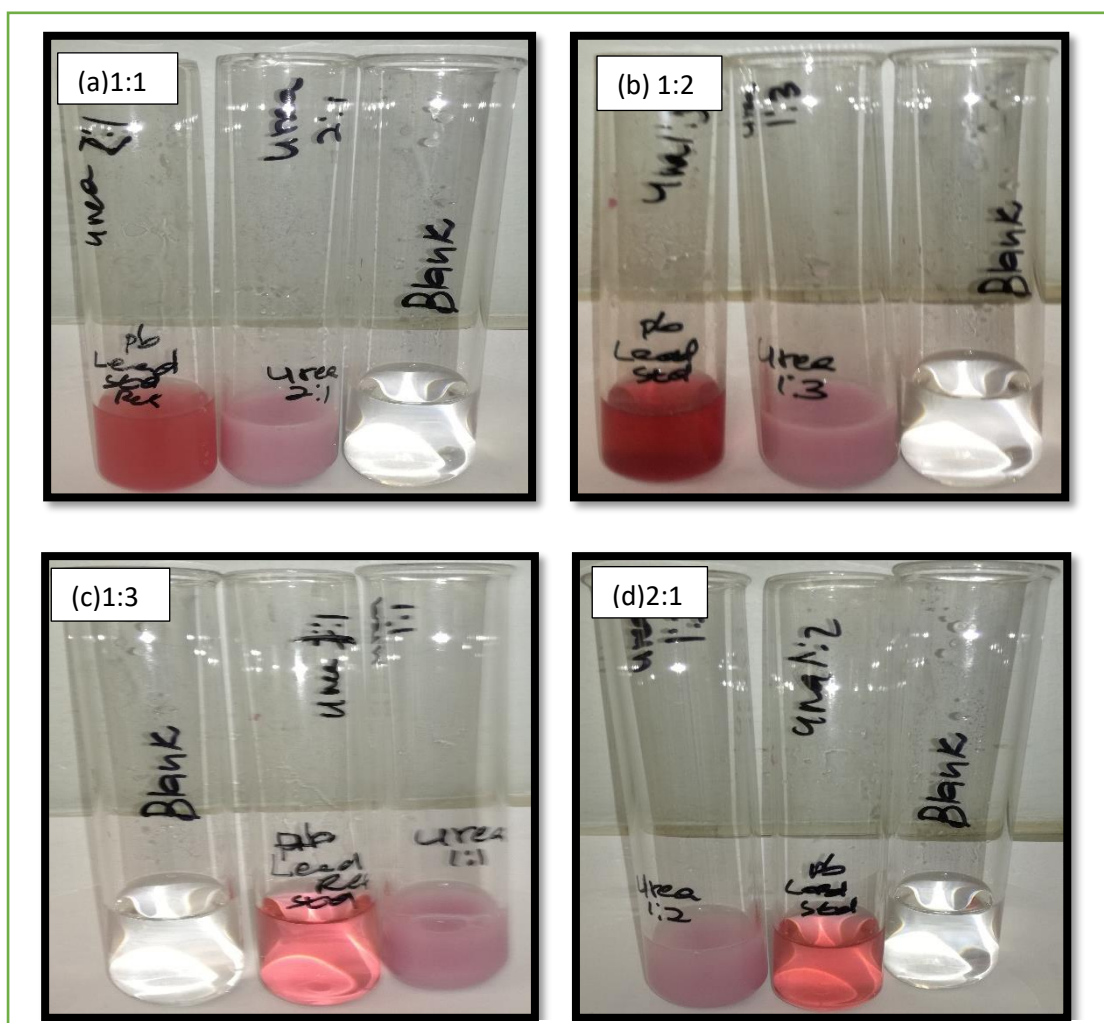


Figure 4.21: Cobalt/Urea nanoparticles heavy metal results

The nanoparticles were tested against 10ppm of lead which showed to have less metals when compared to lead stock. Ratio 1:1 to 2:1 showed same colour light darker than the lead, It witnesses that the cobalt/urea nanoparticles have less metals (Figure 4.21).

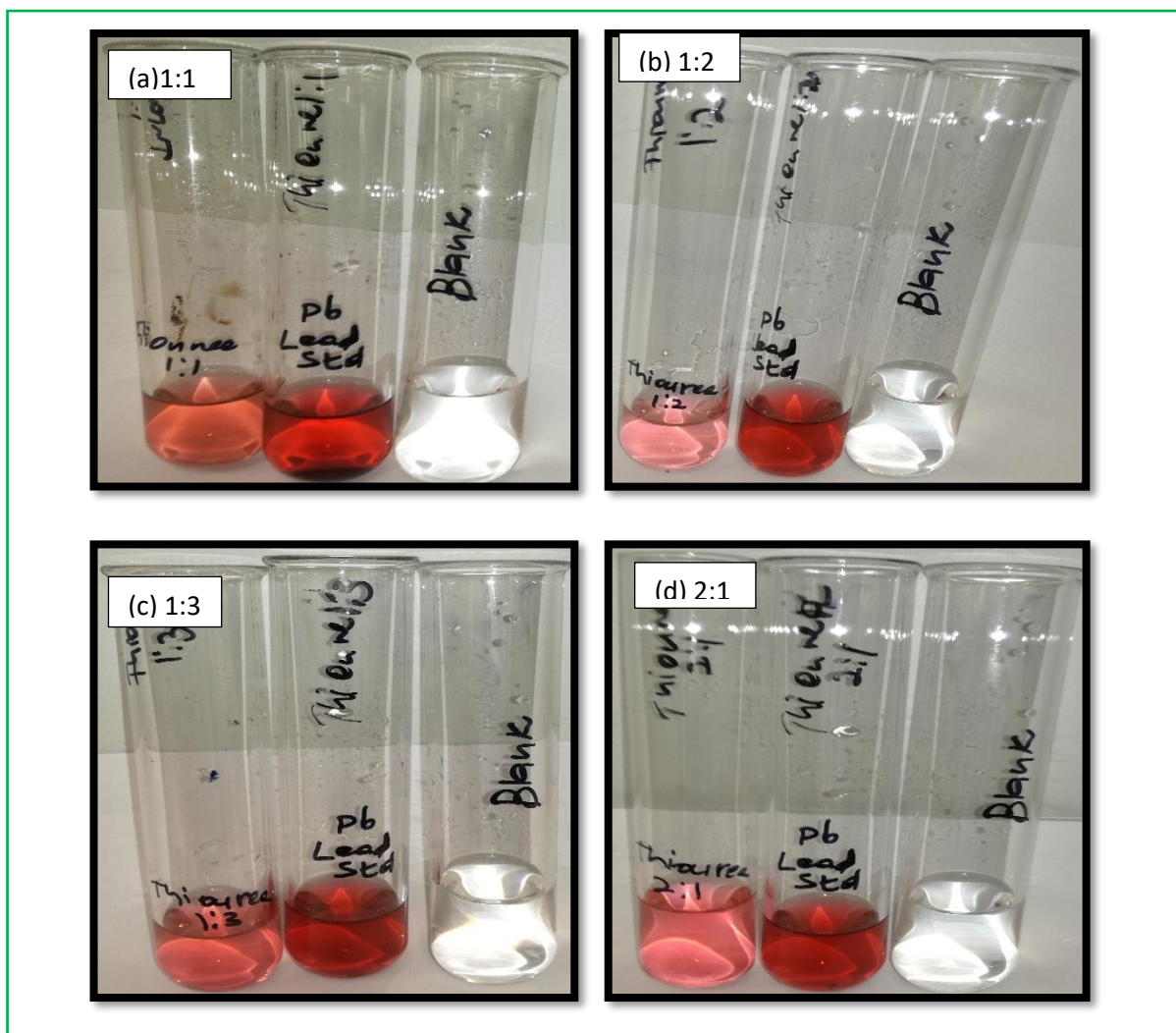


Figure 4.22: Cobalt/Thiourea heavy metal results

Heavy metals results showed that Cobalt/Thiourea nanoparticles from ratio 1:1 to 2:1 showed same colour lighter from the lead stock. These confirms that the nanoparticles have less metals (Figure 4.22).

CHAPTER 5

ANTIMICROBIAL RESULTS

5.1 Introduction

This chapter deals with the antibacterial activity of the nanomaterials. The antibacterial testing procedures are outlined in Chapter 3. In this chapter data was collected and analysed using the following microorganisms, five Gram-negative - *Escherichia coli*, *Pseudomonas aeruginosa*, *Salmonella enterica*, *Salmonella typhi* and *Shigella sonnei*; pathogenic bacteria and two fungal strains - *Aspergillus niger* and *Candida albicans*. Doped cobalt, Co/Urea and Co/Thiourea were tested on the different bacterial and fungal strains.

5.2 Minimum Inhibitory concentration

The minimum inhibitory concentration (MIC) is the lowest concentration of an antimicrobial agent that prevents visible growth of a microorganism after overnight incubation in broth (Nagaraj *et al.*, 2014). This precise method of susceptibility allows for quantification of the exact concentration (in $\mu\text{g/mL}$) of the antibiotic needed to inhibit the bacterial growth. Comparing an MIC value allows determining whether a bacterium is susceptible, intermediate or resistant to an antibiotic at certain concentrations. This information is most often used as a research tool to determine the *in-vitro* activity of new antimicrobials (Ivanova *et al.* 2013).

Minimum inhibitory concentration of the nanoparticles, the viability of the microorganisms when exposed to varying concentrations of doped cobalt, Co/Thiourea and Co/Urea nanoparticles were determined using an oxidation-reduction assay. Resazurin dye, a redox sensitive dye, was used to indicate cell viability. Metabolically active cells reduce the non-fluorescent blue resazurin to fluorescent red resorufin. Non-living cells do not reduce the resazurin and thus indicate cell death. This visible change in colour and fluorescence indicates the cells are viable.

Freshly grown and diluted bacterial cultures in MH broth were exposed to Co, Co/Thiourea and Co/Urea nanoparticles at concentrations ranging from 0.3 to 50 mg/ml.

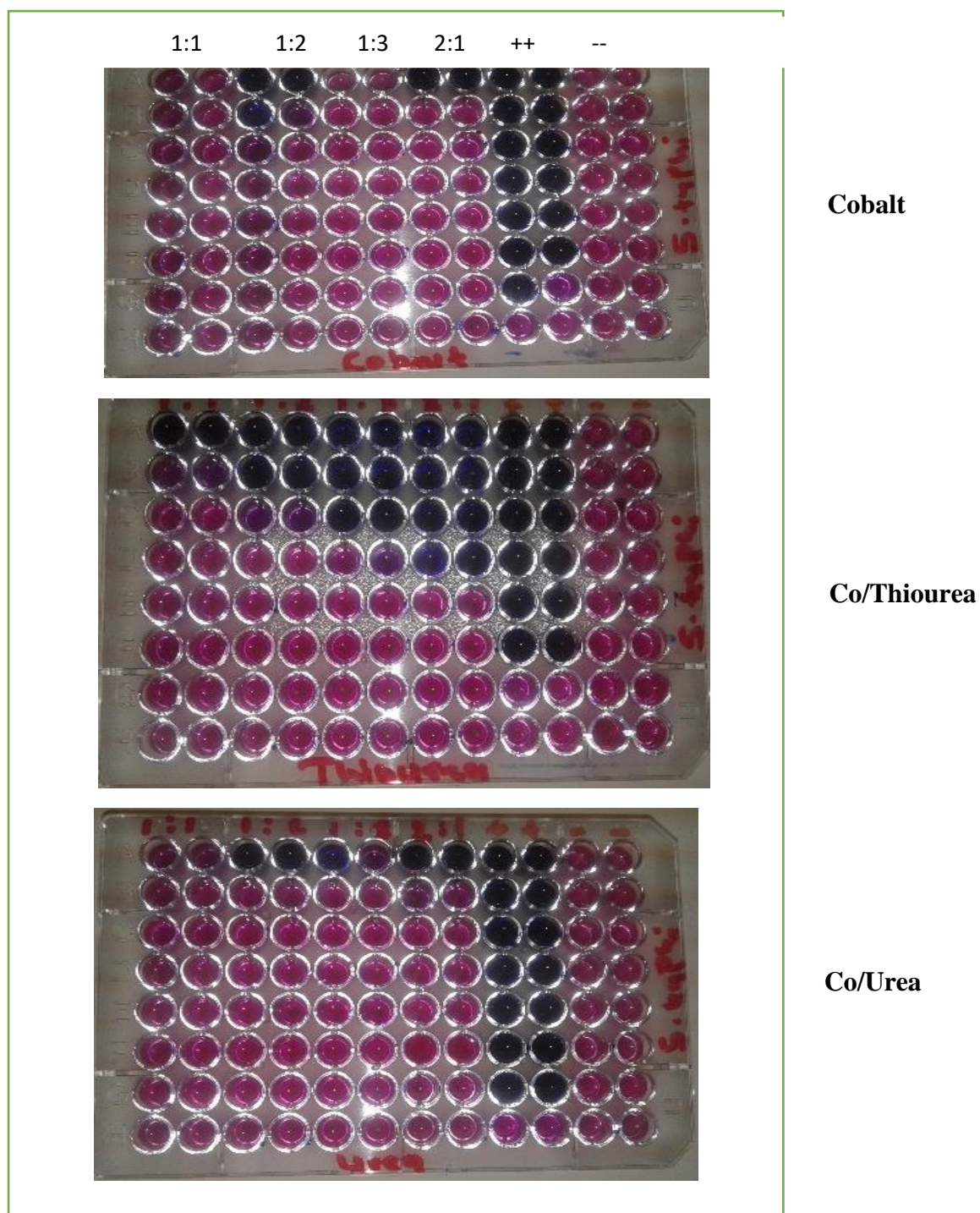


Figure 5.1: MIC results of *S. typhi*

In Figure 5.1, *S. typhi* cells were rendered non-viable after treatment with 12.5 $\mu\text{g/ml}$ of Co/Thiourea and Cobalt nanoparticles. *S. typhi* was inactivated with 25 $\mu\text{g/ml}$ of Co/Urea nanoparticles. This indicates that *S. typhi* is more susceptible to the antimicrobial effects of neomycin than Cobalt, Co/Thiourea or Co/Urea (Kumar *et al.*, 2013).

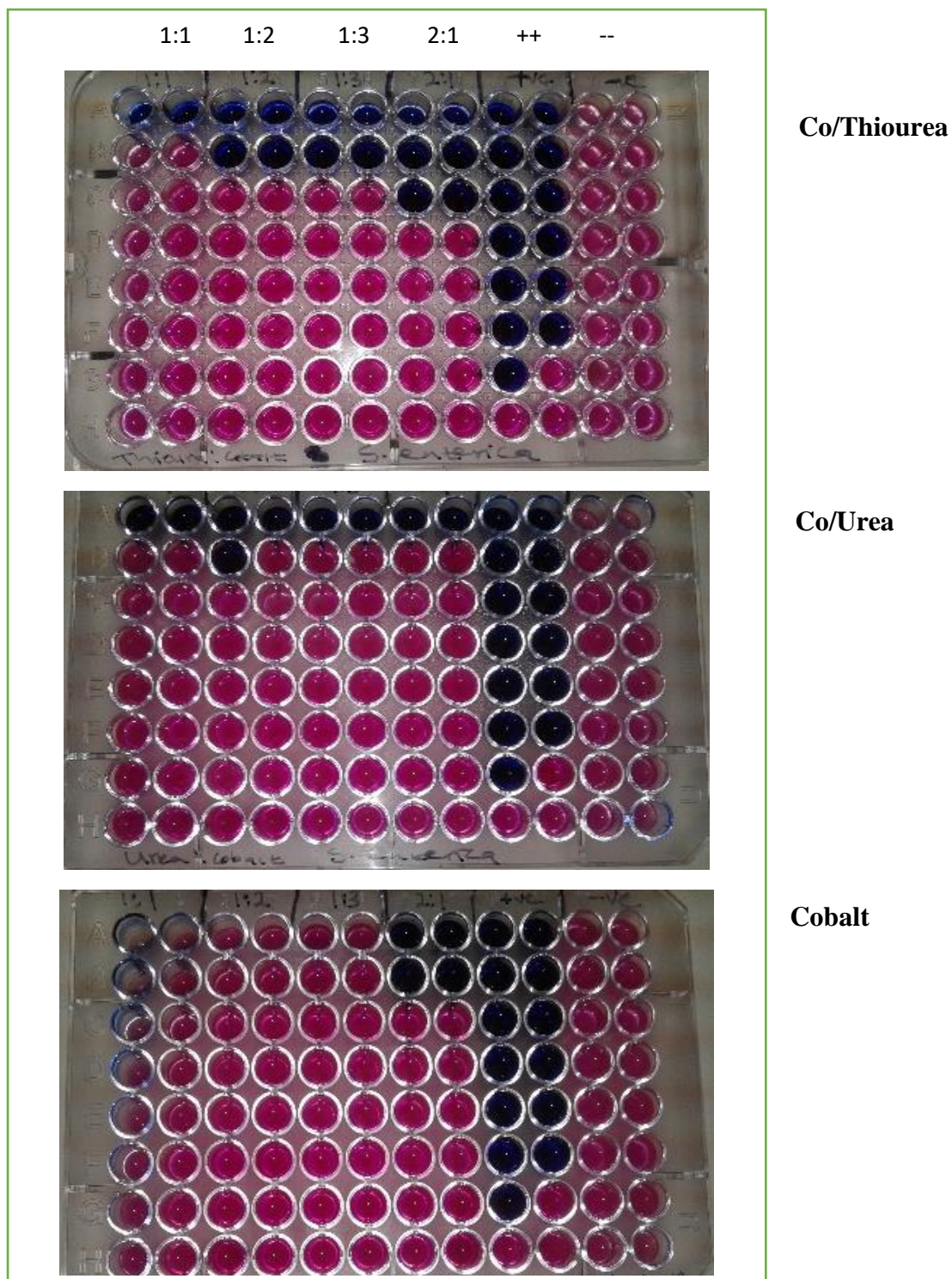


Figure 5.2: MIC results for *S. enterica*

Figure 5.2 shows the MIC of Cobalt, Co/Thiourea and Co/Urea nanoparticles on *S. enterica*. The results show that all the nanoparticles were not effective against *S. enterica* at ratios tested. This claim is supported by the appearance of the purple colour. However, neomycin as a positive control was effective against all the organisms as compared to all the three

nanoparticles. This indicates that the *S. enterica* is more susceptible to positive control than all the nanoparticles tested (Poole, 2004).

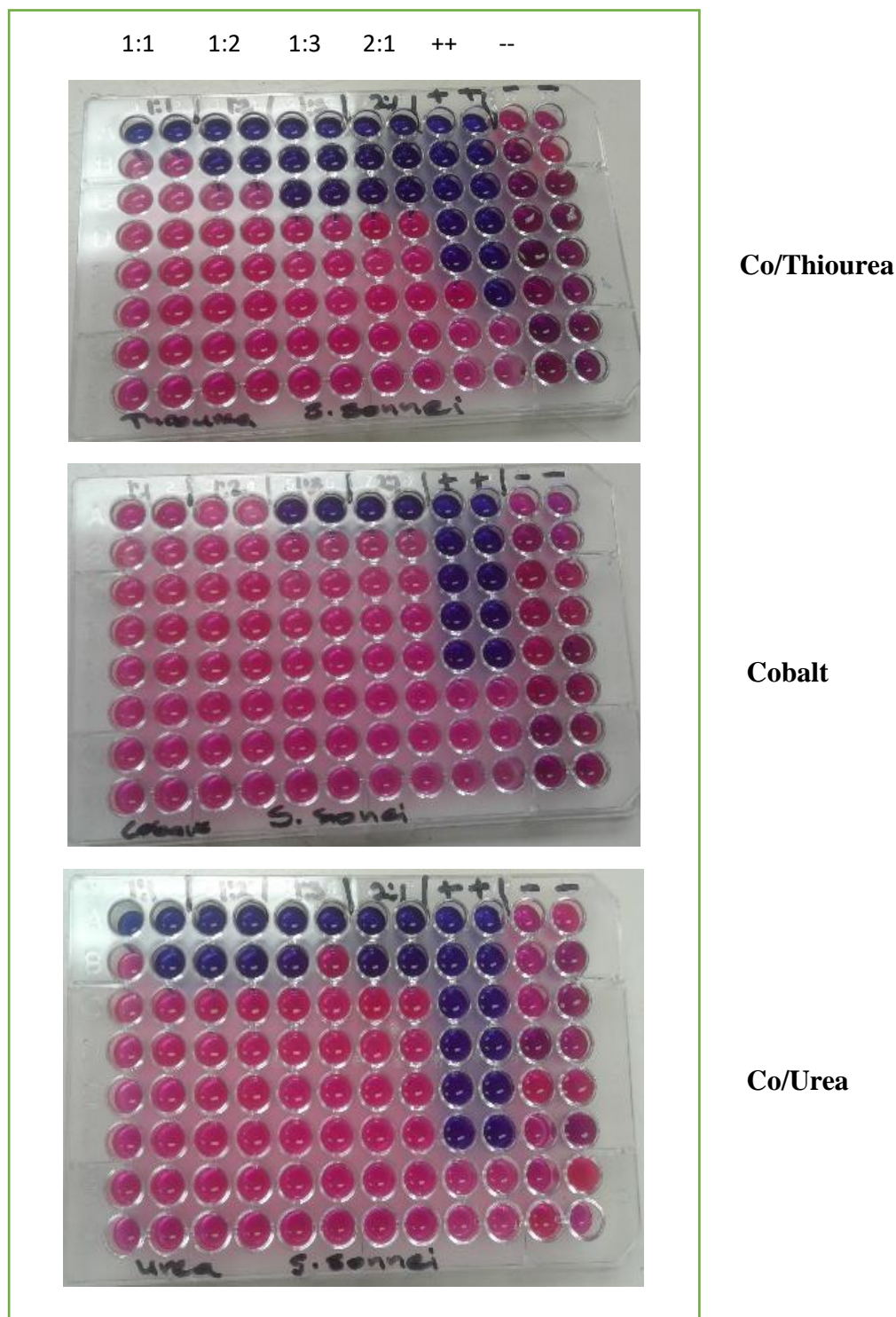


Figure 5.3: MIC results for *S. sonnei*

The serial dilution and MIC of *S. sonnei* by Cobalt, Co/Thiourea and Co/Urea are presented in Figure 5.3. Cobalt nanoparticles were less effective against *S. sonnei*. Co/Thiourea and

Co/Urea nanoparticles were effective against *S. sonnei*. The results also showed that positive control was more effective than the nanoparticles with the inhibition of 0.14 $\mu\text{l/ml}$ (Poole, 2004).

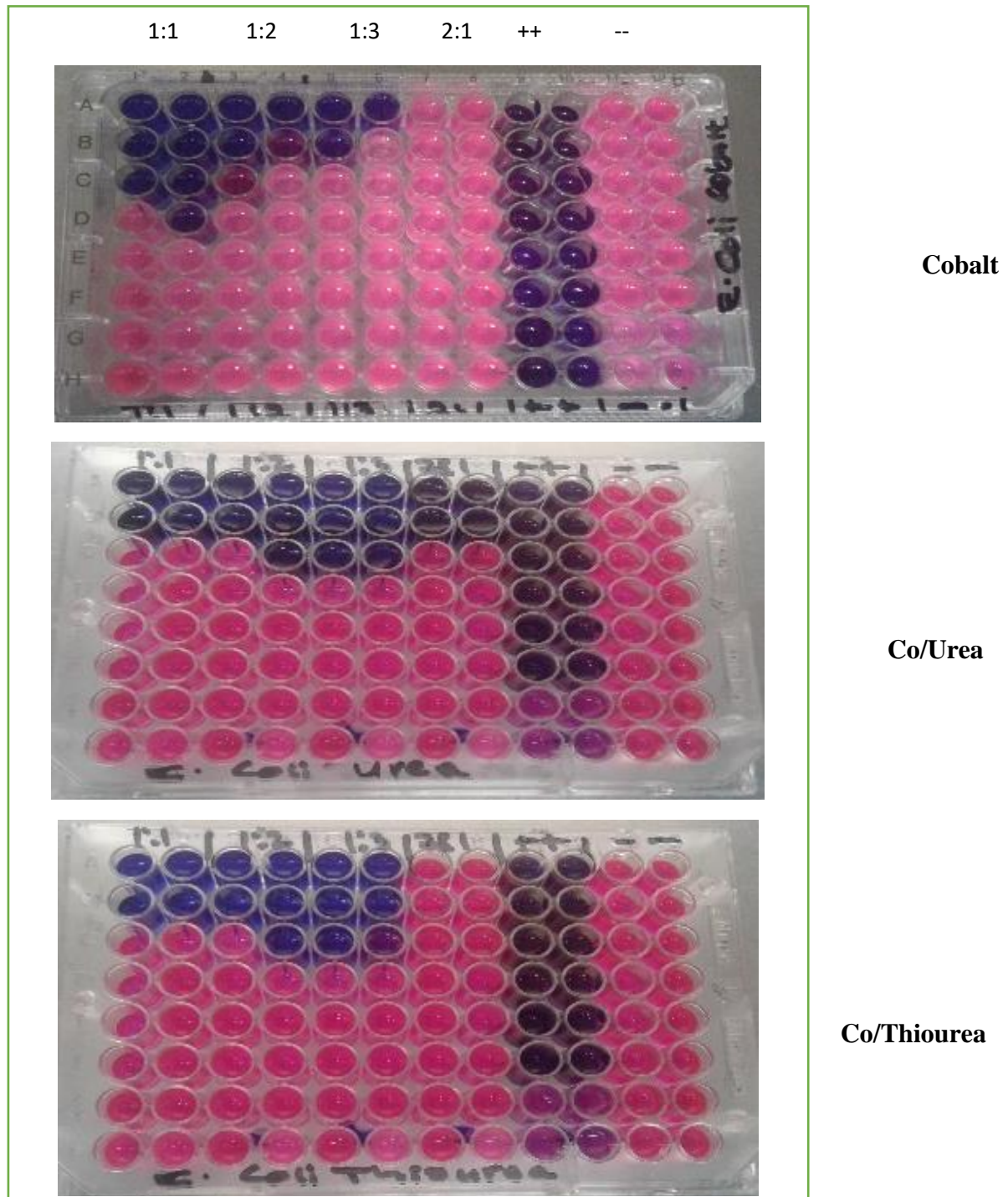


Figure 5.4: MIC for *E. coli*

Figure 5.4 presented the inhibition of *E. coli* by the nanoparticles. A urea nanoparticle was more effective against the *E. coli*. At ratio, 2:1 urea was effective with 50.0 μl However, the cobalt

and thiourea were not effective against *E.coli* at ratio 2:1. At ratio, 1:1 cobalt was more effective compared to Cobalt/Urea and Cobalt/Thiourea. Positive control was more effective to all the nanoparticles with 0.01 $\mu\text{l/ml}$ (Plaza *et al.*, 2013).

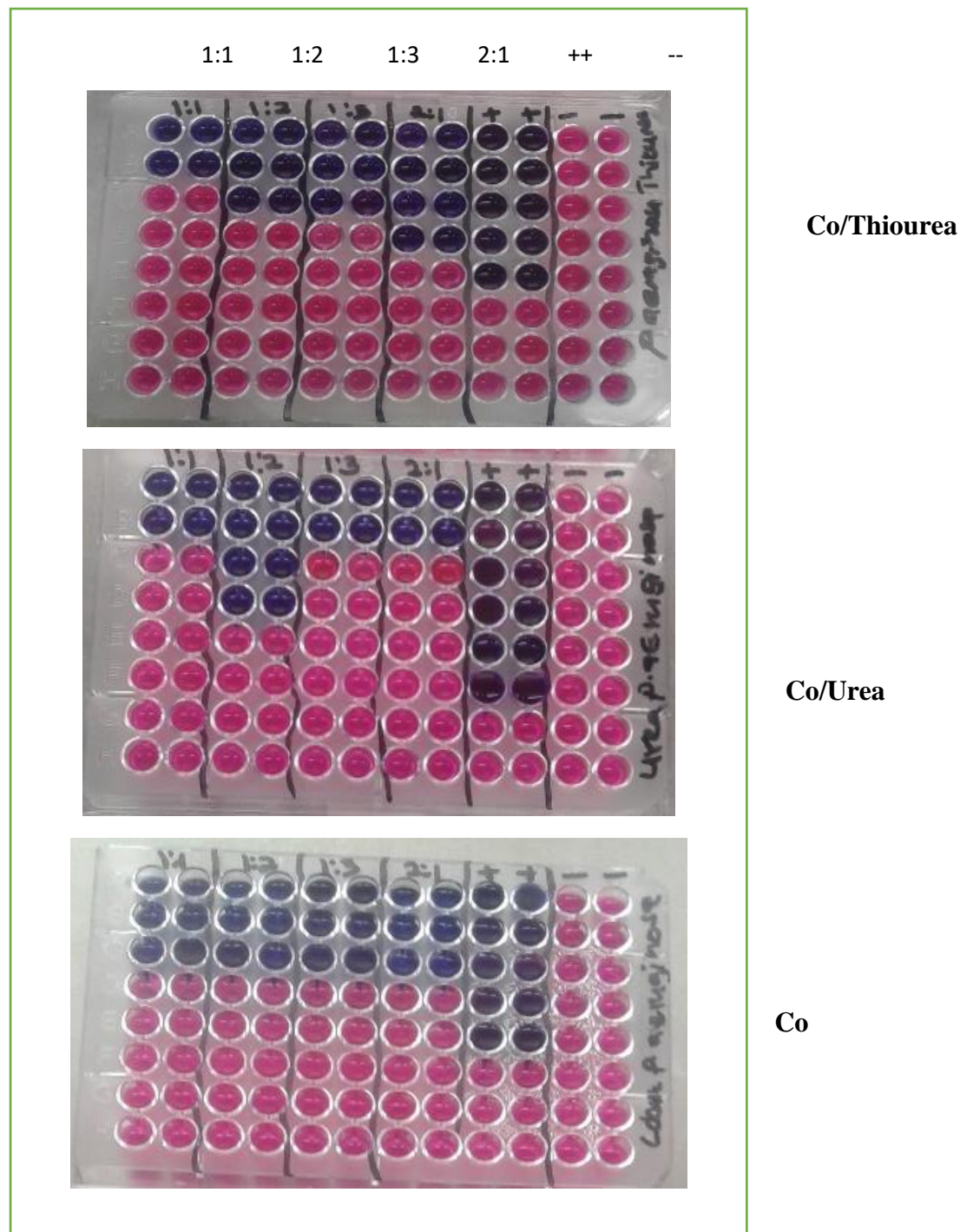


Figure 5.5: MIC of Co, Co/Tu and Co/U nanoparticles on *P.aeruginosa*.

Figure 5.5 shows the MIC of Co, Co/Tu and Co/U nanoparticles on *P.aeruginosa*. The results show that all the nanoparticles were effective against the microorganism at all concentrations

that were tested. The results also show that the positive control was more effective at all nanoparticles. The results indicate that the antibiotic is more susceptible to the *P. aeruginosa* than the tested nanoparticles.

5.3 Well agar diffusion method

The results of this methods reflected varieable antimicrobial activities against the growth of different strains tested. Nanoparticles demonstrated a dose related response where there was zone of inhibition (Figure 5.6).The zones of growth inhibition were not comparable against neomycin during antibacterial testing. However nanoparticles showed comparable results to Amphotericin B when tested against *Aspergillus niger* and *Candida albicans*. In some instances, Co/Thiourea was more effective than Amphotericin (Seil & Webster, 2012).

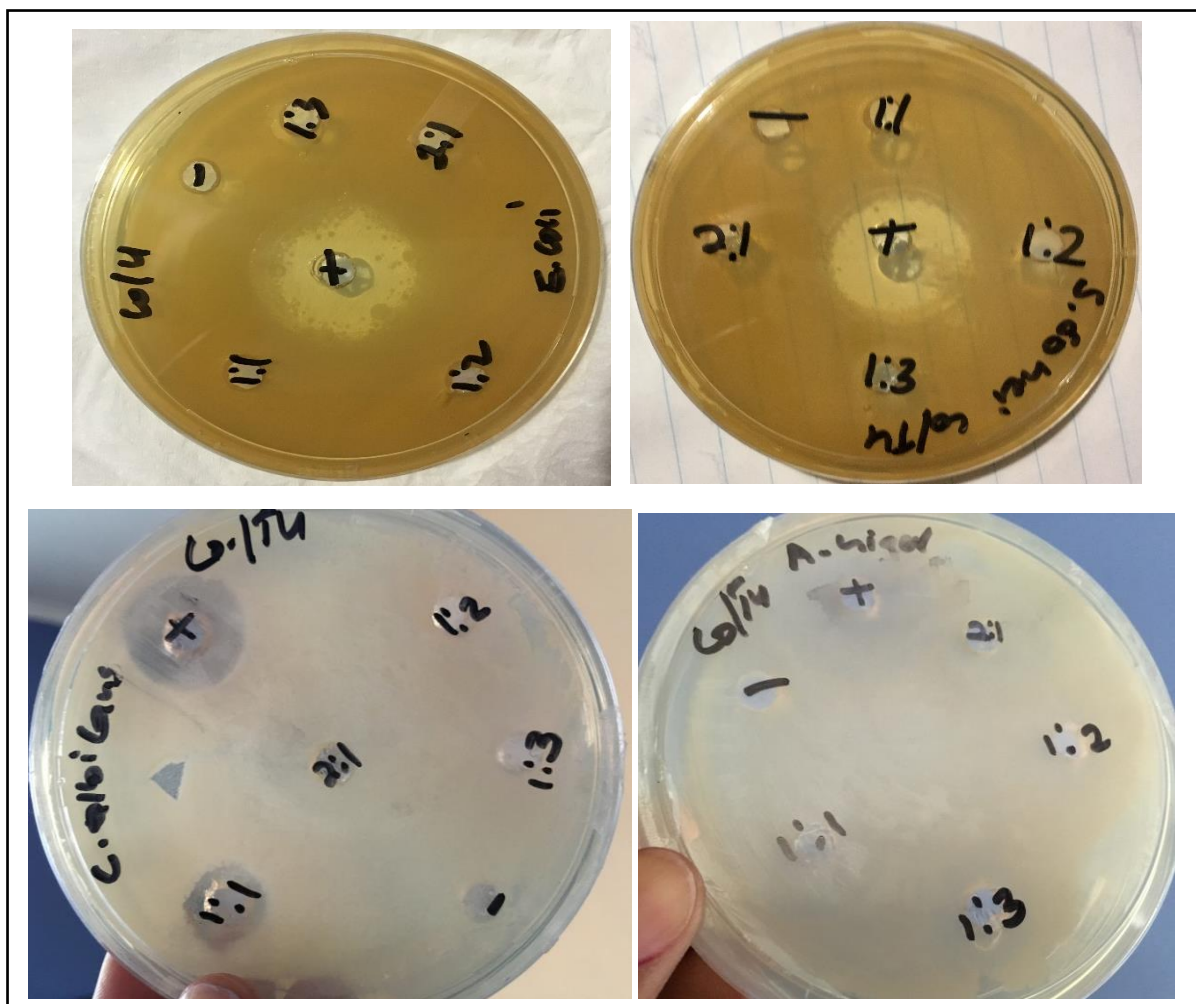


Figure 5.6: Well diffusion picture of the yeast, mould and bacteria on different ratios.

Figure 5.6 presented the well diffusion results of the microorganisms. Co/Tu represent cobalt thiourea, (Co/U) Cobalt urea nanoparticles and (Co) cobalt nanoparticles, (-) Mueller Hinton

broth as negative control and (+) neomycin as positive control used for the bacteria and amphotericin B used for yeast and mold.

5.4 Antibacterial activities of nanoparticles

The antibacterial nanoparticles were analysed and compared with positive controls in the form of neomycin. Bar columns were constructed using Microsoft Excel 2016. Student t-test was used to statistically analyse the *in-vitro* data obtained during this study.

5.4.1 Cobalt on *E. coli*.

Cobalt showed minimal growth inhibition against *E. coli*, especially at ratio 1:2 and 2:1. It showed zone of inhibition measuring 0.76 mm compared to neomycin which measured about 8.42 mm. No inhibition was shown for ratios 1:1 and 1:3. The difference was considered to be extremely statistically significant at $p = 0.0001$. Figure 5.7 below depicts the mean distribution of nanoparticles and neomycin against *E. coli* growth.

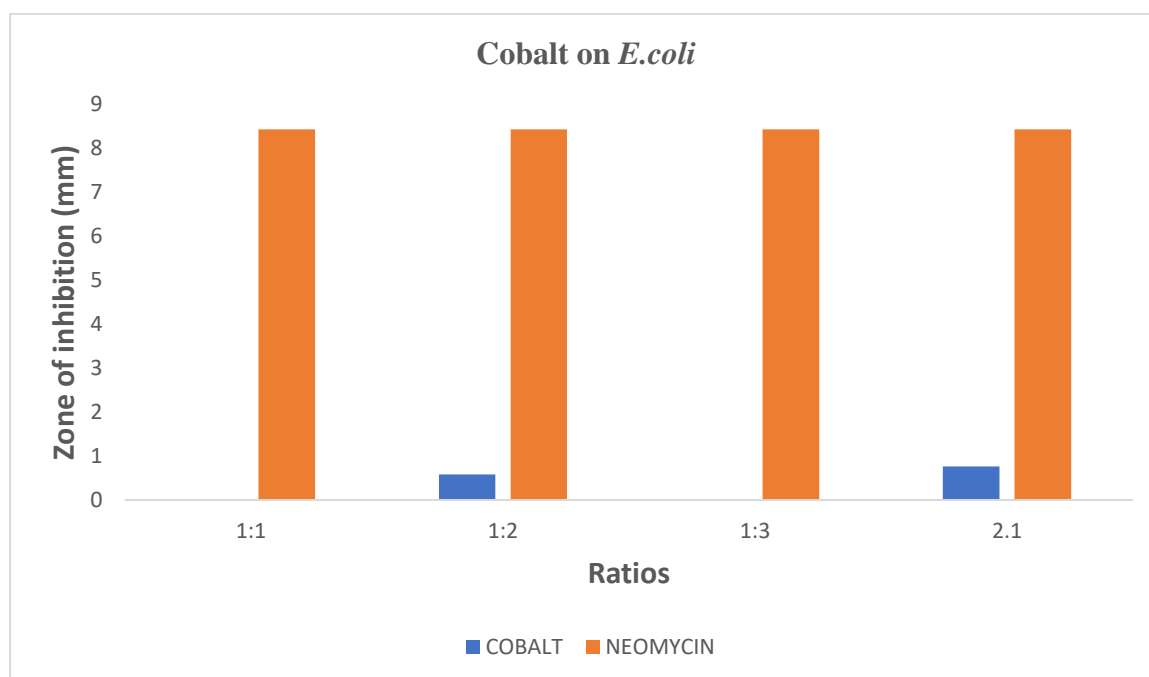


Figure 5.7: The mean inhibition diameter of Cobalt nanoparticles and neomycin on *E.coli*

The above Figure 5.7 is a graphic representation of the mean results for well diffusion method from Table 5.1 below, comparing the zone of inhibition between Cobalt and neomycin. After conducting student t- test statistical analysis the two tailed P value was 0.0001 and the mean of Cobalt minus neomycin was -7.7125. At 95% confidence interval the difference was between

-8.2108 to 7.7125. The intermediate values used in the calculations were as follow, $t = 33.1984$, $df = 14$ and standard error of difference = 0.232. Table 5.1 below depicts statistical calculation from the t-test (Plaza *et al.*, 2013).

Table 5.1: The difference in median values of *E.coli* treated with Cobalt and Neomycin

	Cobalt	Neomycin
Mean	0.1675	7.8800
SD	0.3139	0.5773
SEM	0.1110	0.2041
N	8	8

5.4.2 Cobalt on *S. typhi*

Cobalt showed a positive zone of inhibition against *S. typhi*. It showed zone of inhibition measuring 5.13 mm compared to neomycin which measured about 16.04 mm. By conventional criteria, this difference was considered to be extremely statistically significant at $p = 0.0001$. The 1:2 ratio showed the most inhibition of all the Co ratios. Figure 5.8 below depicts the mean distribution of nanoparticles and neomycin against *S. typhi* growth.

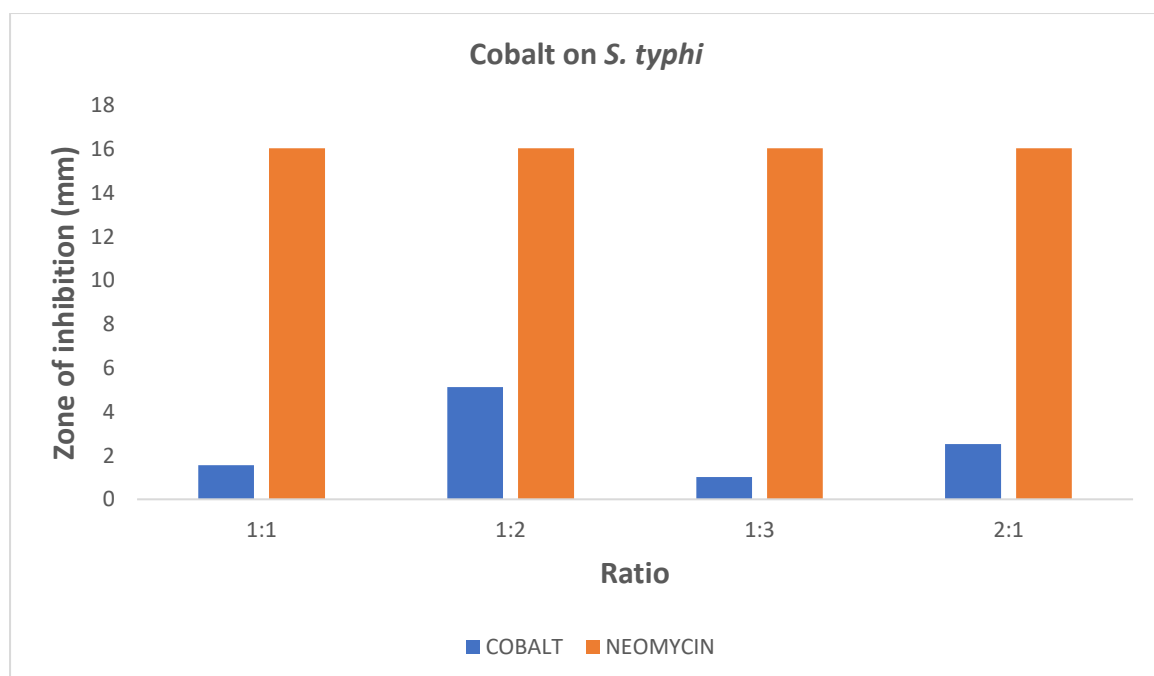


Figure 5.8: The mean inhibition diameter of Cobalt nanoparticles and neomycin on *S. typhi*

The above column on Figure 5.8 is a graphic representation of the mean results for well diffusion method, comparing the zone of inhibition between Cobalt and Amphotericin B. After conducting student t- test statistical analysis the two tailed P value was 0.0001 and the mean of cobalt minus neomycin was -14.2275. At 95% confidence interval the difference was between -15.5111 to -13.0439. The intermediate values used in the calculations were as follows, $t = 25.7804$, $df = 14$ and standard error of difference = 0.552. Table 5.2 below depicts statistical calculation from the t-test (Kumar *et al.*, 2013).

Table 5.2: The difference in median values of *S. typhi* treated with Cobalt and Neomycin

Group	Cobalt	Neomycin
Mean	1.7525	15.9800
SD	1.5596	0.0641
SEM	0.5514	0.0227
N	8	8

5.4.3 Cobalt on *S. sonnei*

Cobalt also showed inhibition of *S. sonnei*. It showed zone of inhibition measuring 2.16 mm compared to neomycin which measured about 12.3 mm. The difference was considered to be extremely statistically significant at $p = 0.0001$. Figure 5.9 below depicts the mean distribution of cobalt and neomycin against the growth of *S. sonnei*.

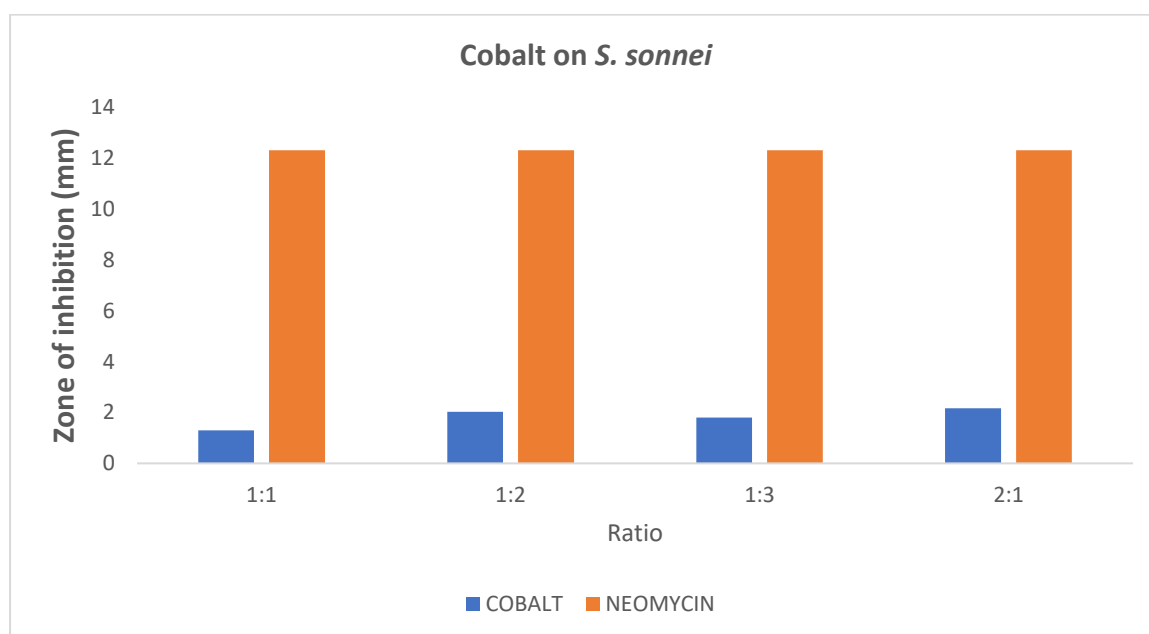


Figure 5.9: The mean inhibition diameter of cobalt nanoparticles and neomycin on *S. sonnei*

Figure 5.9 above is a graphic representation of the mean results for well diffusion method, comparing the zone of inhibition between cobalt and neomycin. After conducting student t-test statistical analysis the two tailed P value was 0.0001 and the mean of cobalt minus neomycin was -10.4875. At 95% confidence interval, the difference was from -11.0525 to -9.9225. The intermediate values used in the calculations were as follow, $t = 39.8103$, $df = 14$ and standard error of difference = 0.263. Table 5.3 below depicts statistical calculation from the t-test.

Table 5.3: The difference in median values of *S. sonnei* treated with Cobalt and Neomycin

Group	Cobalt	Neomycin
Mean	1.5915	12.0850
SD	0.7088	0.2298
SEM	0.2506	0.0813
N	8	8

5.4.4 Cobalt on *P. aeruginosa*

Cobalt showed the largest inhibition for *P. aeruginosa*. The zone of inhibition was 4.49 mm for the 1:3 ratio and 5.96 mm for the 2:1 ratio compare to 2.16 mm compared to neomycin which measured about 6.9 mm (Figure 5.10).

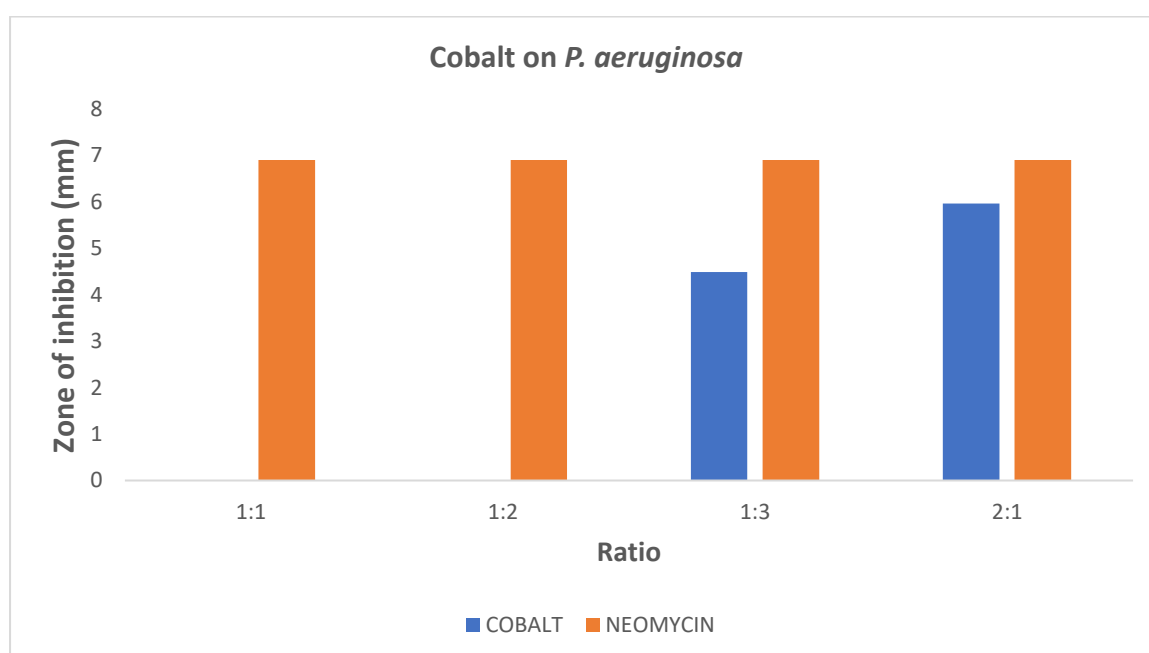


Figure 5.10: The mean inhibition diameter of cobalt nanoparticles and neomycin on *P. aeruginosa*

The conducting Student t- test statistical analysis the two tailed P value was 0.0001 and the mean of cobalt minus neomycin was -4.3037. At 95% confidence interval the difference was between -6.3505 to -2.2570. The intermediate values used in the calculations were as follows, $t = 4.5098$, $df = 14$ and standard error of difference = 0.954. Table 5.4 below depicts statistical calculation from the t-test (Okafor *et al.*, 2013).

Table 5.4: The difference in median values of *P. aeruginosa* treated with Cobalt and Neomycin

Group	Cobalt	Neomycin
Mean	2.2463	6.7900
SD	2.6966	0.1871
SEM	0.9534	0.0416
N	8	8

5.4.5 Cobalt for *S. enterica*

Cobalt showed a zone of inhibition against *S. enterica*. It showed a zone of inhibition measuring 3.62 mm compared to neomycin which measured about 11.4 mm. The difference was considered to be extremely statistically significant at $p = 0.0001$. Figure 5.11 below depicts the mean distribution of Cobalt and neomycin against *S. enterica*.

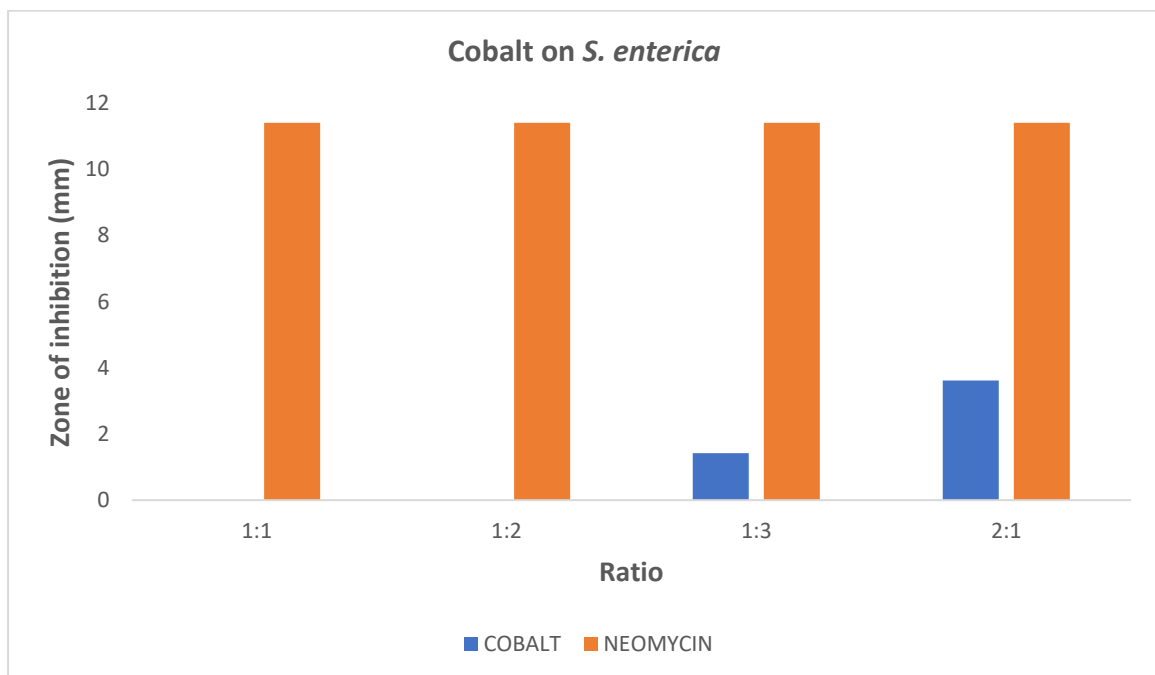


Figure 5.11: The mean inhibition diameter of cobalt nanoparticles and neomycin on *S. enterica*

The above column on figure 5.11 is a graphic representation of the mean results for well diffusion method, comparing the zone of inhibition between Cobalt and neomycin. After conducting Student t- test statistical analysis the two tailed P value was 0.0001 and the mean of cobalt minus neomycin was -10.2687. At 95% confidence interval the difference was from -11.3286 to -9.2089. The intermediate values used in the calculations were as follows, $t = 20.7813$, $df = 14$ and standard error of difference = 0.494. Table 5.5 below depicts statistical calculation from the t-test (Poole, 2004).

Table 5.5: The difference in median values of *S. enterica* treated with cobalt and Neomycin

Group	Cobalt	Neomycin
Mean	0.8963	11.1650
SD	1.3749	0.2512
SEM	0.4861	0.0888
N	8	8

5.4.6 Co/Urea on *E. coli*

Co/Urea depicted inhibition against *E. coli*. It showed a zone of inhibition measuring 2.69 mm compared to neomycin which measured about 8.46 mm. The difference was considered to be extremely statistically significant at $p = 0.0001$. Figure 5.12 below depicts the mean distribution of Co/Urea and neomycin against *E.coli*.

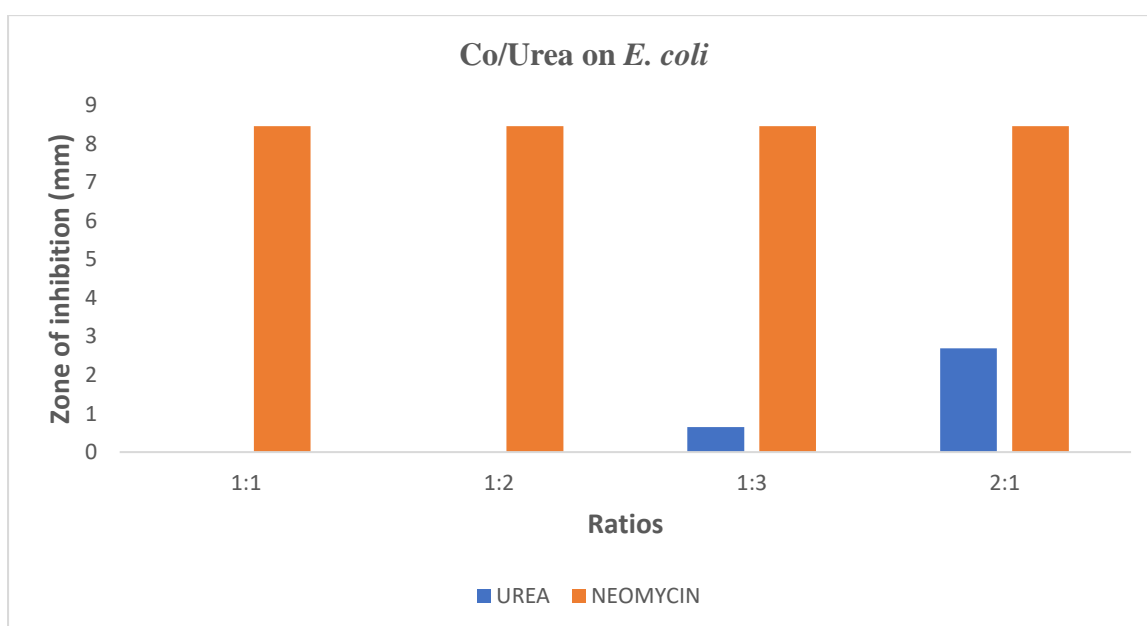


Figure 5.12: The mean inhibition diameter of Co/Urea nanoparticles and neomycin on *E.coli*

Figure 5.12 is a graphic representation of the mean results for well diffusion method, comparing the zone of inhibition between Co/Urea and neomycin. After conducting Student t-test statistical analysis the two tailed P value was 0.0001 and the mean of Co/Urea minus Neomycin was -7.4463. At 95% confidence interval the difference was from -8.2527 to -6.6398. The intermediate values used in the calculations were as follows, $t = 19.8027$, $df = 14$ and standard error of difference = 0.376. Table 5.6 below depicts statistical calculation from the t-test (Plaza *et al.*, 2013).

Table 5.6: The difference in median values of *E.coli* treated with Co/Urea and Neomycin

Group	Cobalt	Neomycin
Mean	0.7138	8.1600
SD	1.0140	0.3207
SEM	0.3585	0.1134
N	8	8

5.4.7 Co/Urea on *S. typhi*

Co/Urea showed a zone of inhibition against *S. typhi* although not comparable to that of neomycin. It showed zone of inhibition measuring 7.55 mm compared to neomycin which measured about 14.26 mm. The difference was considered to be extremely statistically significant at $p = 0.0001$. Figure 5.13 below depicts the mean distribution of Co/Urea and neomycin against *S.typhi*.

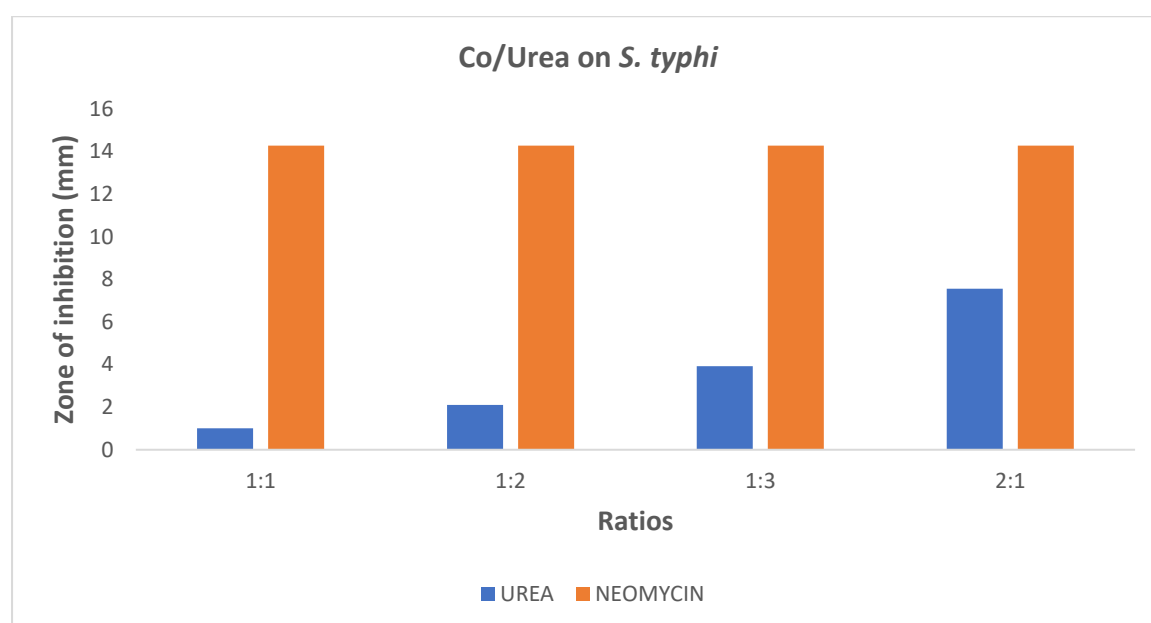


Figure 5.13: The mean inhibition diameter of Co/Urea nanoparticles and neomycin on *S.typhi*

Figure 5.13 is a graphic representation of the mean results for well diffusion method, comparing the zone of inhibition between Co/Urea and Neomycin. After conducting Student t-test statistical analysis the two tailed P value was 0.0001 and the mean of Cobalt/Urea minus neomycin was -0.1375. At 95% confidence interval the difference was from -9.6302 to -5.9223. The intermediate values used in the calculations were as follows, $t = 8.9964$, $df = 14$ and standard error of difference = 0.864. Table 5.7 below depicts statistical calculation from the t-test (Kumar *et al.*, 2013).

Table 5.7: The difference in median values of *S.typhi* treated with Co/Urea and neomycin

Group	Co/Urea	Neomycin
Mean	3.1338	10.9100
SD	2.2943	0.8445
SEM	0.8112	0.2986
N	8	8

5.4.8 Co/Urea on *S. sonnei*.

Co/Urea depicted a zone of inhibition against *S. sonnei*. It showed zone of inhibition measuring 2.17 mm compared to neomycin which measured about 10.84 mm. The difference was considered to be extremely statistically significant at $p = 0.0001$. Figure 5.14 below depicts the mean distribution of Urea and neomycin against *S. sonnei*.

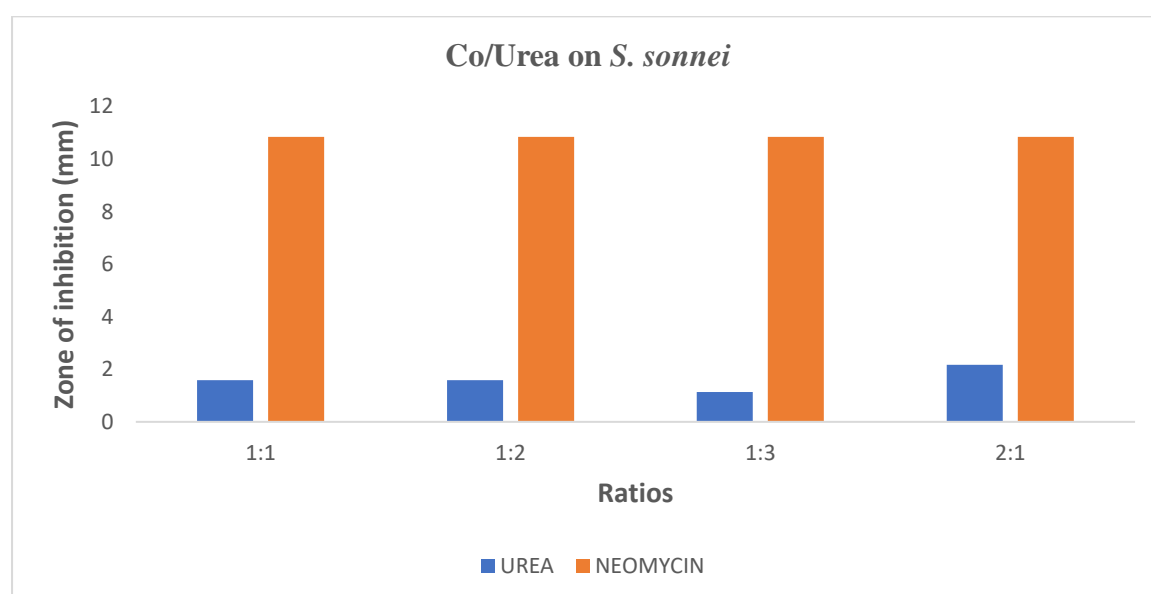


Figure 5.14: The mean inhibition diameter of Co/Urea nanoparticles and neomycin on *S. sonnei*

Figure 5.14 is a graphic representation of the mean results for well diffusion method, comparing the zone of inhibition between Co/Urea and neomycin. After conducting Student t-test statistical analysis the two tailed P value was 0.0001 and the mean of Co/Urea minus Neomycin was -9.2363. At 95% confidence interval the difference was from -9.6469 to -8.8256. The intermediate values used in the calculations were as follows, $t = 48.2353$, $df = 14$ and standard error of difference = 0.191. Table 5.8 below depicts statistical calculation from the t-test (Okafor *et al.*, 2013).

Table 5.8: The difference in median values of *S. sonnei* treated with Co/Urea and neomycin

Group	Urea	Neomycin
Mean	1.5588	10.7950
SD	0.5395	0.0481
SEM	0.1907	0.0170
N	8	8

5.4.9 Co/Urea on *P. aeruginosa*.

Co/Urea showed a zone of inhibition against *P. aeruginosa*. It showed zone of inhibition measuring 5.96 mm compared to neomycin which measured about 8.34 mm. By convention criteria, this difference was considered to be extremely statistically significant at $p = 0.0001$. Figure 5.15 below depicts the mean distribution of Co/Urea and neomycin against *P. aeruginosa*.

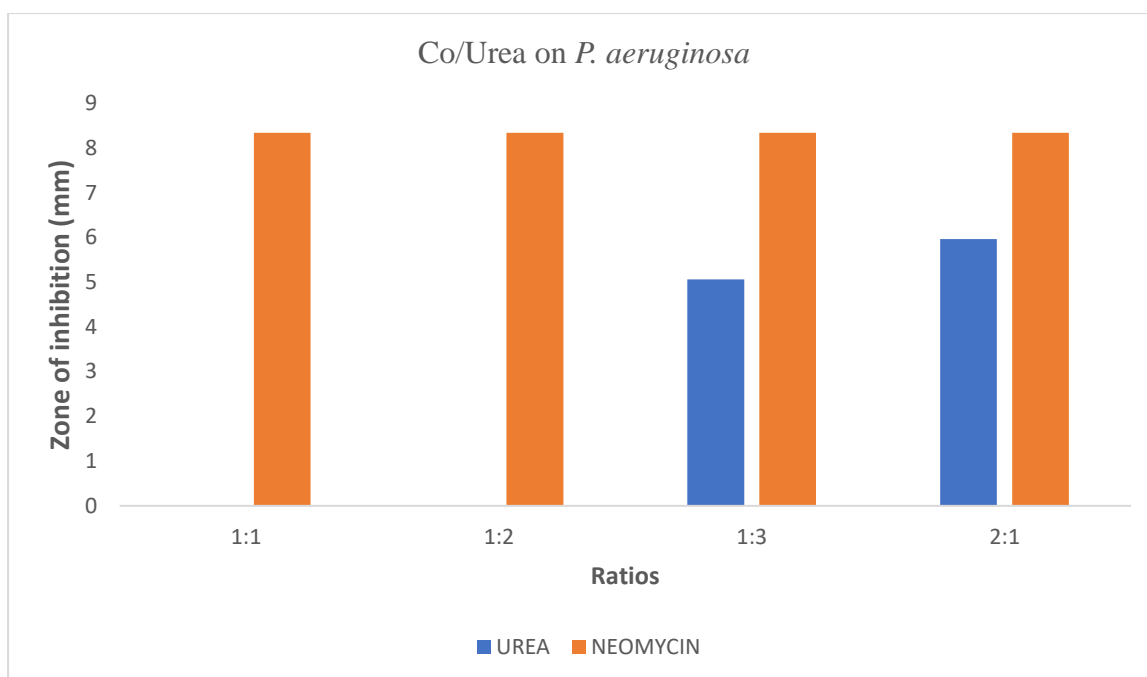


Figure 5.15: The mean inhibition diameter of urea nanoparticles and neomycin on *P. aeruginosa*

After conducting Student t- test statistical analysis the two tailed P value was 0.0001 and the mean of Co/Urea minus Neomycin was -5.3288. At 95% confidence interval the difference was between -7.4637 to -3.1938. The intermediate values used in the calculations were as follows, $t = 5.3534$, $df = 14$ and standard error of difference = 0.995. Table 5.9 below depicts statistical calculation from the t-test (Hardalo & Edberg, 1997).

Table 5.9: The difference in median values of *P. aeruginosa* treated with Co/Urea and Neomycin

Group	Co/Urea	Neomycin
Mean	2.5713	7.9000
SD	2.7758	0.4704
SEM	0.9814	0.1663
N	8	8

5.4.10 Co/Urea on *S. enterica*.

Co/Urea showed a zone of inhibition against *S. enterica*. It showed zone of inhibition measuring 4.58 mm compared to Neomycin which measured about 14.36 mm. The difference

was considered to be extremely statistically significant at $p = 0.0001$. Figure 5.16 below depicts the mean distribution of Co/Urea and neomycin against *S. enterica*.

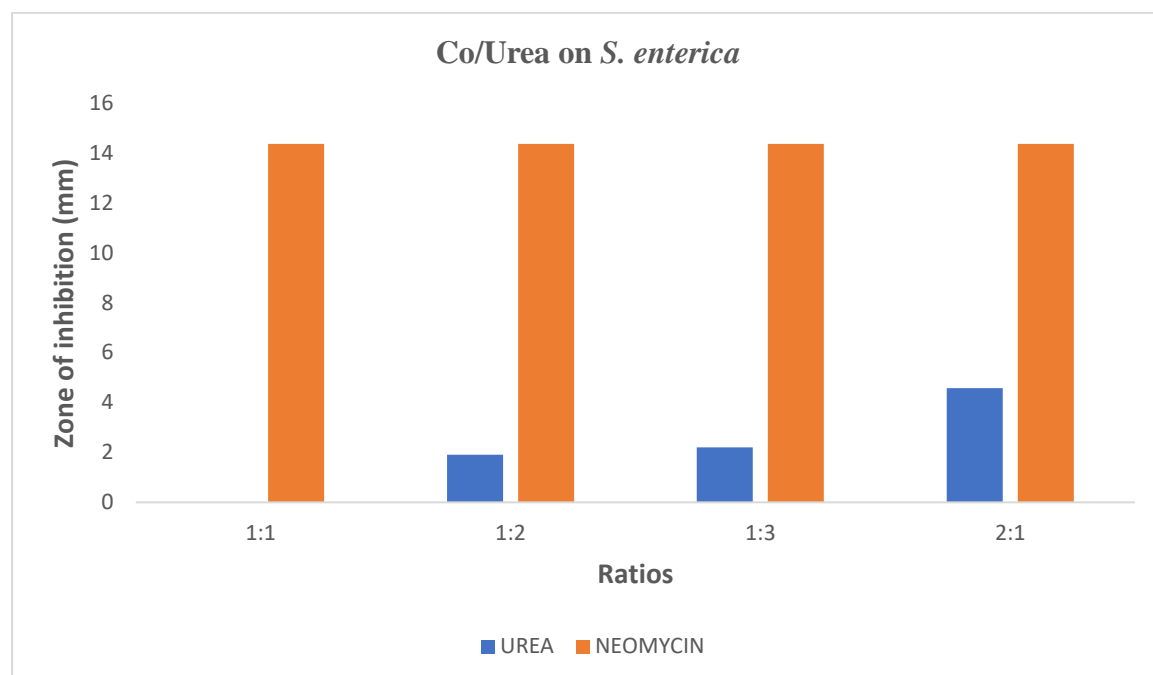


Figure 5.16: The mean inhibition diameter of Co/urea nanoparticles and neomycin on *S. enterica*

After conducting student t- test statistical analysis the two tailed P value was 0.0001 and the mean of Urea minus neomycin was -10.7975. At 95% confidence interval the difference was from -12.7866 to -8.8084. The intermediate values used in the calculations were as follow, $t = 11.6425$, $df = 14$ and standard error of difference = 0.927. Table 5.10 below depicts statistical calculation from the t-test (Poole, 2004).

Table 5.10: The difference in median values of *S. enterica* treated with Co/Urea and Neomycin

Group	Co/Urea	Neomycin
Mean	1.6225	12.4200
SD	1.6061	2.0739
SEM	0.5679	0.7333
N	8	8

5.4.11 Co/Thiourea on *E. coli*.

Figure 5.17 below, is a graphic representation of the mean results for well diffusion method, comparing the zone of inhibition between Co/Thiourea and neomycin. Co/Thiourea depicted a positive zone of inhibition against *E. coli*. It showed zone of inhibition measuring 3.48 mm compared to neomycin which measured about 11.13 mm. The difference was considered to be extremely statistically significant at $p = 0.0001$. Figure 5.17 below depicts the mean distribution of Co/Thiourea and neomycin against *E. coli*.

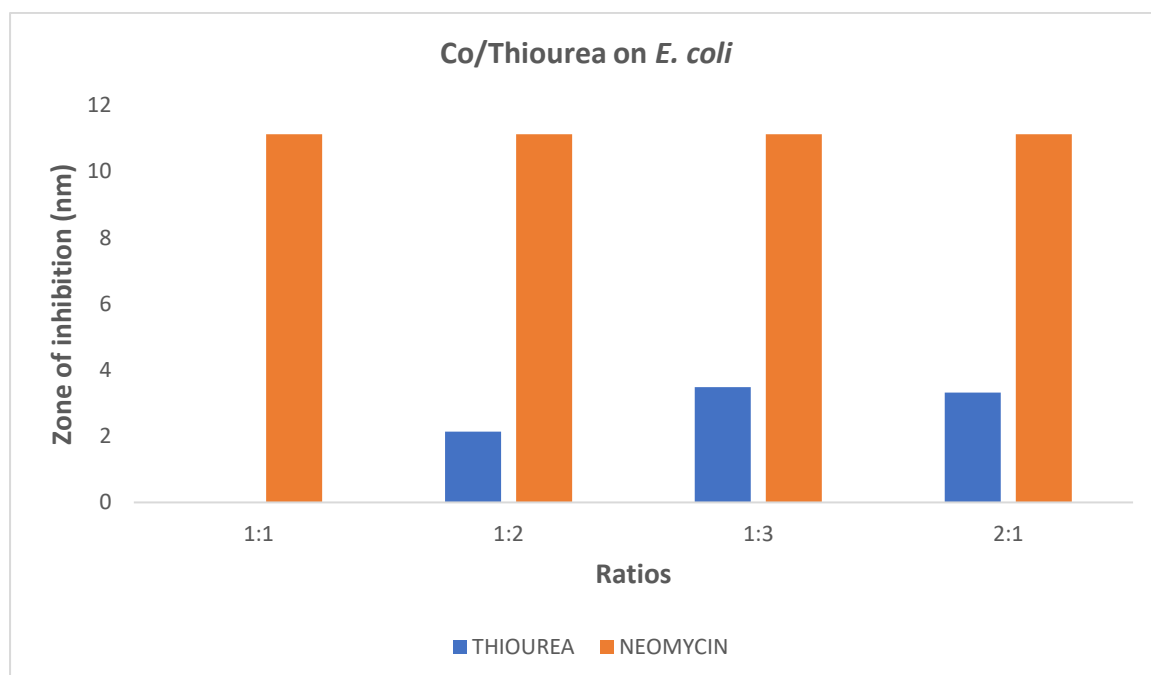


Figure 5.17: The mean inhibition diameter of Co/thiourea nanoparticles and neomycin on *E.coli*

After conducting Student t- test statistical analysis the two tailed P value was 0.0001 and the mean of Co/Thiourea minus neomycin was -7.2025. At 95% confidence interval the difference was from -9.1031 to -5.3019. The intermediate values used in the calculations were as follows, $t = 8.1279$, $df = 14$ and standard error of difference = 0.0886. Table 5.11 below depicts statistical calculation from the t-test (Plaza *et al.*, 2013).

Table 5.11: The difference in median values of *E.coli* treated with Co/thiourea and neomycin

Group	Co/Thiourea	Neomycin
Mean	2.3575	9.5600
SD	1.8614	1.6784
SEM	0.6581	0.5934
N	8	8

5.4.12 Co/Thiourea on *S. typhi*.

The histogram, Figure 5.18, is a graphic representation of the mean results for well diffusion method, comparing the zone of inhibition between Co/Thiourea and neomycin. Co/Thiourea showed a positive zone of inhibition against *S. typhi*. It reflected the largest zone of inhibition measuring 6.55 mm compared to neomycin which measured about 14.26 mm. The difference was considered to be extremely statistically significant at $p = 0.0001$. Figure 5.18 below depicts the mean distribution of Thiourea and neomycin against *S. typhi*.

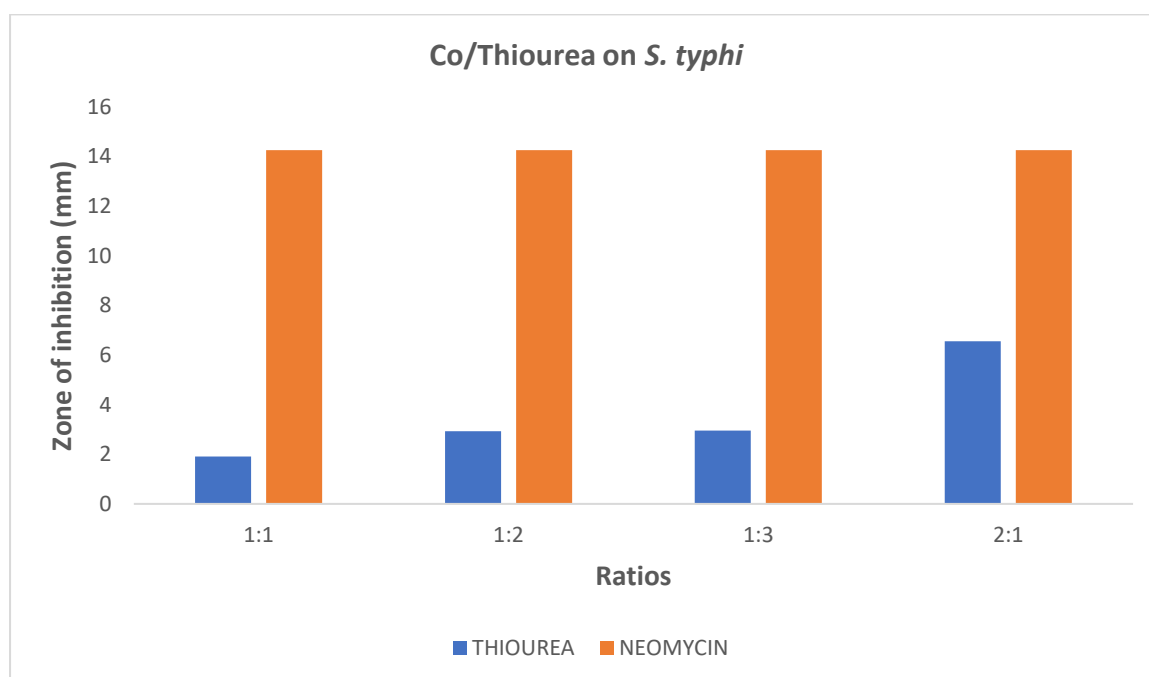


Figure 5.18: The mean inhibition diameter of Co/Thiourea nanoparticles and neomycin on *S.typhi*

After conducting Student t- test statistical analysis the two tailed P value was 0.0001 and the mean of Thiourea minus neomycin was -10.9425. At 95% confidence interval the difference was between -12.3977 to -9.4873. The intermediate values used in the calculations were as

follows, $t = 16.1275$, $df = 14$ and standard error of difference = 0.679. Table 5.12 below depicts statistical calculation from the t-test (Okafor *et al.*, 2013).

Table 5.12: The difference in median values of *S.typhi* treated with Co/thiourea and Neomycin

Group	Co/Thiourea	Neomycin
Mean	3.3175	14.2600
SD	1.9191	0.0000
SEM	0.6785	0.0000
N	8	8

5.4.13 Co/Thiourea on *S. sonnei*.

Figure 5.19 is a graphic representation of the mean results for well diffusion method, comparing the zone of inhibition between Co/Thiourea and neomycin. Co/Thiourea showed a zone of inhibition against *S. sonnei*. It showed zone of inhibition measuring 4.61 mm compared to neomycin which measured about 10.99 mm. The difference was considered to be extremely statistically significant at $p = 0.0001$. Figure 5.19 below depicts the mean distribution of Thiourea and neomycin against *S. sonnei*.

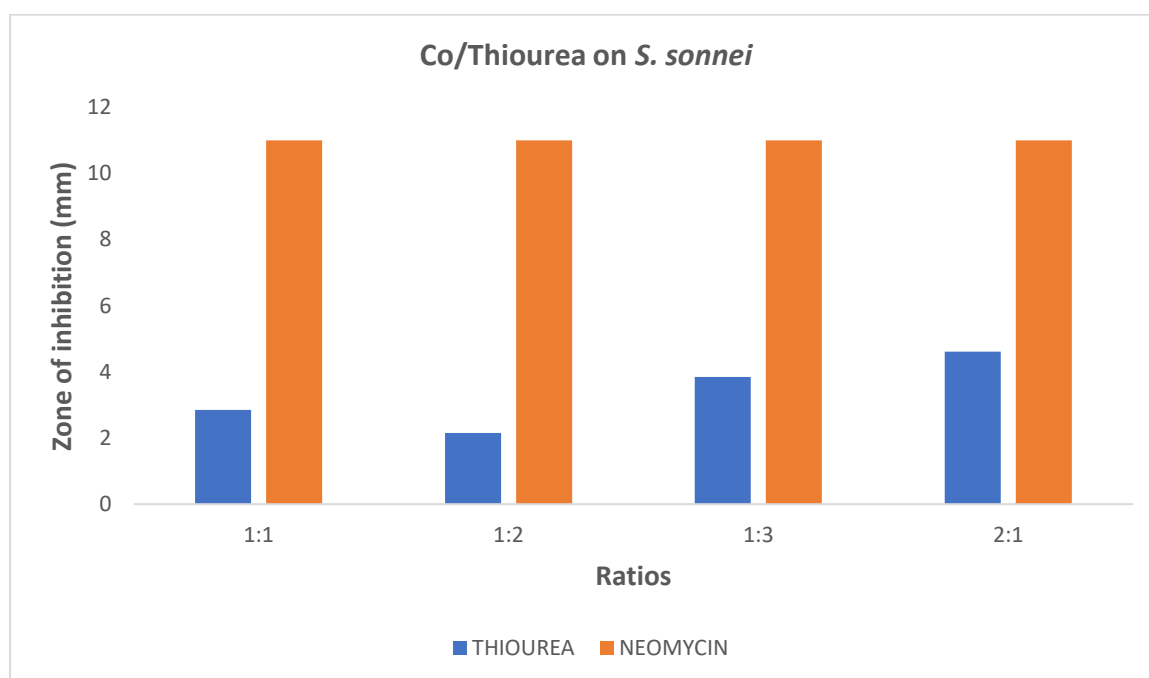


Figure 5.19: The mean inhibition diameter of Co/thiourea nanoparticles and neomycin on *S.sonnei*

After conducting student t- test statistical analysis the two tailed P value was 0.0001 and the mean of Co/Thiourea minus neomycin was -7.2763. At 95% confidence interval the difference

was between -8.0632 to -6.4893. The intermediate values used in the calculations were as follow, $t = 19.8299$, $df = 14$ and standard error of difference = 0.367. Table 5.13 below depicts statistical calculation from the t-test (Okafor *et al.*, 2013).

Table 5.13: The difference in median values of *S. sonnei* treated with Co/thiourea and Neomycin

Group	Co/Thiourea	Neomycin
Mean	3.1525	10.4288
SD	0.8836	0.5444
SEM	0.3124	0.1925
N	8	8

5.4.14 Co/Thiourea on *P. aeruginosa*

Co/Thiourea showed a zone of inhibition against *P. aeruginosa*. It showed zone of inhibition measuring 4.78 mm compared to neomycin which measured about 6.11 mm. The difference was considered to be extremely statistically significant at $p = 0.0001$. Figure 5.20 below depicts the mean distribution of Co/Thiourea and neomycin against *P. aeruginosa*.

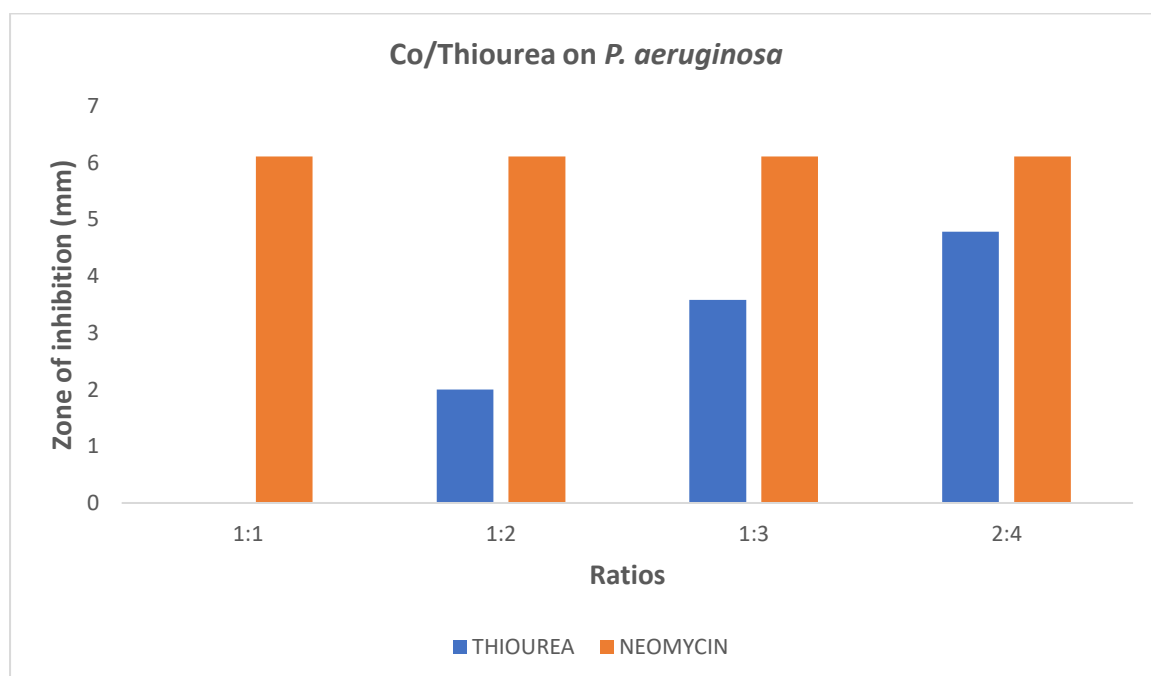


Figure 5.20: The mean inhibition diameter of Co/Thiourea nanoparticles and neomycin on *P. aeruginosa*

After conducting Student t- test statistical analysis the two tailed P value was 0.0001 and the mean of Co/Thiourea minus neomycin was -4.5500. At 95% confidence interval the difference was between -5.9652 to -3.1348. The intermediate values used in the calculations were as follows, $t = 6.8956$, $df = 14$ and standard error of difference = 0.660. Table 5.14 below depicts statistical calculation from the t-test (Botzenhart & Doring, 1993).

Table 5.14: The difference in median values of *P. aeruginosa* treated with Co/Thiourea and Neomycin

Group	Co/Thiourea	Neomycin
Mean	2.2400	6.7900
SD	1.8626	0.1176
SEM	0.6585	0.0416
N	8	8

5.4.15 Co/Thiourea on *S. enterica*

Co/Thiourea showed a zone of inhibition against *S. enterica*. It showed zone of inhibition measuring 3.42 mm compared to neomycin which measured about 15.98 mm. The difference was considered to be extremely statistically significant at $p = 0.0001$. Figure 5.21 below depicts the mean distribution of Thiourea and neomycin against *S. enterica*.

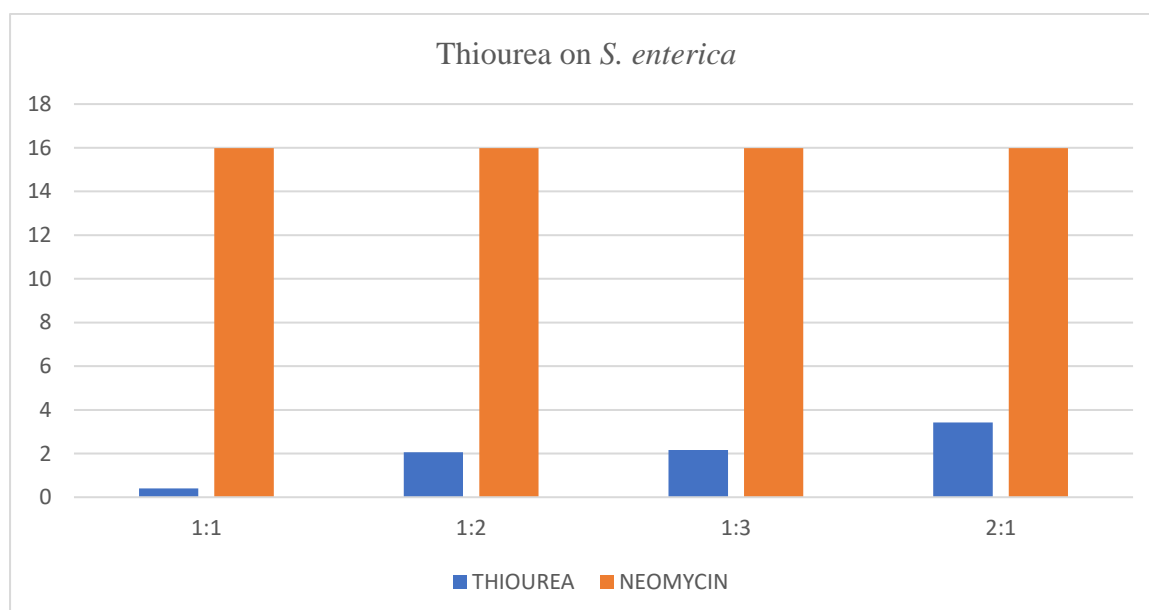


Figure 5.21: The mean inhibition diameter of Co/thiourea nanoparticles and neomycin on *S. enterica*

After conducting Student t- test statistical analysis the two tailed P value was 0.0001 and the mean of Co/Thiourea minus neomycin was -11.8100. At 95% confidence interval the difference was from -14.1435 to -9.4765. The intermediate values used in the calculations were as follows, $t = 10.8547$, $df = 14$ and standard error of difference = 1.088. Table 5.15 below depicts statistical calculation from the t-test.

Table 5.15: The difference in median values of *S. enterica* treated with Co/Thiourea and neomycin

Group	Co/Thiourea	Neomycin
Mean	1.5400	13, 3500
SD	1.2510	2.8116
SEM	0.4423	0.9940
N	8	8

5.5 Antifungal activities of nanoparticles

The antifungal activities of nanoparticles were analysed and compared with positive controls in the form of neomycin and Amphotericin B. Bar charts were constructed using Microsoft Excel 2016. Student t-test was used to statistically analyse the *in-vitro* data obtained during this study.

5.5.1 Cobalt on *Aspergillus. niger*.

Cobalt showed inhibition against *A. niger*. It showed zone of inhibition measuring 2.30 mm compared to Amphotericin B which measured about 2.75 mm. There was no statistical significant difference between the Cobalt and Amphotericin B with regards to zone of inhibition ($p = 0.0921$). Figure 5.22 below depicts the mean distribution of effects Cobalt and Amphotericin B against *A. niger* growth inhibition (Gade *et al.*, 2008).

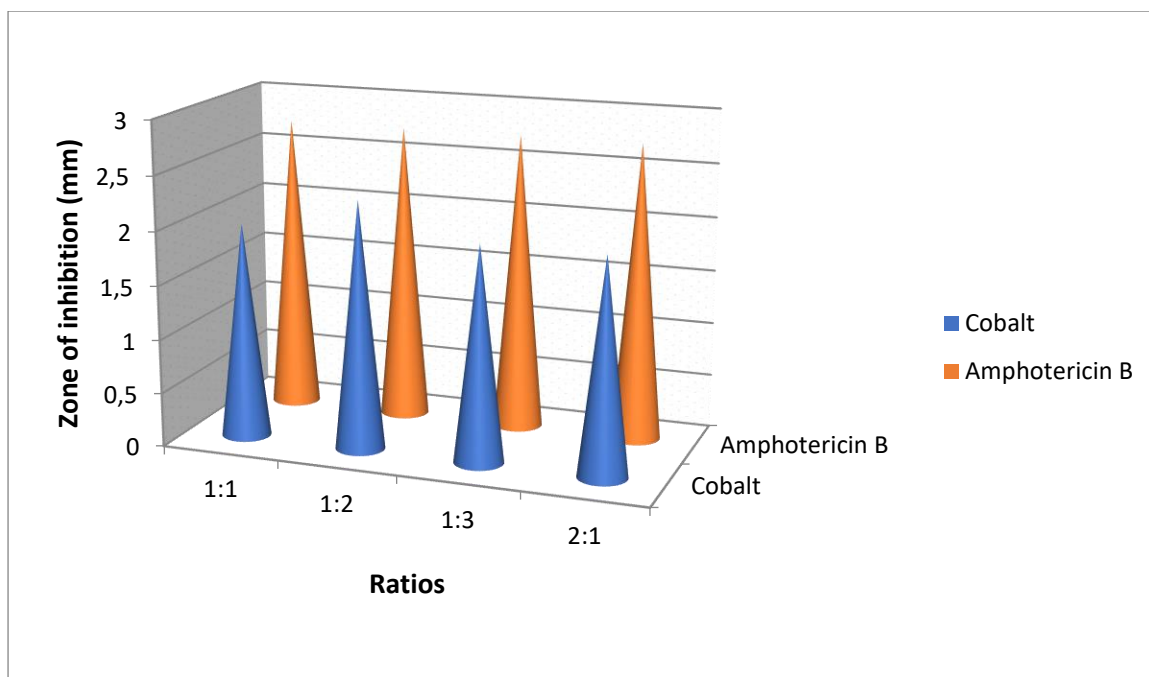


Figure 5.22: The mean inhibition diameter of cobalt nanoparticles and amphotericin B on *A. niger*

The above 3-D cone column on Figure 5.22 is a graphic representation of the mean results for well diffusion method, comparing the zone of inhibition between Cobalt and Amphotericin B. After conducting Student t- test statistical analysis the two tailed P value was 0.0921 and the mean of Cobalt minus Amphotericin B was -0.1375. At 95% confidence interval the difference was from -0.3006 to 0.0256. The intermediate values used in the calculations were as follows, $t = 1.8084$, $df = 14$ and standard error of difference = 0.076. Table 5.16 below depicts statistical calculation from the t-test.

Table 5.16: The difference in median values of *A. niger* treated with Cobalt and Amphotericin B

Group	Cobalt	Amphotericin B
Mean	2.63	4.00
SD	1.60	0.00
SEM	0.56	0.00
N	8	8

5.5.2 Co/Urea *Aspergillus niger*.

Co/urea showed inhibition against *A. niger*. It showed zone of inhibition measuring 2.63mm compared to Amphotericin B which measured about 4.00. There was statistical significant difference between the Urea and Amphotericin B with regards to zone of inhibition against *A. niger* ($p = 0.0289$). Figure 5.23 below depicts the mean distribution of Urea and Amphotericin B against *A. niger*.

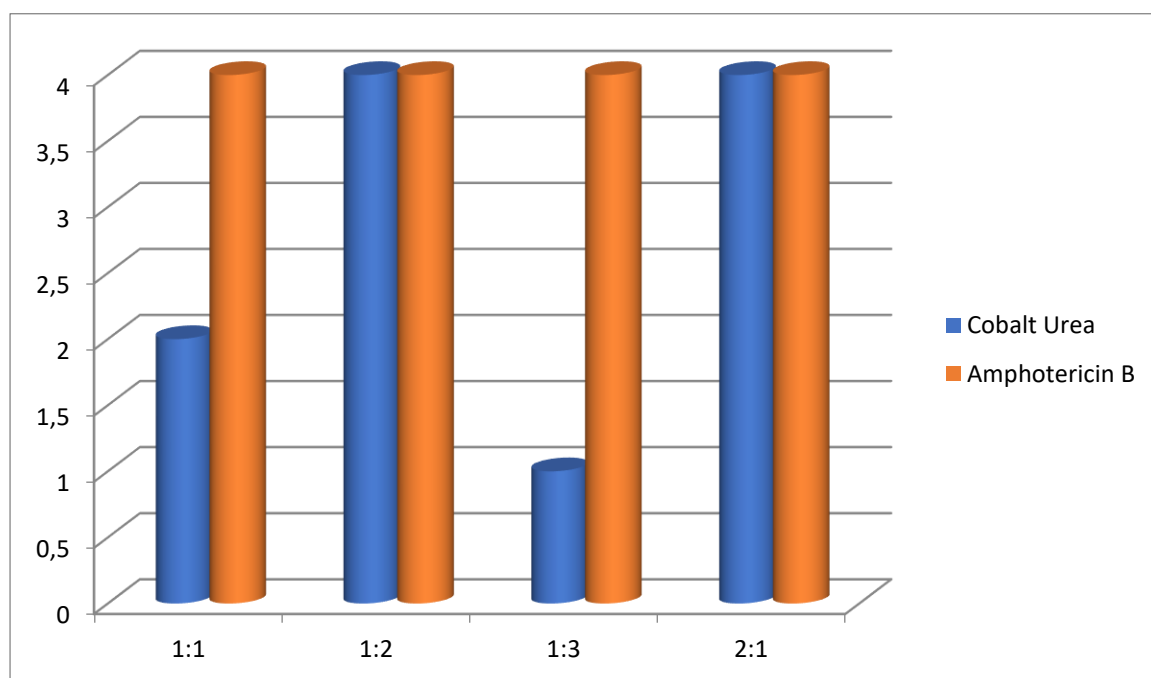


Figure 5.23: The mean inhibition diameter of urea nanoparticles and neomycin on *A.niger*

The above column on figure 5.23 is a graphic representation of the mean results for well diffusion method, comparing the zone of inhibition between Urea and amphotericin B. After conducting Student t- test statistical analysis the two tailed P value was 0.0921. The mean of Urea minus Amphotericin B was -1.38. The t-test value was $t = 2.4337$ with $df = 14$ and standard error of difference = 0.565. At 95% confidence interval the difference was between - 2.59 to -0.16. Table 5.15 below depicts statistical calculation from the t-test.

Table 5.17: The difference in median values of *A.niger* treated with Urea and Amphotericin B

Group	Co/urea	Amphotericin B
Mean	2.63	4.00
SD	1.60	0.00
SEM	0.56	0.00
N	8	8

5.5.3 Co/Thiourea on *Aspergillus niger*.

Co/Thiourea depicted inhibition against *A. niger*. It showed zone of inhibition measuring 5.380 mm compared to Amphotericin B which measured about 4.00. There was no statistically significant difference between Co/Thiourea and Amphotericin ($p = 0.0537$). Figure 5.24 below depicts the mean distribution of Co/Thiourea and Amphotericin B against *A. niger* (Gade *et al.*, 2008).

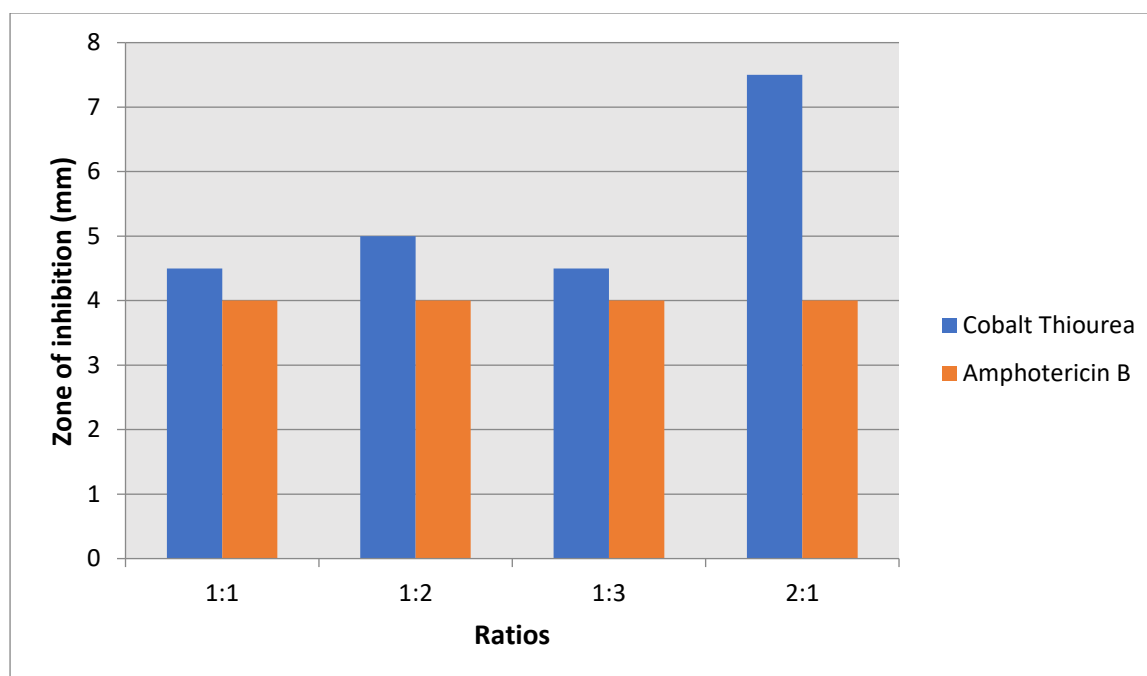


Figure 5.24: The mean inhibition diameter of Co/thiourea nanoparticles and amphotericin B on *A. niger*

The above histogram column on Figure 5.24 is a graphic representation of the mean results for well diffusion method, comparing the zone of inhibition between Co/Thiourea and

Amphotericin B. After conducting Student t- test statistical analysis the two tailed P value was 0.0537 and the mean of Co/Thiourea minus Amphotericin B was -1.38. At 95% confidence interval the difference was between -0.03 to 2.78. The intermediate values used in the statistical analysis are $t = 2.1058$, $df = 14$ and standard error of difference = 0.653. Table 5.18 below depicts statistical calculation from the t-test.

Table 5.18: The difference in median values of *A. niger* treated with Co/Thiourea and Amphotericin B

Group	Co/Thiourea	Amphotericin B
Mean	5.38	4.00
SD	1.51	1.07
SEM	0.53	0.38
N	8	8

5.5.4 Cobalt on *C. albicans*.

Cobalt depicted inhibition against *C. albicans*. It showed zone of inhibition measuring 2.50 mm compared to Amphotericin B which measured about 1.50 ($p = 0.6971$). This difference is considered to be not statistically significant. Figure 5.26 below illustrate the well diffusion results (Seil & Webster, 2012).

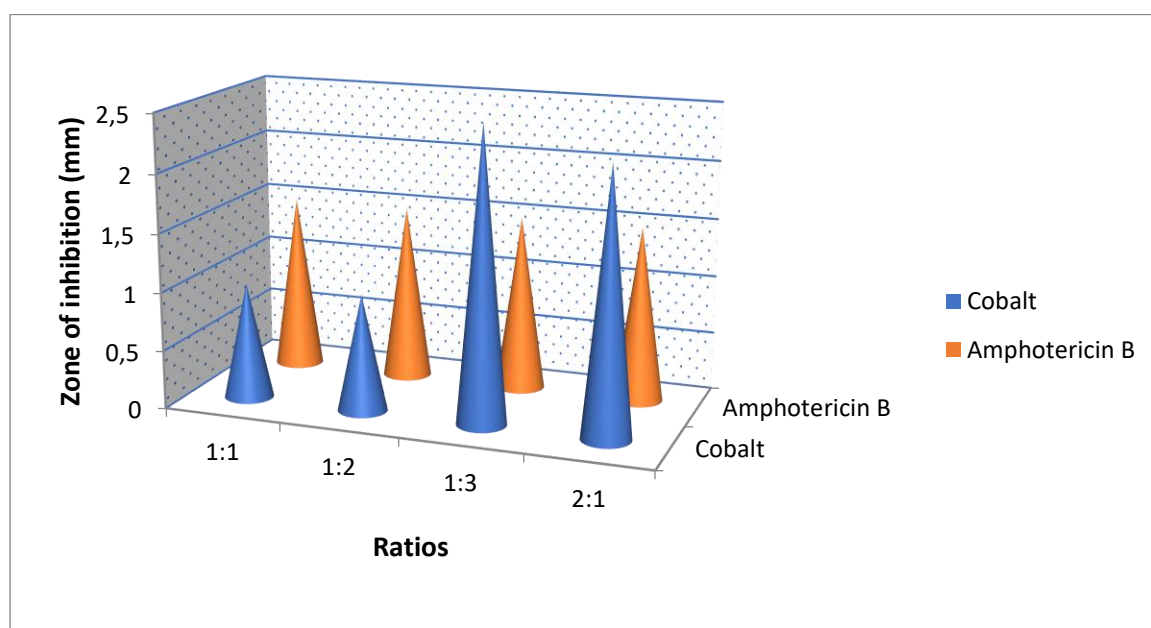


Figure 5.25: The mean inhibition diameter of cobalt nanoparticles and amphotericin on *C. albicans*

The above 3-D cone column on Figure 5.25 is a graphic representation of the mean results for well diffusion method, comparing the zone of inhibition between Cobalt and amphotericin B. After conducting Student t- test statistical analysis the two tailed P value was 0.6971 and the mean of Cobalt minus Amphotericin B was -0.1375. At 95% confidence interval the difference was from -0.825 to 1.200. The t value was $t = 0.3974$. The intermediate values used in calculations were as follows; $t = 0.3974$, $df = 14$ and standard of difference = 0.472. Table 5.19 below depicts statistical calculation from the t-test.

Table 5.19: The difference in median values of *C. albicans* treated with Cobalt and Amphotericin B

Group	Cobalt	Amphotericin B
Mean	1.688	1.500
SD	1.22	0.535
SEM	0.432	0.189
N	8	8

5.5.5 Co/Urea on *C. albicans*.

Co/Urea showed inhibition against *C. albicans*. It reflected the largest zone of inhibition measuring 2.88 mm compared to Amphotericin B which measured about 3.50 (P value = 0.3822). This difference is considered to be not statistically significant. Figure 5.27 below illustrate the well diffusion results.

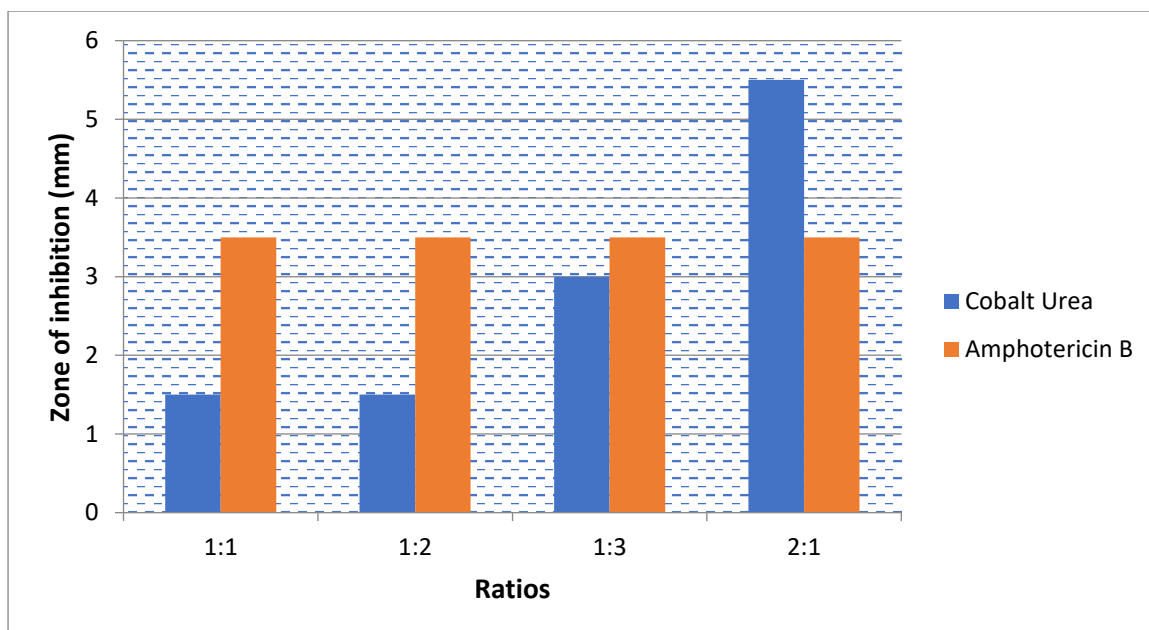


Figure 5.26: The mean inhibition diameter of Co/Urea nanoparticles and amphotericin B *C.albicans*

The above column on Figure 5.27 is a graphic representation of the mean results for well diffusion method, comparing the zone of inhibition between Co/Urea and amphotericin B. After conducting Student t- test statistical analysis the two tailed P value was 0.3822 and the mean of Co/Urea minus Amphotericin B was -0.63. At 95% confidence interval the difference was from -2.11 to 0.86. The t value was $t = 1.8084$. The intermediate values used in the calculations were as follows, $t = 0.9022$, $df = 14$ and standard error of difference = 0.693. Table 5.20 below depicts statistical calculation from the t-test.

Table 5.20: The difference in median values of *C. albicans* treated with Co/Urea and Amphotericin B

Group	Co/Urea	Amphotericin B
Mean	2.88	3.50
SD	1.89	0.53
SEM	0.67	0.19
N	8	8

5.5.6 Co/Thiourea on *C. albicans*.

Co/Thiourea showed inhibition against *C. albicans*. It showed zone of inhibition measuring 2.63 mm compared to Amphotericin B which measured about 3.00 mm (P value = 0.6849).

This difference is considered to be not statistically significant. Figure 5.28 below illustrate the well diffusion results.

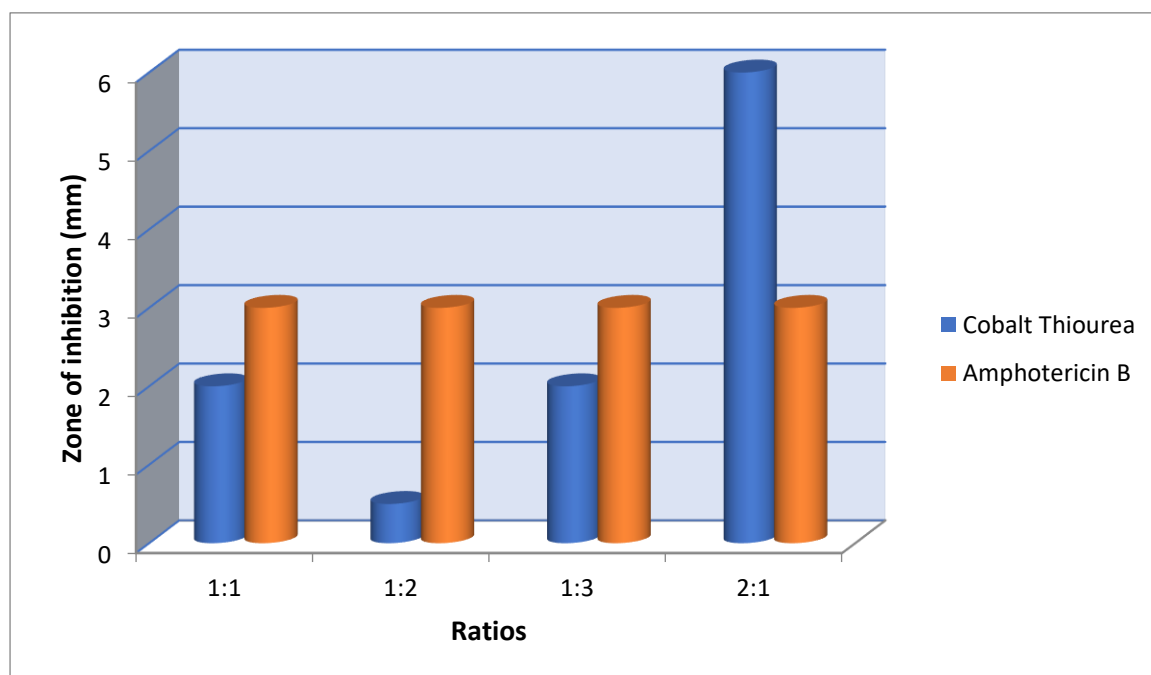


Figure 5.27: The mean inhibition diameter of Co/Thiourea and Amphotericin B on *C.albicans*

The above column on Figure 5.27 is a graphic representation of the mean results for well diffusion method, comparing the zone of inhibition between Co/Thiourea and Amphotericin B. After conducting Student t- test statistical analysis the two tailed P value was 0.6849 and the mean of Co/Thiourea minus Amphotericin B was -0.38. At 95% confidence interval the difference was between -2.32 to 1.57. The intermediate values used in the calculations were as follows, $t = 0.4143$, $df = 14$ and the standard error of difference = 0.905. Table 5.21 below depicts statistical calculation from the t-test.

Table 5.21: The difference in median values of *C.albicans* treated with Co/Thiourea and Amphotericin B

Group	Co/Thiourea	Amphotericin B
Mean	2.63	3.00
SD	2.33	1.07
SEM	0.82	0.38
N	8	8

CHAPTER 6

CONCLUSION AND RECOMMENDATIONS

6.1 INTRODUCTION

In this chapter the researcher will discuss the research findings, then describe the limitations of this study, and lastly make recommendations based on the research findings.

6.2 SUMMARY AND INTERPRETATION OF RESEARCH FINDINGS

The study was carried out to synthesis, characterize and investigate antimicrobial properties of Cobalt, Co/Urea and Co/Thiourea nanoparticles on five Gram-negative—*Escherichia coli*, *Pseudomonas aeruginosa*, *Salmonella enterica*, *Salmonella typhi* and *Shigella sonnei* bacteria; and two fungal strains—*Aspergillus niger* and *Candida albicans*.

6.2.1 CHARACTERIZATION OF COBALT, Co/UREA AND Co/THIOUREA

Cobalt and cobalt complexes based on urea and thiourea were successfully synthesized. All complexes were obtained in reasonable yields, easy to prepare and very stable. The complexes were analysed optically and structurally by several spectroscopic techniques such as UV-Vis, PL, FTIR, TEM, SEM, XRD and TGA.

Morphology demonstrated the size of the particles with different concentration as well as the size distribution. The Co particles are in a mixture of rod, agglomerates with irregular shapes around 50 – 100 nm in diameter. The Co/Thiourea particles appear to be around 10 – 30 nm in size. The Co complexed with Urea images showed what appear to be spherical to hexagonal shape with 50 nm size in diameter.

The UV-Vis absorption band edges for Co and Co/Urea are blue shifted to their bulk band-edges whereas the absorption band edges of the core-shells nanoparticles are red-shifted from low to high concentration all as results of quantum confinement. Photoluminescence spectra show a red shift from their respective band edges, however Co/Thiourea is blue shifted from their respective band edges as results of irregular shapes and agglomeration of nanoparticles. XRD matches well with TEM and SEM, broader and narrow peaks favouring small and larger particles respectively.

Thermogravimetric analyses of all the complexes were conducted to check the stability of use as reagents for nanoparticles at low and high temperature. Complexes start to decompose at

low temperature about 100°C and the last decomposition step was at about 800-900°C, which is convenient to thermal decomposition of precursors in high boiling solvents.

6.2.2 ANTIBACTERIAL PROPERTIES OF COBALT, UREA AND THIOUREA

The antibacterial properties of Cobalt, Urea and Thiourea were tested against five Gram-negative—*Escherichia coli*, *Pseudomonas aeruginosa*, *Shigella enterica*, *Salmonella typhi* and *Salmonella sonnei*; human pathogenic bacteria. However, Cobalt showed a positive consistent zone of inhibition against *S. typhi* and *S. sonnei* growth production. *E. coli* showed to be the most resistant bacteria against Cobalt with an inhibitory zone ranging from 0.58 mm (at 1:2) to 0.76 mm (at 2:1). Second to *E. coli* was *S. enterica* with growth inhibition from 1.42 mm (at 1:3) to 3.62 mm (at 2:1). *P. aeruginosa* was inhibited by Cobalt 1:2 (measured 4.9 mm) and Cobalt 2:1 which measured 5.6 mm. The results of this study is contradictory to a study conducted by Schade (1949) who demonstrated the antibacterial activity of Cobalt on the growth of a number of Gram-positive and Gram-negative bacteria tested, the minimal inhibitory concentration of Cobalt varied from 1 to 100 parts per million.

Co/Urea showed a positive inhibition ranging from 1.3 mm to 2.1 mm at ratio 1:3 and 2:1 respectively. It showed dose dependent relationship with *S. typhi* and *S. enterica*. Urea showed a larger zone of inhibition measuring 5.06 mm and 5.96 mm at ratio 1:3 and 2:1 respectively.

Co/Thiourea showed a positively zone of inhibition against all five organisms studied. These results are very encouraging although they are not statistically comparable with the zone of inhibition yielded by neomycin which acted at a positive control. These results are supported by Glory and co-workers (2016) who demonstrated that Urea and Thiourea derivatives have gained research interest due to their different biological and pharmacological activities such as anti-bacterial anti-proliferative, antiviral, anti-cancer, anti-inflammatory and insecticidal properties.

6.2.3 ANTIFUNGAL PROPERTIES OF COBALT, Co/UREA AND Co/THIOUREA

Cobalt showed dose dependent zone of inhibition against both *A. niger* and *C. albicans* that are statistically comparable to Amphotericin B. This result can be observed from statistical calculation and column bar showed on chapter 5 above.

Urea was not comparable to Amphotericin B when tested against the growth of *A. niger*. Although it showed comparable zone of inhibition at ratio 1:2 (4 mm) and 2:1 (4 mm) it was overall not comparable to the mean inhibition of the positive control. However, it was

comparable to Amphotericin B when tested against *C. albicans*, where there was no statistical difference between the Urea and Amphotericin B.

Thiourea was highly effective against *C. albicans* where the zone of inhibition ranged from 4.5 mm at ratio 1:1 to 7.5 mm at ratio 2:1. There was a statistical difference between Thiourea and Amphotericin B. Thiourea was more effective than Amphotericin B in this case.

6.3 RECOMMENDATIONS

Due to the scope of the study it is not possible to make generalisation regarding the antibacterial and antifungal effects of Cobalt, Co/Urea and Co/Thiourea, the main recommendation is related to further research on this topic.

6.3.1 Recommendation regarding antibacterial properties

As the study only focused on *Escherichia coli*, *Pseudomonas aeruginosa*, *Salmonella enterica*, *Salmonella typhi* and *Shigella sonnei* pathogenic bacteria, it is therefore recommended that future studies be designed to include all bacteria found in wastewater.

6.3.2 Recommendation regarding the antifungal

It is recommended that a larger sample of pathogenic fungal strains found in water be investigated further before nanoparticles can be widely used to treat fungus in both wastewater and fresh drinking water.

6.3.3 Recommendation on study design

Research design that will include heavy metal testing and toxicity studies should be employed to further determine the use and safety of these nanoparticles.

6.4 CONTRIBUTIONS OF THE STUDY

Although the antibacterial results of doped cobalt, Co/urea and Co/thiourea do not show a statistically significance comparable neomycin, statistically significant antifungal properties of doped cobalt, Co/Urea and Co/Thiourea were observed when tested *in-vitro*. It also supports other studies which have showed the *in-vitro* antibacterial and antifungal effects of nanoparticles and possible use in water treatment and other spheres of health care. Since water contamination is a public health concern and since there is a drive to find new cheaper, effective and safer ways to treat wastewater and contaminated fresh water, it will be necessary that any potential agents be investigated with the aim of finding a solution towards treating wastewater and fresh contaminated water.

6.5 LIMITATIONS OF THE STUDY

This study encountered some limitations. The main limitations for this study as identified by the researcher include scope and research designs.

For the purposes of this study the researcher focused on synthesis, characterisation and evaluation of antimicrobial activity only on the selected applicable microorganisms, as it was difficult to cover all microbial common in wastewater and fresh water contaminations. Because the study focused on available at microbiology laboratory of the VUT, the results may not be generalizable to all different strains of microbial commonly found in wastewater. However, they can be used as a foundation for more sensitive research designs.

6.6 CONCLUDING REMARKS

In conclusion, Cobalt, Co/Urea and Co/Thiourea nanoparticles were synthesised, characterised and evaluated for their inhibitory activities on the growth of pathogenic bacteria and fungi. They have exhibited promising antibacterial and antifungal activity. Among the Cobalt, Co/Urea and Co/Thiourea nanoparticles: Co/Thiourea and Co/Urea nanoparticles have shown more activity compared to Cobalt nanoparticles. Cobalt, Co/Urea and Co/Thiourea have shown antifungal activity that is comparable to Amphotericin B in the inhibition of *C. albicans*. The nanoparticles of Cobalt showed no statistical difference against *A. niger* compared to Amphotericin B. Co/Urea was however, not comparable to Amphotericin B even though it had a positive zone of inhibition. However, Co/Thiourea was very effective as compared to Amphotericin B in inhibiting the *A. niger* growth. The most striking feature of this study is that nanoparticles Cobalt, Co/Urea and Co/Thiourea nanoparticles have antifungal activity comparable or incomparable (as in case of Co/Thiourea on *A. niger*) to Amphotericin B and; nearly promising antibacterial activity although not comparable to neomycin. Thus, the present findings provide new opportunity for the development of novel antimicrobials to overcome the ever-increasing problem of drug resistance.

REFERENCES

- Akpor, O.B. & Muchie, M. (2011). Environmental and Public Health implications of wastewater quality. *African journal of Biotechnology*. Vol 10(13): pp 2379-2387.
- Akpor, O.B., Ohiobor, G.O. & Olaolu, T.B. Heavy metals pollutants in wastewater effluents sources, effects and remediation. (2014). *Advances in Bioscience and Bioengineering*. Vol.2 (4): pp. 37-43.
- Amin, M.T., Alazba, A.A. & Manzoor, U. (2014). A Review of Removal of Pollutants from Water/Wastewater Using Different Types of Nanomaterial. *Advances in Materials Science and Engineering*. 2014. P. 1-24.
- Amutha, R., Mumghanadham, G.J. & Lee, J.J. (2011). Facile microwave-combustion synthesis of wurtzite Cd's nanoparticles journal of nanoscience & nanotechnology. Vol, 11.09. pp7940-7944
- Anderson, K., Rosemarin, A., Lamizana, B., Kvarnström, E., McConville, J., Seidu, R., Dickin, S. and Trimmer, C. (2016). *Sanitation, Wastewater Management and Sustainability: from Waste Disposal to Resource Recovery* Archived 1 June 2017 at the [Wayback Machine](#).. Nairobi and Stockholm: United Nations Environment Programme and Stockholm Environment Institute. [ISBN 978-92-807-3488-1](#), p. 56
- Anitha, p., Mohammad, T.H.N. & Mansoor, A.K. (2004). Response surface methodology for optimization and characterization of limonene-based coenzyme Q10 self-nanoemulsified capsule dosage form. 26 (10). pp. 1208.
- Annerberg, A., Hietala, S.F., Martensson, A., Ngasal, B., Cahlstrom, S., Premji, Z., Farnet, A., Gil, P., Bjorkman, A. & Ashton, M. (2010). Population pharmacokinetics and pharmacodynamics of artemether and lumefantrine during combination treatment in children with uncomplicated falciparum malaria in Tanzania. *Antimicrobial Agents Chemotherapy*. 54(11). pp.4780-4788.
- Ayanda, O.S., Petrik, L.F. (2014). Nanotechnology: The Breakthrough in Water and Wastewater Treatment, *International Journal of Chemical, Material and Environmental Research*. Pp. 1-2.
- Babbie, E. & Mouton, J. (2010). The practice of social Research 10th edition. Republic of South Africa. *Oxford University Press Southern Africa*. Capetown.

Balcht A & Smith R (1994). *Pseudomonas aeruginosa: Infections and Treatment. Informa Health Care*. pp. 83–84. [ISBN 0-8247-9210-6](#).

Balouiri, M., Bouhdid, E., Harki, E. (2015). Antifungal activity of Bacillus spp. Isolated from Calotropis procera AIT. Rhizosphere against *Candida albicans*. *Asian J. pham. Clin. Res.* 8. pp. 213-217

Bao, Y., Beerman, M., Pakhomov, A.B. & Kumar, C.S.S.R. (2005). Controlled crystalline structure and surface stability of cobalt nanocrystals. *Journal of Physics Chemistry B*. 109. p. 7220-7222.

Bhushan, B., Jung, Y.C. & Koch Kerstin (2009). *Phil. Trans. R.Soc.A*. 367. pp.1631-1672..
Roduner, E. (2006). Size matters: Why nanomaterials are different: *Chemical Society Reviews* 35 (7): pp 583-592.

Binzet, G., Kavak, G.H., Kuku, N., Ozbey, S., Florke, V. & Arslan, H., (2013). Synthesis and Characterization of Novel Thiourea derivatives and their Nickel and Copper complexes. *Journal of Chemistry*.vol (2013)

Bodey, G.P., Bolivar, R. Fainstein, V. & Jadeja, L. Infectious caused by *Pseudomonas aeruginosa*. *Rev infect Dis* vol 5 (2): pp 279 – 313.

Bodzek, M. Dudziak, M. & Luks-Betlej. (2004). Application of Membrane Techniques to Water Purification. Removal of Phthalates, Desalination, Vol. 162, No. 1-3, Pp. 121-128

Bolong. N. Ismail, A.F. Salim, M.R. & Matsuura, T. (2009). A Review of The Effects of Emerging Contaminants in Wastewater and Options for Their Removal, Desalination, Vol. 238, No. 1-3, Pp. 229-246.

Bora, T. & Dutta, J. (2014). Applications of nanotechnology in wastewater treatment. *Journal of nanoscience and nanotechnology*. 14: (1). pp 613-626

Born, P., Murray, E., Weber, A. & Krans, T. (2006). Robust, Ultrasmall organosilica nanoparticles without silica shells. *ARC centre of excellence for electromaterials science*.

Bottero, J.Y. Rose, J. & Wiesner, M.R. (2006). Nanotechnologies: Tools for Sustainability in A New Wave of Water Treatment Processes, Integrated Environmental Assessment and Management, Vol. 2, No. 4, Pp. 31-395.

Botzenhart, K. & Doring, G. (1993). Ecology and Epidemiology of *Pseudomonas aeruginosa*. From book of *Pseudomonas aeruginosa* as an opportunistic pathogen. Pp. (1-18).

Braeken. L. Bettens. B. & Boussu. K. (2006). Transport Mechanisms of Dissolved Organic Compounds in Aqueous Solution During Nano Filtration. *Journal of Membrane Science*, Vol. 279, No. 1-2, Pp. 311-319.

Bragg, W.H. & Bragg, W.L. (1949). The reflection of X-rays by crystals. *Proc. R.Soc.Cond.A*. 88.(605): pp. 428-438.

Brar, S. K., Verma, M., Tyagi, R.D and Surampalli, R.Y. (2010). Engineered nanoparticles in wastewater and wastewater sludge evidence and impacts. *Waste management*. 30 (3). pp. 504-520.

British Pharmacopeia Commission Secretariat 2014 Vol (5) 7th edition. *Ph.Eur.method* 2.4.8 Method A Appendix VII V-A261.

Bruce, R., Harvey, E. B., Sergey, V., Patrik, K., Gallagher, A. R. (2008). Thermal Analysis of polymers fundamentals and applications.

Carter, R. & Howsam, P. (1997). Water pollution control – A guide to the use of water Quality Management Principles. *Water quality Assessments 2nd edition. WHO/UNEP*.

Chandra, S. & Kumar, A. (2012). Modulation of synthetic parameters of cobalt nanoparticles. *Journal of Molecular and Biomolecular Spectroscopy*. 98. p. 23-26.

Chauhan, R., Kumar, A. & Abraham, J. (2013). A biological approach to the synthesis of Silver nanoparticles with *Streptomyces* sp JAR1 and its antimicrobial activity. *Sci. Pharm*. 81: p. 607 – 621.

Chen, H & Zhang, M. (2013). Occurrence and removal of resistance genes in municipal wastewater and rural domestic sewage treatment systems in eastern China. *Environmental International*. 55: pp. 9-14.

Classen, T., Haller, L., Walker, D., Bartram, J and Cairncross S. (2007). Cost-effectiveness of water quality interventions for preventing diarrhoeal disease in developing countries. *Journal of water* Vol 5 (4).

Crane. R.A & Scott. T.B. (2012), Nano Scale Zero – Valent Iron: Future Prospects for An Emerging Water Treatment Technology. *J Hazard Mater*, Pp. 211 – 212.

Craun, G.F., Brunkard, J.M., Yoder, J.S., Roberts, V.A., Carpenter, J., Wade, T., Calderon, R.L., Roberts, J.M., Beach, M.J. & Roy, S.L. (2006). C. Causes of outbreaks associated with drinking water in the United States from 1971 to 2006. *American Society for Microbiology*. Vol 23. (3).

Crump, J. A.; Sjölund-Karlsson, M. G., Melita A.P. Christopher M. (2016). "Epidemiology, Clinical Presentation, Laboratory Diagnosis, Antimicrobial Resistance, and Antimicrobial Management of Invasive Salmonella Infections". *Clin Microbiol Rev*. 28 (4): 901–937. doi:10.1128/CMR.00002-15. ISSN 0893-8512. PMC 4503790. PMID 26180063.

Das, A., Slaughter, B.D., Unruh, J.R., Bradford, W.D., Alexander, R., Rubinstein, B. & Li, R. (2012). Flippase-mediated phospholipid asymmetry promotes fast Cdc42 recycling in dynamic maintenance of cell polarity. *Nat Cell Biol* 14(3):304-10.

Dhermendra, K., Tiwari B.J & Prasenjit, S. (2008). Application of Nanoparticles in Waste Water Treatment World Applied Sciences Journal. 3(3): 417-33.

Dhillon, G.G., Brar, S.K., Kaur, S. & Verma, M. (2012). Green approach for nanoparticle biosynthesis by fungi: current trends and applications. *Crit. Rev. Biotechnology*. 32: p. 49-73.

Diallo, M.S. Christie, S. & Swaminathan, P. (2005). Dendritic Chelating Agents. Cu(II) Binding to Ethylene Diamine Core Poly(Amidoamine) Dendrimers in Aqueous Solutions, *Langmuir*, Vol. 20, No. 7, Pp. 2640-2651.

Elmi, A., Eleanor, Watson., Pamela, S., Dominic, C., Mills, N. & Lisa, I. (2011). *Campylobacter jejuni* Outer Membrane Vesicles Play an Important Role in Bacterial Interactions with Human Intestinal Epithelial Cells. Faculty of Infectious & Tropical Diseases, London School of Hygiene & Tropical Medicine.

Eng, S.K.; Pusparajah, P.; Mutalib, N. S.; Ser, H. L.; Chan, K.G. & Lee, L. H (2015). "Salmonella: A review on pathogenesis, epidemiology and antibiotic resistance". *Taylor & Francis Online*. 8 (3): 284–293. doi:10.1080/21553769.2015.1051243.

Fàbrega A, Vila J (2013). "[Salmonella enterica serovar Typhimurium skills to succeed in the host: virulence and regulation](#)". *Clinical Microbiology Reviews*. 26 (2): 308–41.

Farah, C.S., Lynch, N. & McCullough, M.J. (2010). Oral fungal infections: an update for the general practitioner. *Aust Dent J* 55: pp. 48-54.

- Feller, L., Khammissa, R.A., Chandran, R., Altini, M. & Lemmer, J. (2014) Oral candidosis in relation to oral immunity. *J Oral Pathol Med* 43: pp. 563-9
- Fenwick, A. (2006). Waterborne infectious diseases. *Scientific research*. 313: pp. 1077-1081.
- Fewtrell, L., Kaufmann, R.B., Kay, D., Enanoria, W., Haller, L & Colford, J.M. (2005). Water, Sanitation & hygiene interventions to reduce diarrhea in less developed countries: A systematic review and meta-analysis. *The Lancet Infectious Diseases*. Vol 5 (1): pp 42-52.
- Funk, C., Pete, P., Martin, L., Diego, P., James, V., Shraddhanand, S., Gregory, H., James, R., Laura, H., Andrew, H. & Joel, M. (2015). The climate hazards Infrared precipitation with stations – a new environmental record for monitoring extremes.
- Gabriella, G., Paola, R., Guido, B. & Fabio, C. (2015). Cobalt nanoparticles mechanically deposited on α -Al₂O₃: a competitive catalyst for the production of hydrogen through ethanol steam reforming
- Gade, A.K., Bonde, P., Ingle, A.P., Marcato, P.D., Duran, N. & Rai, M.K. (2008). Exploitation of *Aspergillus niger* for synthesis of silver nanoparticles. *J. Biobased Mater. Bioenergy*. 2: p. 243 – 247.
- Gaffield, S., Goo, R., Richards, L., & Jackson, R. (2003). Public health effects of inadequately managed stormwater runoff . *American Journal of Public Health*, 93(9), 1527-1533. Retrieved from CINAHL Plus with Full Text database.
- Gal-Mor O, Boyle EC, Grassl GA (2014). ["Same species, different diseases: how and why typhoidal and non-typhoidal Salmonella enterica serovars differ"](#). *Frontiers in Microbiology*. 5: 391.
- Gao, P., Munir, M. & Xagorarakis, L. (2012). Correlation of tetracycline and sulphonamide antibiotics with corresponding resistance genes and resistant bacteria in a conventional municipal wastewater treatment plant. *Science Total Environmental*, 421-422: pp. 173-183.
- Grosset, A.A., St-Amaud, K., aubertin, K., strupler, M., Madore, W.J., Petrecca, K., Trudel, D. & Leblond, F. (2018). Development and characterization of a handheld hyperspectral Raman imaging probe system for molecular characterization of tissue on mesoscopic scales. *Med Phys*. 45(10): pp 328-339.
- Guo, M., Diao, P. & Cai Sheng, M. (2004). Electrochemical properties of highly oriented ZnO nanotube array films on ITO substrates, *chinese chem. Lett*. 15. Pp.1113.

- Gupta, K., Hooton, T.M., Naber, K.G., Wullt, B., Colgan, R., Miller, L.G., Moran, G.J., Nicolle, L.E., Raz, R., Schaeffer, A.J. & Soper, D.E. (2013). International clinical practice guidelines for the treatment of acute uncomplicated cystitis and pyelonephritis in Women: Infectious Diseases Society of America and the European Society for Microbiology and Infectious Diseases. 52 (5): pp. 103-120.
- Hangchang, S. (2011). Industrial waste-water types, amounts and effects. Encyclopaedia of life support systems (EOLSS); Available: www.eolss.net/sample-chapters/c09/e4-11-02-02.
- Hardalo, C. & Edberg, S.C. (1997). *Pseudomonas aeruginosa*: Assessment of risk from drinking water. *Journal of microbiology*. 23 (1): pp. 47-75.
- Hari, P. & Kulmala, M. (2005). Station for measuring Ecos Boreal Environment. Res. 10: pp. 315-322.
- Hollyoak, V., allison, D. & Summers, J. (1995). Wound infection associated with a nursing homes whirlpool bath. *Communicable disease report. CDR review*: 5(7).
- Holt, K.E., Thieu Nga, T.V., Thanh, D.P., Vinh, H., kim, D.W., Vu Tra, M.P., Campbell, J.L., hoang, N.V., Vinh, N.T., Minh, P.V., Thuy, C.T., Nga, T.T., Thompson, C., Dung, T.T., Nhu, N.T., Vinh, P.V., Tuyet, P.T., Phuc, H.L., Lien, N.T., Phu, B.D., Ai, N.T., Tien, N.M., Dong, N., Parry, C.M., Hien, T.T., Farrar, J.J., Parkhill, J., Dougan, G., Thompson, N.R. & Baker, S. (2013). Tracking the establishment of local endemic populations of an emergent enteric pathogen. *Proc Nati Acad Sci U.S.A* vol 110 (43): pp 17522-175227.
- Hu, M., Fan, B., Wang, H., Qu, B., Zhu, S., (2016). Construction the ecological sanitation: a review on technology and methods. *Journal of Cleaner Production*. 125.pp 1-21.
- Hulkoti, N. I. & Taranath, T.C. (2014). Biosynthesis of nanoparticles using microbes- a review. *Journal of colsurfb*. (05). 027
- Ivanova, L., Cabello, F.C., Godfrey, H.P., Tomova, A., Dolz, H., Millanao, A. & Buschmann, A.H. (2013). Antimicrobial use in aquaculture re-examined: its relevance to antimicrobial resistance and to animal and human health. 15 (7): pp. 1917-1942.
- Jain, Sanjay K.; Gupta, Amita; Glanz, Brian; Dick, James; Siberry, George K. (2005). "Antimicrobial-Resistant *Shigella sonnei*". *The Pediatric Infectious Disease Journal*. 24 (6): 494–7.

- Janet, M. & Szafert, S. (2017). Synthesis, characterization and thermal properties of T8 type amido-POSS with p-halophenyl end-group. *Journal of organometallic Chemistry. Organometallic Chemistry from stereochemistry to catalysis* 847: pp 173-183.
- Jantsch J, Chikkaballi D, Hensel M (2011). "Cellular aspects of immunity to intracellular *Salmonella enterica*". *Immunological Reviews*. 240 (1): 185–95.
- Jiang, J., Oberdorster, G & Biswas, P. (2009). Characterization of size, surface charge, and agglomeration state of nanoparticle dispersions for toxicological studies. *J. Phys.Chem*:107. P. 668-677.
- Jianxi, Y., Gaoling, Z. & Gaorong, H. (2003). Synthesis and characteristics of the thiourea-capped Cds Nanoparticles. *Journal of materials science letters*. 22. p. 1491-1493.
- Kanchi, S. (2014). Nanotechnology for Water Treatment. *J Environ Anal Chem* 1: E102.Doi: 10.4172/Jreac.1000e102.
- Karak, T. & Bhattacharyya, P. Human Urine as a Source of Alternative natural fertilizer in agriculture: (2011). *A flight of fancy or an achievable reality, resource, conservation and recycling*. Vol 55: (4). Pp. 400-408.
- Kathiresan, K., Manivannan, S., Nabeel, M.A. & Dhivya, B. (2009). Studies on silver nanoparticles synthesized by a marine fungus, *Penicillium fellutanum* isolated from coastal mangrove sediment. *Colloids Surfactant B*. 71: p. 133-137.
- Kgalushi, R., Smite, S. & Eales, K. (2004). People living with HIV/AIDS in a context of rural poverty: The importance of water and sanitation services and hygiene education, JHB: Mvula Trust and Delft: IRC International Water and Sanitation Centre.
- Khan, A., Rashid, A., Younas, R. & Chong, R. (2016). A chemical reduction approach to the synthesis of copper nanoparticles. *International Nano Letters*, 6(1). pp. 21-26.
- Konate, K., Mavoungou, J.F., Lepengue, A.N. (2012). Antibacterial activity against B-lactamase producing Methicillin and Ampicillin-resistants *Staphylococcus aureus*: Fractional Inhibitory Concentration Index (FICI) determination. *Ann.Clin.Microbiology.Antimicrob*.11.p. 18
- Kumar, A., Kaur, K. & Sharma, S. (2013). Synthesis, characterization and antibacterial potential of silver nanoparticles by *Morus nigra* leaf extract. *Indian. J.Pharm.Biol.Res*.1:p. 16 – 24.

- Laurent, P. (2005). Household drinking water systems and their impact on people with weakened immunity. *Public Health Department*
- Lens, P.N.L., Virkutye, J., Jegatheesan, V., Kim, S.H., Al-Abed, S. (2013). Nanotechnology for Water and Wastewater Treatment, Iwa Publishing.
- Levantesi, C., Bonadonna, L., Briancesco, R., Grohmann, E., Toze, S. & Tandoi, V. (2012). *Salmonella* in surface and drinking water: occurrence and water – mediated transmission. *Food Research International*. 45.pp.587-602.
- Li, H., Chen, Q. Zhao, J. & Urmila, K. (2015). Enhancing the antimicrobial activity of natural extraction using the synthetic ultrasmall metal nanoparticles. *Scientific reports*. (5). pp 11033.
- Li, J., Carlson, B.E., & Lacis, A.A. (2014) Application of spectral analysis techniques in the inter-comparison of aerosol data, Part 4: Synthesized analysis of multisensor satellite and ground-based AOD measurements using combined maximum covariance analysis. *Atmos. Meas. Tech.*, **7**, 2531-2549, doi:10.5194/amt-7-2531-2014.
- Li, R., Zhang, Y., Lou, H., Li, J. & Feng, Z. (2011). Synthesis of ZrB₂ nanoparticles by sol-gel method. *Journal of sol-gel science and technology*, 58(2). pp. 580-585
- Lili, W. & Youshia, W. (2007). Synthesis and optical characteristic of ZnO nanorod. *Journal. Material.Sci.*42. pp. 1113.
- Makarov, V.V., Love, A.J., Sinitsyna, O.V., Makarova, S.S., Yaminsky, I.V., Talianky, M.E. & Kalinina, N.O. (2014). Green nanotechnologies: Synthesis of metal nanoparticles using plants. *Acta Naturae*. 6: p. 35-44.
- Mandal, D., Bolander, M.E., Mukhopadhyay, D., Sarkar, G. & Mukherjee, P. (2006). *Application of microbiology and Biotechnology*. 69: p. 485 – 492.
- Mara, D.D. (2003). Water, sanitation and hygiene for the health of developing nations. *Public Health*. 117(6). p. 452-456.
- Marcells A. O., Omowunmi, S.K., & Isaac, K. (2009). Nanostructured Materials for Improving Water Quality: Potentials and Risks. *Nanotechnology Applications for Clean Water*. Pp 233-247.
- Michler, G.H. & Balta-Calleja, F.J. (2012). Nano and micromechanics of polymer; Hanser. Institute of physics, Martin Luther University Halle-Wittenberg, Halle Saale Germany

- Mohammed, E., Syed, A., Scott, F., Paul, D., Mark, M., Roger, M. & Ibrahim, M.B. (2016). US National Library of Medicine National Institutes of Health. Biotechnology letters. Pp38: 1015-1019.
- Moloto, M.J., Thema, F.T., Dikio, E.D., Nyangiwe, N.N., Kotsedi, L., Maaza, M. And Khenfouch, M. (2013). Synthesis and characterization of Graphene thin Films by Chemical Reduction of Exfoliated and Intercalated Graphite Oxide. *Journal of Chemistry, Vol.2013*
- Muirhead, R.W. & Monaghan, R.M. (2012). A two-reservoir model to predict *Escherichia coli* losses to water from pastures grazed by dairy cows. *Environ Int* 40: pp. 8-14
- Mukherjee, P., Senapati, S., Mandal, D., Ahmad, A., Khan, M.I., Kumar, R. & Sastry, M. (2002). Extracellular synthesis of gold nanoparticles by the fungus *Fusarium oxysporum*. *ChemBioChem*. 3: p. 461-463.
- Nagaraj, V.H., Mukhopadhyay, S., Dayarian, A. & Sengupta, A.M. (2014). Breaking an epigenetic chromatin switch: curious features of hysteresis in *Saccharomyces cerevisiae* telomeric silencing. 9 (12): pp. 113516
- Narayan, K.B. & Sakthivel, N. (2010). Biological synthesis of metal nanoparticles by microbes. *Adv Colloid Interface Sci*. 22 (1-2). pp. 1-13.
- Narayanan, K.B & Sakthivel, N. (2010). Biological synthesis of metal nanoparticles by microbes. *Adv. Colloid Interface Sci*. 156: p. 1-3.
- Nassar, N.N. (2013). The Application of Nanoparticles for Wastewater Remediation, Applications of Nanomaterial for Water Quality, Published by Future Science Ltd.
- Nemade, K.R & Waghuley, S.A. (2013). UV-VIS spectroscopic study of one pot synthesized strontium oxide quantum dots. # *Res.Phys*.3.pp. 52-54
- Niara, M., Yuri, L., Lonal, J.L., Diniz, B., Maria, F. (2015). Microscopic and UV/Vis spectrophotometric characterization of *Cissampelos pareira* of Brazil and Africa. *Brazilian Journal of Pharmacognosy*. 26 (2016). pp. 135-146.
- Obare, S.O. & Meyer, G.J. (2004). Nanostructured Materials for Environmental Remediation of Organic Contaminants in Water. *Journal of Environmental Science and Health Part-A*. 39(10): 2549 – 2582.
- Oikonomou, A., Katsiapi, M., Karayanni, H., Moustaka-gouni, M. & Kormas, K.A. (2012). Plankton microorganisms coinciding with two consecutive mass fish kills in a newly reconstructed lake. *Sci world*. Pp. 1-4

- Okafor, F., Janen, A., Kukhtaneva, T., Edwards, V. & Curley, M. (2013). Green synthesis of silver nanoparticles, their characterization, application and antibacterial activity. *International journal of Environmental Research and Public Health*. 10:5221 – 5238.
- Olushola, S.A., Leslie, F.P. (2014). Nanotechnology: The Breakthrough in Water and Wastewater Treatment. *International Journal of Chemical Material and Environmental Research*. 1(1): 1-2.
- Omar, B. I. (2012). Pelagria research library. *Advances in applied science research*. 3(6). p. 3522-3539.
- Pankaj T.K., Ravikant S., Smriti V., Dharmendra K & Shruti T. (2012). Nanomaterial's Use in Waste Water Treatment, International Conference on Nanotechnology and Chemical Engineering. Bangkok. P.21-22.
- Pendergast, M.M. & Hoek, E.M.V., (2011). A Review of Water Treatment Membrane Nanotechnologies, Energy and Environmental Science. 4(6), Pp. 1946 – 1971.
- Plaza, G., Turek, A & Szczyglowska R (2013). Characterization of E.coli strains obtained from wastewater effluent. *Int J Environ Res* 2:67-74
- Poole, K. (2004). "Efflux-mediated multiresistance in Gram-negative bacteria". *Clinical Microbiology and Infection*. **10** (1): pp. 12-26
- Prabhu, S. & Poulouse, E.K. (2012). Silver nanoparticles: Mechanism of anti-microbial action, synthesis, medical applications and toxicity effects. 2: pp. 1-10.
- Prachi, P. G., Deepa, M., Gautam, P. & Brijesh Nair, A.N. (2013). Nanotechnology in Wastewater Treatment: *International Journal of Chemtech Research*. Vol. 5, Pp. 2303 – 2308.
- Privette, C. & Smink, J. (2017). Assessing the Potential Impacts of WWTP Effluent Reductions within the Reedy River Watershed. *Journal of Ecological Engineering*. Vol 98 (11-16).
- Qu, X., Alvarez, P.J.J., Li, Q. (2013). Applications of Nanotechnology in Water and Wastewater Treatment, *Water Research*, 47. Pp. 391-3946.
- Rana, S. & KalaiChelvan, P.T. (2013). Ecotoxicity of nanoparticles. *ISRN Toxicology*
- Ricco, J.B. & Assadian, O. (2011). Antimicrobial Silver Grafts for prevention and treatment of Vascular Graft Infection. *Semin. Vasc. Surg.* 4: pp. 234-241.
- Roduner, E. (2006) Size matters: why nanomaterials are different. *Chem Soc Rev*

Ross, J. A., Rich, M., Molzen, J. & Pensak, M.. 1988. Family planning and child survival in one hundred developing countries. *New York: Center for Population and Family Health, Columbia*

Russo, D., Avner, S. & Dani, O. (2015). Balancing water scarcity and quality for sustainable irrigated agriculture. *Water resources research*. Vol 51 (5): pp 3419-3436.

Ryan, I. K.J & Ray, C.G., (2004). Sherris Medical Microbiology (4th ed.). *McGraw Hill*. pp. 362–8.

Sadiq, R. & Rodriguez, M.J. (2004). Disinfection By-Products (Dbps) In Drinking Water and Predictive Models for Their Occurrence: A Review, *Science Of The Total Environment*, Vol. 321, No. 1-3, Pp. 21-46.

Saini, M., Chandra, S., Sign, Y., Basu, B. & Tripathi, A. (2013). X-Ray diffraction and scanning electron microscopy – energy dispersive spectroscopic analysis of ceramometal interface at different firing.

Salata, O.V. (2004). Applications of nanoparticles in Biology and medicine. *Journal of nanobiotechnology*. 12. Pp. 15-20.

Saliby, E.L., Shon, I.J., Kandasamy, H.K., Vigneswaran, J., (2013). Nanotechnology for Wastewater Treatment: In Brief, *Water and Wastewater Treatment Technologies*.

Salman, S.A., Usami, T., Kuroda, K. & Okido, M. (2014). Synthesis and characterization of Cobalt Nanoparticles using hydrazine and citric acid. *Journal of Nanotechnology*. p. 1-6.

Schade, A. L. (1949). Cobalt and Bacterial Growth, with special reference to *Proteus vulgaris*. *Journal of Bacteriology*, Vol.58 (96). pp: 811-22 ref.18

Seil, J.T. & Webster, T.J. (2012). Antimicrobial applications of nanotechnology: Methods and literature. *Int.J. Nanomedicines*. 7: p. 2767-2781.

Sharma, V. & Sharma, A. (2013). Nanotechnology: An Emerging Future Trend in Wastewater Treatment with Its Innovative Products and Processes, *International Journal of Enhanced Research in Science Technology and Engineering*, Vol. 2. Issue 1.

Singh, R.P., Shukla, V.K., Yadav, R.S., Sharma, P.K. & Pandey, A.C. (2011). Biological approach of zinc oxide nanoparticles formation and its characterization. *Adv. Mater. Lett.* 2: p. 313-317.

Steven I, Percival D, & Williams W. (2014). [*Microbiology of Waterborne Diseases \(Second Edition\)*](#). Microbiological Aspects and Risks: Pages 223-236.

Sudha, S.S., Karthic, R. & Rengaramanujam, J. (2013). Microalgae mediated synthesis of silver nanoparticles and their antibacterial activity against pathogenic bacteria. *Indian J. Exp. Biology*. 51: p. 393-399.

Sun, H., Ahmad, M. & Zhu, J. (2013). Morphology-controlled synthesis of Co₃O₄ porous nanostructures for the application as lithium-ion battery electrode. *Electrochim Acta* 89, pp.199-205.

Sun, S. & Murray, C.B. (1999). Synthesis of monodisperse cobalt nanocrystals and their assembly into magnetic superlattices. *Journal of applied physics*. 85(8). p. 4325-4330.

Szylak-Szydlowski, M., Kulig, A. & Miaskiewics-Peska, E. (2016). Seasonal changes in the concentrations of airborne bacteria emitted from a large wastewater treatment plant. *International Biodeterior Biodegradation*, 115: pp. 11-16

Tchobanoglous, G., Stensel, H.D., Tsuchihashi, R., Burton, F. (2014). Wastewater Engineering: Treatment and Resource Recovery, 5th Edition, New York, Mcgraw-Hill.

Terashi, Y., Purwanto, A., Wang, W., Iskandar, F. & Okuyama, K. (2008). Role of urea addition in the preparation of tetragonal BaTiO₃ nanoparticles using flame-assisted spray pyrolysis. *Journal of the European Ceramic Society*. Vol 28 (13). Pp. 2573-2580.

Theron, M., Barkhuizen, N., & Du Plessis, Y. (2014). Managing the academic talent void: Investigating factors in academic turnover and retention in South Africa. *SA Journal of Industrial Psychology/SA Tydskrif vir Bedryfsielkunde*, 40(1). pp. 1117

Tilley, E., Ulrich, L., Luthi, C., Reymond, P.H. & Zurbrugg, C. (2016). Compendium of Sanitation Technologies- 2nd Ed. Swiss Federal Institute of Aquatic Science and Technology (Eawag). Duebendorf, Switzerland. pp. 175

U.S. Pharmacopeia 35/National Formulary 30, Rockville, MD: US Pharmacopeial Convention, Inc; 2012: 344-386

United Nations Children's Fund (UNICEF). (2010). *Progress on Sanitation and Drinking Water*. New York: UNICEF.

Vidyasagar, D. (2007). Global minute: water and health - walking for water and water wars *Journal of Perinatology* .27. pp56-58.

- Vorosmarty, C.J., Green, P., Salisbury, J. & Lammers, R.B. (2000). Global water resources: *Vulnerability from climate change and population growth, science*. 289. pp. 284-288.
- Wadekar, K.F., Nemade, K.R. & Waghuley, S.A (2017). Chemical synthesis of Cobalt Oxide (Co₃O₄) nanoparticles using cobalt – precipitation method. *Research journal of chemical Sciences*. Vol. 7 (1). P. 53-55.
- Walha, K., Amar, R.B., Firdaous, L., Quemeneur, F. & Jaouen, P. (2007). Brackish groundwater treatment by nano filtration, Reverse Osmosis and Electro dialysis in Tunisia: Performance and cost comparison, desalination, Vol.207, No. 1-3, pp. 95-106.
- Wang, D., Xin, H.L., Hovden, R., Wang, H., Yu, Y., Muller, D.A. & Abruna, H.D. (2013). Structurally ordered intermetallic platinum-cobalt core-shell nanoparticles with enhanced activity and stability as oxygen reduction electrocatalysts. *Nature materials*. 12 (1). Pp. 81-87.
- Wang, F., Nimmo, S.L., Cao, B. & Mao, C. (2012). Oxide formation on biological nanostructures via a structure-directing agent: Towards an understanding of precise structural transcription. *Chem. Sci*. 3. P. 2639-2645.
- Wang, J., Sheng, Y. & Tong, T.D. (2014). Satellite-based daily water extents in Poyang Lake region. China, *Pangaea*. 2000-2011.
- Wang, Y., Boguski, M., Riggs, M., Rodgers, L. & Wigler, M. (1991). Sar1, a gene from *Schizosaccharomyces pombe* encoding a protein that regulates ras1. *Cell Regulation*. 2(6): pp. 453-465.
- World Health Organization (2006). *Guidelines for the safe use of wastewater, excreta and greywater*. WHO. P. 31.
- World Health Organization. (2010). *UN-water global annual assessment of sanitation and drinking-water*. WHO. P. 12
- World Health Organization. (2014). *Water and sanitation in the European region*. WHO. P. 46
- WWAP (United Nations World Water Assessment Programme) (2017). The United Nations World Water Development Report 2017 wastewater. The untapped Resource. Paris ISBN 978-92-3-100201-4
- Yoon, Y. Westerhoff, P. Snyder, S.A. & Wert, F.C. (2006). Nano Filtration and Ultrafiltration of endocrine disrupting compounds, Pharmaceuticals and personal care products, *Journal of Membrane Science*, Vol. 270. pp. 1-2.

Zhang, B., Yu, Q., Wang, Y., Xiao, C., Dong, Y., Xu, N., Wang, L. & Li, M. & (2015). The actin-related protein Sac1 is required for morphogenesis and cell wall integrity in *Candida albicans*. *Fungal Genetic Biology*. 81: 261-270.

Zhang, K., An, Y., Wang, F., Lin, L. & Guo, H. (2011). Experimental investigation on water treatment by the combined nano MgO-nanofiltration technique. *Water Science and Technology*. 63: 2542-2546.

Zhang, L.W., Fu, J.Y., Hua, H. & Yan, Z.M. (2015). Efficacy and safety of miconazole for oral candidiasis: *a systematic review and meta-analysis*.

Zhang, Y., Li, Z., Zhao, Y., Chen, S., Manhood, I.B. & (2013). Stabilization of source-separated human urine by chemical oxidation. *Water Science and Technology*. 67: pp. 1901-1907.